Universitat Autònoma de Barcelona

Implementation and Characterization of In-to-out Body Radio Transmissions for a Ruminal Bolus

Lu Wang

Implementation and Characterization of In-to-out Body Radio Transmissions for a Ruminal Bolus

Lu Wang

Universitat Autònoma
de Barcelona

Implementation and Characterization of In-to-out Body Radio Transmissions for a Ruminal Bolus

PhD dissertation

Electrical and Telecommunication Engineering
Department of Microelectronics and Electronic Systems
Autonomous University of Barcelona

Author:
Lu Wang

Directors:
Carles Ferrer Ramis and Marta Prim Sabrià

2019

Implementation and Characterization of In-to-out Body Radio Transmissions for a Ruminal Bolus
Implementación y caracterización de las transmisiones radiofrecuencia intracorporales para bolos ruminales
Implementació i caracterització de les transmissions radiofreqüència intracorporals per a bolus ruminals

A thesis submitted in conformity with the requirements for the Degree of Doctor of Philosophy in Electrical and Telecommunication Engineering

PhD candidate: Lu Wang
Signature

Supervisors: Carles Ferrer Ramis and Marta Prim Sabrià
Signatures

Autonomous University of Barcelona
Department of Microelectronics and Electronic Systems
Edifici Q, C/Sitges
08193 Cerdanyola del Valles, Spain

February 5, 2019

Abstract

In recent years, using indwelling wireless sensor nodes to collect and transmit essential bioclimatic data from the reticulo-ruminal chamber is gaining a global recognition in cattle management. Benefits of these devices, usually referred to as ruminal (sensing) boluses, include real-time supervisions of rumen stability, loss prevention, and improved animal welfare. As the major export party of global dairy products, Europe has been pioneering in the research and development of ruminal boluses, mostly working at the license-free industrial, scientific, and medical radio band of 433.05 MHz—434.79 MHz. Meanwhile, the increasing need to apply adequate ruminal boluses to monitor the health status of small ruminants, such as sheep and goats, is bringing new challenges to researchers. In consideration of the much smaller body size compared to cows, a notable downsizing of device form-factor is indispensable. However, this would affect not only the radiation efficiency but also the shelf life of the small ruminal boluses, since both the radio component and the power unit would benefit from abundant space. For devices used in wireless body area networks, power consumption is closely related to system configurations in view of the wireless channel: not only the radiation elements, but also the characteristics of the radio transmission channel. Unfortunately, very few research efforts have been dedicated to the wireless channel of ruminal boluses for small ruminants.

This doctoral thesis focused on the search of a radio solution for ruminal boluses targeted on small ruminants, which could balance the restrictions in device dimension and performance. This radio solution consists of the implementation of a small antenna that could fit for a compact ruminal bolus working at 433 MHz, and the characterization of the in-to-out body radio transmission channel between a small ruminal bolus and an on-body receiver. A small spiral antenna was devised for integration into a ruminal bolus for small ruminants, taking into consideration of the other encapsulated components and mediums, as well as the in-body environment where the ruminal bolus resides. To investigate the radio link between the spiral antenna

and a reference receiver, theoretical path loss models were developed, by means of both laboratory measurement in a tissue-simulating liquid and numerical analysis with 3-dimensional computational electromagnetic tools. Link viability was verified on a system level through link budget analysis, utilizing the theoretical path loss models. Beyond the theoretical channel studies, the actual radio transmission channel also exhibits time-varying features, some of which are aligned with biological behaviors of the ruminant animals. On-site studies were therefore carried out with a rumen-cannulated animal in a barn. Series of in vivo measurement campaigns were arranged to investigate the radio channel's characteristics in the authentic scenarios. A diurnal path loss pattern was developed through continuous observations based on a prototype of the small bolus and an on-body receiver. Variances of path loss in the radio channel across the day were demonstrated and associated with ruminal digestive statuses. A power-reduction plan was then proposed combining the diurnal path loss pattern to the existing power profile of the small ruminal bolus.

Resumen

Actualmente, los nodos de sensores inalámbricos que residen en la cámara retículo-ruminal de los animales rumiantes para recolectar y transmitir datos bioclimáticos vitales están ganando un reconocimiento mundial en el manejo del ganado. Los beneficios de estos dispositivos, generalmente conocidos como bolos ruminales (de detección), incluyen la supervisión en tiempo real de la estabilidad del rumen, la prevención de pérdidas y la mejora del bienestar animal. Europa, con la mayor exportación de productos lácteos del mundo, ha sido pionera en la investigación y el desarrollo de bolos ruminales, la mayoría de los cuales trabajan en la banda de frecuencia de uso abierto y sin licencia dentro de las áreas científica e industrial de 433,05 MHz – 434,79 MHz. Por otro lado, la creciente necesidad de aplicar bolos ruminales adecuados al monitoreo de la salud de los pequeños rumiantes, como son las ovejas y las cabras, presenta nuevos desafíos para los investigadores. Teniendo en cuenta que el tamaño corporal de estos rumiantes es mucho más pequeño en comparación con las vacas, es indispensable reducir el tamaño del bolo ruminal. Esto afecta no solo la eficiencia de la transmisión radio, sino también a la vida útil del pequeño bolo ruminal, como resultado de las limitaciones de espacio tanto para su componente de radiofrecuencia como para la unidad de potencia. Así pues, para los dispositivos utilizados en redes inalámbricas de área corporal, el consumo de energía suele estar estrechamente relacionado con las configuraciones del sistema dado que en el canal inalámbrico, no solo los elementos de transmisión, sino también influyen las características de transmisión de radiofrecuencia en el canal. Desafortunadamente, se han dedicado muy pocos esfuerzos de investigación al canal inalámbrico de bolos ruminales para pequeños rumiantes.

Esta tesis doctoral se ha centrado en la búsqueda de una solución de radiofrecuencia para bolos ruminales destinados a pequeños rumiantes, que equilibrar las restricciones en la dimensión y el rendimiento del dispositivo. Dicha solución de radiofrecuencia ha consistido en la implementación de una pequeña antena que puede ajustarse a un pequeño bolo ruminal que funciona a 433 MHz y la caracterización del canal de transmisión de radiofrecuencia

desde dentro del cuerpo con un pequeño bolo ruminal hacia fuera del cuerpo con un receptor externo. El trabajo de investigación comenzó con el diseño de una antena en espiral, con una estructura geométrica simple y personalizada para el entorno de propagación de radiofrecuencia deseado. Para investigar el enlace de radiofrecuencia entre la antena espiral y un receptor de referencia, se desarrollaron modelos teóricos de pérdida de trayectoria, mediante mediciones de laboratorio con líquidos de simulación de tejidos y análisis numérico con herramientas electromagnéticas computacionales tridimensionales. La viabilidad del enlace se verificó a nivel de sistema mediante el análisis de la estimación del enlace, utilizando los modelos teóricos de pérdida de trayectoria. Más allá de los estudios de canales teóricos, el canal de transmisión de radiofrecuencia real también presenta características que varían con el tiempo, algunas de las cuales están alineadas con los comportamientos biológicos de los animales rumiantes. Por lo tanto, los estudios in situ se llevaron a cabo con un animal con el rumen canulado situado en un establo. Se organizaron series de medición in vivo para investigar los comportamientos del canal de radiofrecuencia en los escenarios reales. Se desarrolló un patrón de pérdida de la trayectoria diurna a través de observaciones continuas basadas en un prototipo de un pequeño bolo ruminal y un receptor externo en el cuerpo. Se han demostrado las variaciones en la pérdida de la trayectoria en el canal de radiofrecuencia a lo largo del día y se han asociado con los estados digestivos ruminales. A partir de estos resultados, se ha propuesto un plan de reducción de potencia combinando el patrón de pérdida de la trayectoria diurna con el perfil de potencia existente del pequeño bolo ruminal.

Resum

Actualment, els nodes de sensors sense fils que resideixen a la cambra reticle-ruminal dels animals remugants per recol·lectar i transmetre dades bioclimàtics vitals estan guanyant un reconeixement mundial en el maneig del bestiar. Els beneficis d'aquests dispositius, generalment coneguts com bols ruminals (de detecció), inclouen la supervisió en temps real de l'estabilitat del rumen, la prevenció de pèrdues i la millora del benestar animal. Europa, amb la major exportació de productes lactis del món, ha estat pionera en la investigació i el desenvolupament de bols ruminals, la majoria dels quals treballen a la banda de freqüència d'ús obert i sense llicència dins de les àrees científica i industrial de 433,05 MHz – 434,79 MHz. D'altra banda, la creixent necessitat d'aplicar bols ruminals adequats al monitoratge de la salut dels petits remugants, com són les ovelles i les cabres, presenta nous reptes per als investigadors. Tenint en compte que la mida corporal d'aquests remugants és molt més petit en comparació amb les vaques, és indispensable reduir la mida del bol ruminal. Això afecta no només l'eficiència de la transmissió ràdio, sinó també a la vida útil del petit bol ruminal, com a resultat de les limitacions d'espai tant per al seu component de radiofreqüència com per a la unitat de potència. Així doncs, per als dispositius utilitzats en xarxes sense fil d'àrea corporal, el consum d'energia sol estar estretament relacionat amb que les configuracions del sistema donat que la transmissió sense fil, no només els elements de transmissió, sinó també influeixen les característiques de transmissió de radiofreqüència en el canal. Desafortunadament, s'han dedicat molt pocs esforços d'investigació al canal sense fil de bols ruminals per a petits remugants.

Aquesta tesi doctoral s'ha centrat en la recerca d'una solució de radiofreqüència per bols ruminals destinats a petits remugants, que equilibrar les restriccions en la dimensió i el rendiment del dispositiu. Aquesta solució de radiofreqüència va consistir en la implementació d'una petita antena que pot ajustar-se a un petit bol ruminal que funciona a 433 MHz i la caracterització de la cadena de transmissió de radiofreqüència des de dins del cos amb un petit bol ruminal cap a fora del cos amb un

receptor extern. El treball de recerca va començar amb el disseny d'una antena en espiral, amb una estructura geomètrica simple i personalitzada per a l'entorn de propagació de radiofreqüència desitjat. Per investigar l'enllaç de radiofreqüència entre l'antena espiral i un receptor de referència, es van desenvolupar models teòrics de pèrdua de trajectòria, mitjançant mesuraments de laboratori amb líquids de simulació de teixits i anàlisi numèrica amb eines electromagnètiques computacionals tridimensionals. La viabilitat de l'enllaç es va verificar a nivell de sistema mitjançant l'anàlisi de l'estimació de l'enllaç, utilitzant els models teòrics de pèrdua de trajectòria. Més enllà dels estudis de canals teòrics, el canal de transmissió de radiofreqüència real també presenta característiques que varien amb el temps, algunes de les quals estan alineades amb els comportaments biològics dels animals remugants. Per tant, els estudis in situ es van dur a terme amb un animal amb el rumen fisulat situat en un estable. Es van organitzar sèries de mesurament in vivo per investigar els comportaments de la cadena de radiofreqüència en els escenaris reals. Es va desenvolupar un patró de pèrdua de la trajectòria diürna a través d'observacions contínues basades en un prototip d'un petit bol ruminal i un receptor extern al cos. Es van demostrar les variacions en la pèrdua de la trajectòria al canal de radiofreqüència al llarg del dia i es van associar amb els estats digestius ruminals. A partir d'aquests resultats s'ha proposat un pla de reducció de potència combinant el patró de pèrdua de la trajectòria diürna amb el perfil de potència existent del petit bol ruminal.

Acknowledgement

This doctoral thesis would never have come to be without a lot of people. To name them all would be even more difficult than writing down the thesis. But still, a few have to be named.

I would like to express my sincere gratitude to Prof. Carles Ferrer and Dr. Marta Prim, my directors of the thesis and trusting friends, for their help, great patience, and always being by my side during all the harsh times.

Dr. Joan Oliver for providing me the device platform with lots of guidance, generosity in knowledge sharing, and above all, his passion with work.

Prof. Gerardo Caja and his team for their expertise in veterinarian research and determinations to establish multidisciplinary international collaborations.

Prof. Wout Joseph, Dr. Günter Vermeeren, and the group WAVES of Ghent University for hosting me for internships that opened the door of research for me.

Dr. Josep Parrón and Dr. Ángeles Vazquez-Castro for their generous help and intuitive suggestions when I got stuck with the research.

Everyone at my department, for their ground support and accompany, throughout the years of my doctoral study.

My family and friends, without whom, I would never have walked along this winding road to find a better me.

Thank You All.

Lu Wang

Barcelona, February 2019

Contents

1 Introduction

> *If you want to find the secrets of the universe, think in terms of energy, frequency and vibration.*
>
> **— Nikola Tesla**

The rapid growth of information technologies is bringing different sectors more and more connected. One of the many beneficial applications is telemetric biomedicine: through implant and wearable wireless biosensor nodes, the subjects can receive rapid diagnosis without being hospitalized. In recent years, wireless biosensors are spreading to precision livestock farming, offering early detection of chronic diseases to reduce economic loss and improve animal welfare. These benefits highlight the needs for more in-depth research work as well as adequate devices the animal-targeted wireless body area networks (WBAN). In this chapter, the motivation and essence of the thesis are first provided, within which the objectives and limitations are listed. Next, background knowledge that are required for this thesis are briefly introduced. Thesis structure is provided in the last section of this chapter.

1.1 Motivation and essence of the thesis

Domestic ruminant animals that yield dairy products, such as cows, sheep, and goats, are closely related to human beings for more than 10 000 years [HS10]. With their special digestive physiology, the ruminant animals could produce high-quality dairy product while living mainly on grass and plants. A recent report from the Food and Agriculture Organization of the United Nations indicated that both milk production and milk price have been growing modestly, with the European Union remaining as a major exporter of dairy products [OECa]. Meanwhile, increases in milk imports from major developing countries, as well as the dairy development's impact on poverty reduction, have further demonstrated a growing global need for dairy products [OECb].

Researchers have discovered that high-yielding ruminant animals are more vulnerable to diseases that break the rumen stability in an almost undetectable way, especially at early stage [EJ01; Zos+10]. For decades, farmers and scientists have been attempting to inspect rumen abnormality with various measures, most of which are invasive, not suitable for field applications, and highly dependent on the operator's skills [Duf+04; Mot; Sat+12]. Until recent years, indwelling wireless ruminal sensor nodes have become the trend in cattle health management. Such sensor nodes, referred to as ruminal boluses, are applied orally through the esophagus and reside in the reticulo-ruminal chamber [Alz+07; Sat+12; Nog+17]. Bioclimatic information, such as rumen temperature and pH value, are collected and sent out of the body by the radio transmitter (TX) integrated in the ruminal boluses. The receiver could either be a fixed apparatus [Sat+12; Nog+17] or a wearable device, such as a neck collar [Alz+07; Limb].

Existing ruminal boluses are mostly limited to large livestock ruminants, for example, the dairy cows. It is of relatively lower risk to conduct research work and experiments with dairy cows, since their large body size would impose less dimensional restrictions to the indwelling devices. However, compared with implant and ingestible medical devices used in human medicine, most of the existing ruminal boluses are still at a primary stage: instability in radio transmission has been discovered [Nog+17], and the reported battery life is not satisfactory [Limb; Gmb]– since ruminal boluses cannot be retrieved after administration, permanent indwelling is always desired by veterinarian researchers and farmers [CCK16]. Research and development of ruminal boluses for small ruminant are even farther lagged behind, regardless of the increasing demand on dairy products of sheep and goats [OECb]. Strict limitation in device size is only one of the many challenges. Problems with ruminal boluses for dairy cows would also exist, and get even tougher, in the design and evaluation of ruminal boluses for small ruminants, since the trade-off between dimension and performance applies to most of the electronic components.

Research work in WBAN for humankind could shed light on the evolution of ruminal boluses. With similarities in system components, frequency bands, and application scenarios, methodologies used in developing implant and ingestible medical devices could be transferred to ruminal boluses. Among the many trending topics, radio solution is always attached high importance for implant and ingestible devices [AH09; Lee+11; Sta+16]; however, it is almost neglected in ruminal boluses, which could be a major cause for

the aforementioned problems among existing ruminal boluses. Being closely related to both link viability and power consumption, a qualified radio solution provides not only adequate radio components, but also a proper characterization of the target wireless transmission channel. An in-depth understanding of the channel's behaviors is the first step towards reliable and efficient WBAN communications.

This doctoral thesis aimed at providing a radio solution, which could balance the restrictions in dimension and requirements in performance for a ruminal bolus targeted on small ruminants. The ruminal bolus, working at 433 MHz, was devised in the Autonomous University of Barcelona (referred to as UAB in this thesis work) to facilitate research work in dairy sheep and goats. The older version was developed in 2015, and referred to as UAB bolus'15, in which a spring antenna was integrated and exceeded dimensional requirements for safe use in small ruminants [Oli+18]. A substitute antenna was therefore in need, which was planned to be integrated in the later bolus, UAB bolus'17, and be used for channel characterizations. The objectives of this doctoral thesis include:

- to devise an antenna with reduced form-factor and proper radiation performance at 433 MHz, for integration to a small ruminal bolus: UAB bolus'17.

- to characterize the in-to-out body radio transmission channel with regard to power levels, system range, and time-varying features.

- to propose a power-reduction plan for the ruminal bolus system.

The research work was divided into three parts: antenna implementation, theoretical channel studies, and in vivo channel studies. Computational electromagnetic (CEM) methods were used for the first two parts of research, including antenna parameterization, transmission scenario modelling, and related simulations etc. Moreover, tissue-simulating liquids were prepared for laboratory measurements, which were compared with the results from numerical analysis. A small antenna was fabricated and integrated into UAB bolus'17 for channel studies. In theoretical studies, attenuation profile of radio signal was described with canonical path loss (PL) models. The in vivo investigations were performed with a rumen-cannulated animal, under the permission of Ethics Committee on Animal and Human Experimentation, UAB. Behaviors of the radio channel were studied associated with the authentic

biological behaviors of the animal, and interpreted with PL in the time domain. The results were combined with the power profile of the system for power-reduction designs.

This thesis has involved collaborations among various groups in UAB and Ghent University, Belgium (referred to as UGENT). Although greatly benefited from resource and knowledge sharing, it is also important to define the limitations. First of all, component selection for UAB bolus'17, other than the antenna, was not the concern of this thesis, nor was any modification to those components. Besides, different radio frequency (RF) instrument that belong to various entities were used to carry out the measurements. Problems with instrument precision had certain influence on both methodologies and results, which could not be fixed with the accessible resources. Thirdly, the on-site studies were not designed to be or treated as quantitative research work. Therefore, the results are representative only within a limited group of animals under specific conditions.

1.2 Background knowledge

1.2.1 Using WBAN for health monitoring in dairy farms

Example of ruminal health monitoring platform

More and more modern dairy farms are embracing biotelemetric platforms to instantly gather health information of the livestock ruminants. Real-in-time detection of rumen abnormalities, such as abrupt and unprovoked changes in temperature and pH value, is considered indispensable, especially in high productive dairy farms [Limb; Zos+10]. Some prevalent chronic diseases among the ruminants, such as sub-acute ruminal acidosis (SARA), could result in staggering drop in production, impaired animal welfare, and high rates of involuntary culling.

A health monitoring platform for ruminant animals consists of a control centre, a gateway, and several individual WBANs. Basic elements in an individual WBAN are a ruminal sensing bolus and a receiving device, either be an on-body wearable receiver (RX) or a fixed receiver in the barn. The

ruminal bolus is scheduled to work at certain time intervals collecting bioclimatic data and sending out to the RX. Figure 1.1 illustrates an example of health monitoring platform in a WBAN-equipped modern farm[Gmb].

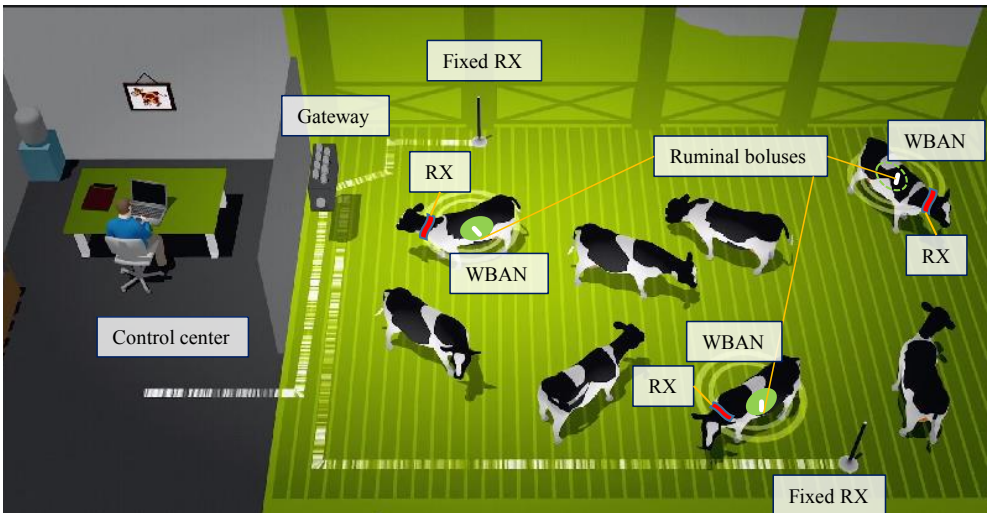

Fig. 1.1: Example health monitoring platform in a modern farm [Gmb]

Frequency considerations

A wide range of the free license industrial, scientific, and medical bands (ISM) are available. Among them, the 433 MHz band is one of the most widely used license-free radio bands throughout Europe [LKW05]. Besides, it has its merits for being very close to the Medical Implanted Communication Services (MICS) band (402 MHz-405 MHz), which has been well regulated Federal Communication Commissions and European Radio-communication Commissions. Consequently, abundant devices and research work using MICS band are available, which could serve as references for using ISM 433 MHz band in this doctoral thesis.

1.2.2 Basic rumen physiology

Unlike monogastrics, the stomach of an adult ruminant has four compartments that occupy almost three quarters of the abdominal cavity. The rumen is the first and the largest stomach compartment with an average capacity of around 180 liters for adult cows and 30 liters for adult goat. Inside the rumen, there are basically three layers: gas cap at the top, fiber mat of recently ingested feed, and more fluid-saturated roughage at the bottom. The

recent consumed feed is churned by rhythmic muscular contractions and later processed into more digestible substances through microbial fermentation. Usually, it takes more than one day for the consumed feed to move on to the second stomach compartment— the reticulum, which is located very close to the heart of the animal. Contractions in the reticulo-ruminal chamber are directly driven by the cardiac beats, which take place every minute. During rumination, such contractions repel the processed feed back to the esophagus for the ruminant to rematiscate. Large amount of saliva is added during the regurgitation[Mot; LMH57]. Figure 1.2 illustrates the internal structure of the reticulo-ruminal chamber, and the movement trails of the feed, which imply that dramatic changes to the composition of the reticulo-ruminal chamber would take place during digestive activities.

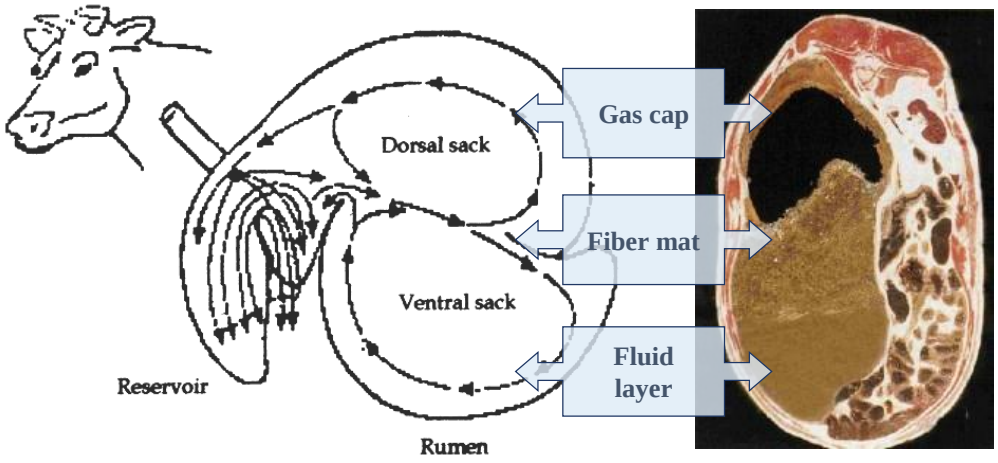

Fig. 1.2: Left view and rear view of reticulo-ruminal chamber composition and feed movement: (a) Schematic cross-sectional representation of the rumen and the reservoir (reticulum). The arrows indicate the movement of the contents. [C+97]; (b) Rumen anatomy [Mot]

1.2.3 Electromagnetic wave propagation in lossy mediums

High absorption of electromagnetic (EM) energy would take place when the radio signals propagate in lossy mediums, which refer to the ruminant's body and ruminal contents in this thesis. The body of ruminant animals consists of many biological tissues and organs, such as muscle, fat, and blood etc. As Gabriel et al. indicated in their research, different tissues and organs

have different dielectric properties which are frequency dependent [GGC96; GLG96a; GLG96b]. Table 1.1 lists the relative permittivity (denoted as ϵ_r) and conductivity (denoted as σ) of some common biological tissues as concluded in [Nik+17].

The dielectric properties and penetration depth in the desired frequency band strongly depend on the water content of these tissues [SF80], which are reported to be in between 70% and 80% [RTR97]. Besides the biological tissues and organs, large amount of radio signal is absorbed by the ruminal contents– mixtures of feed and ruminal liquid, whose water content increases from around 85% in fiber mat to 95% in fluid layer at the bottom of ventral sac due to gravity [Lavb].

Aside from absorption losses, the EM waves also suffer from reflection losses when propagating through the interface of mediums. Such losses would increase when there is a high contrast in the dielectric properties between the mediums, which further decreases the transmitted power. To evaluate the total loss of power from the bolus antenna to the RX antenna, characterization of the PL is essential for channel studies.

Tab. 1.1: EM properties of biological tissues at 434 MHz for some implantable (top) and ingestible (bottom) cases [Nik+17]

Tissue	ϵ_r	σ (S/m)
Fat (lowest overall values)	11.6	0.08
Grey matter	56.8	0.75
While matter	41.7	0.46
Muscle	56.9	0.81
Lung (inflated)	23.6	0.38
Highest overall values	77.3	2.26
Stomach	67.2	1.01
Small intestine	65.3	1.92
Large intestine	62.0	0.87
GI average(cite)	63.0	1.02

1.2.4 Methodologies for channel studies

Computational electromagnetic

Computational electromagnetic (CEM) methods consist of a number of different techniques, all of which utilize computational resources to solve Maxwell equations over large or complex physical objects, either in the

frequency domain or in the time domain. The physical objects are modelled with adequate small geometries. Each CEM method has its specialized application areas considering the dimension of the objects and the computational cost. Multiple methods may be required to solve complex problems. Figure 1.3 demonstrates the most common CEM methods and their specialized application areas.

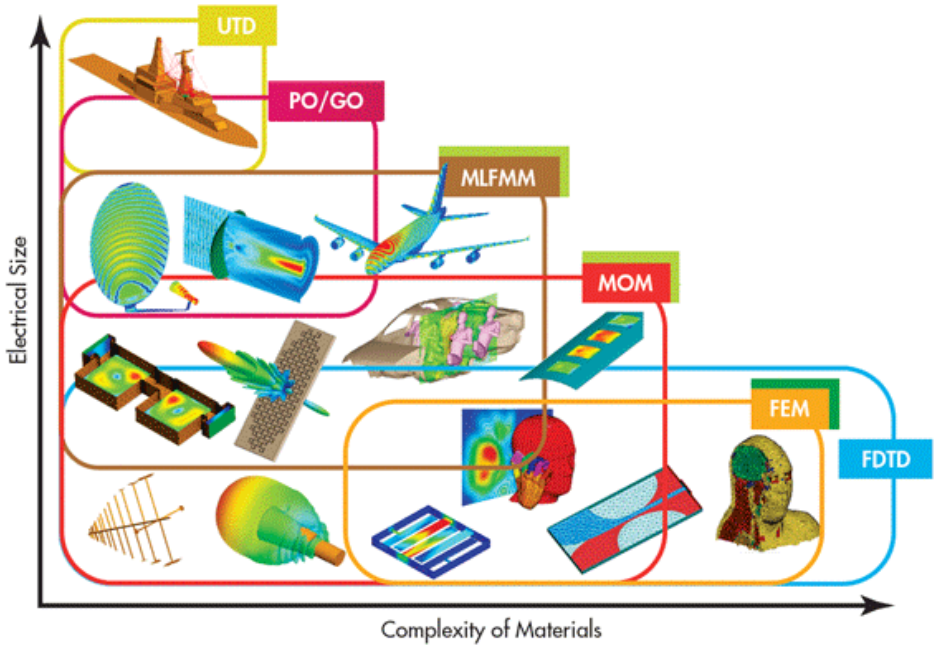

Fig. 1.3: Common CEM methods and their applied areas [DeL; LJ13]

In this thesis, two CEM tools were used for antenna implementation and theoretical channel studies. FEKO (Altair, Michigan, USA), which mainly uses the Method of moment (MoM), was the tool for antenna implementation. Sim4Life (Zurich Med Tech, Switzerland), which employed finite difference time domain method (FDTD), was used for modelling and simulating the in-to-out body radio transmission.

Measurement with bio-equivalent phantoms

In many cases, to avoid using living tissues for radio transmission experiments, liquids that emulate dielectric properties of body tissues at a certain frequency range are used to build up bio-equivalent phantoms. They can help to quantify the interactions between the biological body and the electromagnetic field

[Ito+01]. For the convenience of measurement setup, simple phantoms have been desirable, usually in the form of homogeneous liquid [FFC16].

In vivo studies

Unlike the studies of wearable medical devices, more challenges and concerns are raised around in vivo studies of implant and ingestible medical devices. These studies are usually conducted with animals [Lee+11; Flo+15]. However, ethnic issues with animal experiments are also of great importance, which obliges approval from related ethics committee of each institute or organization.

1.3 Structure of the thesis

The thesis is organized into seven chapters, with current chapter being the first one, which starts with introducing the motivations and essence of thesis, followed by background knowledge in rumen health management, rumen physiology, EM wave propagation in lossy mediums, and methodologies for channel studies.

Chapter 2 reviews the research advances in WBAN with respect to ruminal bolus device development, antenna for ingestible devices, and channel studies etc. Many existing studies are involved and discussed, which contribute to the research methodologies of this thesis work.

Chapter 3 to 5 present the major research work of this thesis, in the order of antenna implementation, theoretical channel studies, and in vivo channel studies. In each of these chapters, essential work, the obtained results, and discussions are presented. Besides, an introduction and a summary for each chapter are also provided.

Chapter 6 draws conclusion of the thesis while the future work are suggested in the last chapter, Chapter 7.

Literature review

2

> *It is best to learn as we go, not go as we have learned.*
>
> **— Leslie Jeanne Sahler**

This doctoral thesis involves multidisciplinary knowledge and experiences, which could be categorized into three major sections (as the organization of the thesis): antenna implementation, theoretical channel studies, and in vivo channel studies. A review of ruminal bolus solutions is first provided that defines the focus and problems. Since very few research work have been dedicated to the antenna and radio channel of ruminal boluses, reference in antenna design and theoretical channel studies for the implant and ingestible applications are presented. Besides, concepts in dynamic channel modelling are introduced to help define the goal of the in vivo channel studies. In addition, measurement set up and execution for in vivo radio channel characterization with animals are discussed.

2.1 Ruminal sensing boluses

2.1.1 Introduction

Before being used for monitoring the bioclimatic data, ruminal indwelling boluses were first proposed for electronic identification of the livestock ruminants [Han76][CLF94]. Such **identification boluses** usually have a capsular shape casing made of biocompatible materials, and could be administrated orally with a balling gun. With the proper size, material, and operation skills, these boluses would retain in the reticulum without causing inconvenience to the animals. Dimension of these devices should be adequate to the size of the ruminants considering the safeness and suitability of lifelong retention [Caj+99; Car+10]. The identification boluses usually work at low frequency (30-300 kHz), for example, 134.2 kHz [Caj+99], and

coil inductors are used as radiators. All these research work and practices on identification boluses have paved the way for integrating biosensors to the indwelling ruminal boluses.

Ever since the pioneering prototypes [Mot+08] to recent commercial products [Gmb], **ruminal sensing boluses** have inherited the appearance and administration method from the identification boluses. Unlike their predecessors, the ruminal sensing boluses have higher requirements on transmission data rate, which would only be possible with larger bandwidth [Poo+15]. Meanwhile, link viability over large amount of lossy tissues as well as strict constraints on device dimensions also need to be evaluated [Wan+17].

It is discovered that most of the existing ruminal boluses, both commercial products and prototypes for research, work at sub-G Hz radio bands. As a consequence, the components and electronic circuitry for ruminal sensing boluses would be quite different from those of ruminal identification boluses. Besides the biosensors, an microcontroller unit (MCU), a specific radio transmitter or transceiver, an antenna, and a battery are indispensable [Mot+08; Zos+10; Nog+17]. Table 2.1 lists several traceable ruminal boluses. In the rest of this section, reviews of the key aspects, including RF band, dimension, antenna selection, cell range, and shell life etc. are provided.

Tab. 2.1: List of existing ruminal sensing boluses (with commercial bolus products on the top and bolus prototypes in research papers on the bottom)

Bolus	Origin	Frequency	Diameter × Length	Range	Source
eCow	UK	432 MHz	27 mm × 135 mm	n/a	[Mot16]
Kahne	NZ	433.9 MHz	27 mm × 145 mm	0.5-30 m	[Lin09]
smaXtec	AT	Sub-GHz configurable	35 mm × 132 mm	n/a	[RF16]
WellCow	UK	433.92 MHz	32 mm × 145 mm	n/a	[Mot+08]
Nogami	JP	315 MHz	30 mm × 70 mm	3 m	[Nog+17]
Sato	JP	429 MHz	30 mm × 145 mm	32 m	[Sat+12]
UAB'17	ES	433.04 MHz	22 mm × 80 mm	2 m	[Wan+17]
Zosel	DE	868 MHz	36 mm × 195 mm	3 m	[Zos+10]

2.1.2 Key aspects of the ruminal sensing boluses in terms of wireless transmission

1. RF band

Most of the ruminal sensing boluses in Table 2.1 work at lower sub-G Hz RF bands. As indicated by Mottram et al. in [Mot+08], the researchers of WellCow bolus chose 434 MHz over 868 MHz after comparisons of the system performance. Besides, the ISM 433 MHz band has larger worldwide acceptance, compared to other sub-G Hz ISM bands [LKW05]. However, it is worth noting that the solution of smaXtec bolus has enabled band selection, which would make their boluses globally applicable [RF16].

2. Device dimension

Besides UAB bolus'17, all of the other boluses have much bigger dimensions and are designed for cows, especially for cows over 18-month old, as indicated in [Gmb]. The bolus for adult sheep and goats is only about 30% in volume of those for adult cows [Oli+18], which reflects the noticeable difference in body size among ruminant animals. Figure 2.1 demonstrates such difference in device dimension [Wan+17]. Caja et al. emphasized that the bolus size for small or young ruminants is more critical since oversized bolus may affect rumination process, which would result in changes in digestibility of the diet [Caj+99]. Therefore, device dimension is the primary concern when devising a ruminal bolus for small ruminants.

3. Antenna selection

Antenna selection for these boluses is seldom discussed or even mentioned in existing literature. Besides the UAB boluses, to the author's knowledge, the Nogami bolus uses a wire antenna [Nog+17], the WellCow bolus uses a spring antenna [Mot+08], and the smaXtec bolus uses a meandered printed circuit board (PCB) antenna [RF16]. However, detailed information about these antennas is not available. As one of the most important criteria to determine system performances, more attention and efforts are needed on the bolus antennas, especially on those for small ruminants. Downscale devices would bring in more restrictions on the electrical length of the bolus antenna, which is directly related to its radiation efficiency. Repetitions in antenna design and evaluation are crucial to improve link viability [Nik+17]. More details about antenna selection is provided in the next section.

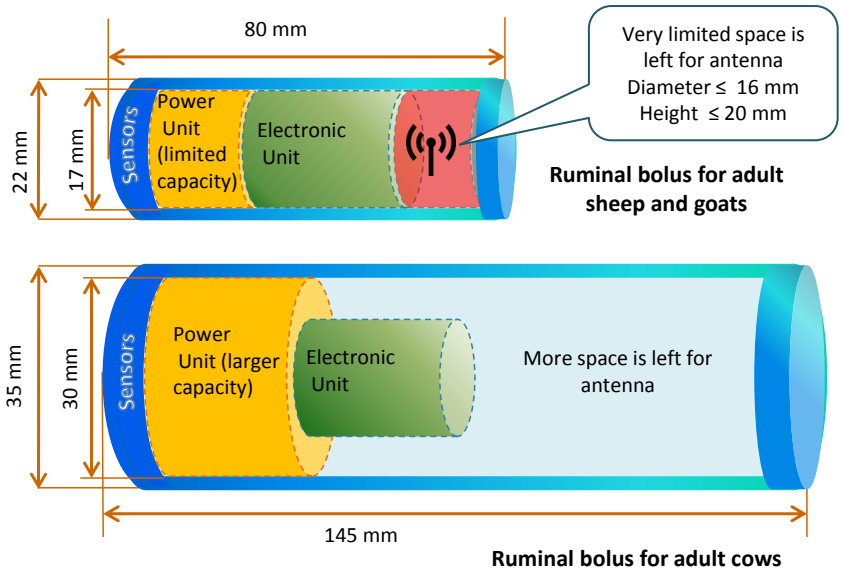

Fig. 2.1: Difference in dimension restrictions between bolus for large ruminants and bolus for small ruminants [Wan+17]

4. Cell range

The reported cell range of these boluses have demonstrated a great variation. As mentioned by the manufacturer of Kahne bolus, whose reported system coverage is from 0.5 m to 30 m, the gut fill would affect signal reception [Lima]. Besides the gut fill, the transmit power, the RX, the environment, and the measurement setup would also have their respective influences on the cell range. Thereby, the data of system range listed in Table 2.1 cannot be solely used to evaluate these boluses.

5. Shell life

Shell life of these boluses are not listed since it depends on multiple factors, such as the duty cycle, the transmit power, and the battery capacity etc. However, it is unquestionable that longer shell life is always preferred since the ruminal boluses cannot be retrieved once administrated. Currently, the majority of the ruminal sensing boluses are powered by lithium-ion battery units [Mot+08; Sat+12; RF16]. Consequently, shell life of the ruminal bolus is directly determined by the battery life, which is not rechargeable. For small-sized ruminal boluses, battery capacity is further restricted by the dimension, which makes the shelf life an even bigger challenge to their acceptability. Besides optimizing the components and system configuration, researchers are also working on introducing new materials and new technologies to

prolong the shell life of indwelling devices. One of the most popular trends is recharging the bolus through wireless power transfer [Min+18].

2.2 Antennas for ingestible devices

2.2.1 Introduction

Regarding the insufficiency of research work on bolus antennas, antennas used by wireless capsule endoscope (WCE) devices are reviewed in this section, since there are many similarities between ruminal sensing boluses and WCE devices [Lee+11][Wan+12][Nik+17].

The first WCE device, with a diameter of 11 mm and a length of 26 mm, was reported to receive American Food and Drug Administration clearance in 2001 [Idd+00]. Since then, WCE devices have been spreading out globally with success [Wan+12]. Until today, opportunities and challenges in WCE antenna design have been discussed comprehensively [NRR07; Lee+11; Nik+17]. As stated by Norris et al., the antennas for the implant (or ingestible) devices that work at sub-G Hz bands would always be "electrically small", which means that the antenna size would be much smaller than a quarter wavelength [NRR07]. Consequently, both the radiation efficiency and the resonant bandwidth would be restricted. Besides, the other encapsulated components and the body tissues would affect the antenna performance significantly [Nik+17]. As a result, careful considerations are necessary for antenna design, including the actual encapsulation condition and the radiation environment.

2.2.2 General considerations on antenna for ingestible devices

1. Dedicated space for the antenna

Form factor of the antenna depends on requirements from the target applications [Rem98]. The space that could be utilized by the antenna should be specified at the component planning stage [Mer+11; Nik+17].

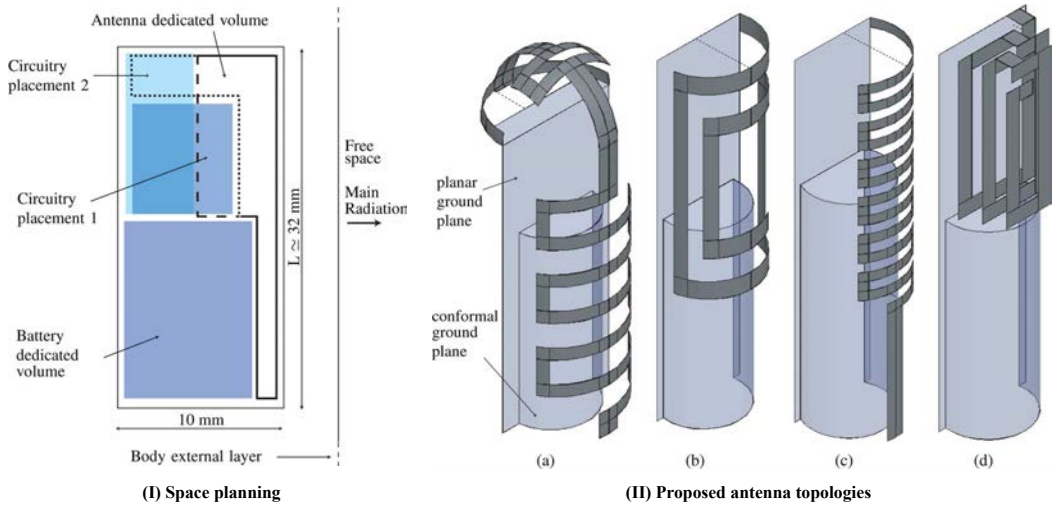

Fig. 2.2: Space planning and antenna typologies for a WCE device [Mer+11]

Merli et al. began the antenna design for a WCE device with space planning of the major electronic components inside a cylinder capsule. Based on different placement methods, four antenna typologies were proposed, as shown in Figure 2.2 and evaluated, with regard to resonant frequency, gain, directivity, and radiation efficiency etc. [Mer+11].

2. Compound vicinity environment

Radiations take place in a compound environment. In the direction of wave propagation, such compound environment consists of the electronic components inside the capsule, the background medium inside the capsule, the capsule, the digestive contents, and the body tissues etc [AH09; Mer+11; LGX14; Nik+17]. Considering their respective physical dimensions, all of these mediums and components could be regarded in the near field of the ingestible antenna through an estimation of the wavelength in the environment [SAH09].

The **digestive contents** inside the human stomach include small particles of food and chyme. In the case of ruminant animals, their reticulo-ruminal chamber can store large amount of undigested feed and liquid. Water content inside either human stomach or reticulo-ruminal chamber could be higher than many other organs [GGC96; RTR97; Lavb], which would result in higher losses during the wireless transmission[SF80]. Experiments of Kahne bolus suggested that cell range of the ruminal bolus is closely related to gut fill, which was measured to be in the range of 0.5 to 30 meters [Lima]. To characterize the influence from digestive contents on signal attenuation, Alomainy et al. suggested using the dielectric parameters of small intestine

to emulate a "full stomach" scenario [AH09].

Wang et al. indicated that larger attenuation would be expected when there is a dramatic difference in the dielectric properties of the transmission medium [WW12]. Among the aforementioned medium and components, the **encapsulated medium** is usually air [Lee+11; Sat+12; Nog+17; Wan+17], which has very different dielectric properties from that of digestive contents or body tissues [GGC96]. Nikolayev et al. suggested that filling the capsule with solid materials of high permittivity and low loss, such as ceramic-powder-loaded polymer [Kou+06] or epoxy [Lee+07], would reduce the attenuation and improve the radiation efficiency [Nik+17]. Besides the capsule filling, they also suggested that using high permittivity and low loss **material for encapsulation** would help to decouple the antenna from surrounding tissues. In their research work, they chose a biocompatibe, low cost and commercially available material 99.7% Al_2O_3 for the capsule [Nik+17]. Other encapsulation materials, such as polymer-ceramic, have also been proposed [Kou+06].

Besides the mediums, the **proximity to electronic circuitry boards** would also affect the antenna's performance. This topic is much less discussed in existing research work, especially those targeted on theoretical studies of the ingestible antennas and transmission channels for WBAN applications [AH09; SAH09; Rom+14]. However, when a real device is concerned, the influence from the adjacent electronic component on the antenna would need to be examined and evaluated. This is because both the resonant frequency and the return loss would be altered, which should be taken into consideration at the beginning of antenna selection and design [Pis+13; PT15; Wan+17]. Some common solutions to verify the robustness of an antenna model considering other electronic components include modelling those components into a perfect electrical conductor (PEC) cylinder for CEM analysis [Mer+11][LGX14][Nik+17], adding a PCB sheet that has the same dimension as the real electronic circuitry to the antenna model for laboratory measurements [Wan+17].

3. Bandwidth

Considering the complexity of the in-body environment, which is composed of different types of body tissues and mass watery digestive contents, the antenna should have enough bandwidth to be insensitive to the lossy mediums [Lee+11; Wan+12; Nik+17]. Lee et al. devised a planar spiral antenna which worked at 500 MHz with a reported bandwidth of over 100

MHz. Meanwhile, it should be noted that there is a trade-off between the bandwidth and radiation efficiency. Nikolayev et al. presented a rough estimation of the antenna's theoretically maximum radiation efficiency with a given bandwidth, which indicated that the narrower the bandwidth, the higher the achievable radiation efficiency [Nik+17]. In order to achieve a balance between bandwidth and radiation efficiency, some researchers examined the range of antenna's resonant frequency when setting different body tissues as background medium [Aug09; SCQ16]. According to Nikolayev et al., whose antenna also targeted on ISM 433 MHz band, a bandwidth of 17 MHz (when $|S_{11}| = -10$ dB) would be sufficient [Nik+17].

4. Radiation pattern

Antennas for either WCE devices or ruminal boluses would be more susceptible to impedance detuning compared to antennas for implant devices. This is because the ingestible antennas work in a dynamic environment: their exact location and orientation are less observable and always on the change. Accordingly, composition of the surrounding medium would be varied and less predictable, that is, through different tissues and contents in the digestive organs[Nik+17]. Therefore, an isotropic radiation pattern is recommended [Lee+11; Nik+17]. On the contrary, for implant antennas, enhancement of directivity towards the desired transmission path is preferred since power absorption in body tissues would be reduced accordingly [Mer+11].

Nikolayev et al. also proved with a 3D human model in CEM simulations that the radiation pattern would strongly depend on the location of the antenna inside the body: the closer it is to the surface, the less directive it would be. For deep in-body locations, the radiation intensity is related to the closeness to body surface [Nik+17].

2.2.3 Example ingestible antennas

An extensive review of the antennas for WCE devices that work at MICS and ISM 433 MHz bands is provided by Wang et al., in which they categorized the existing wireless capsule antennas into two groups based on the structure: **wire antennas** in loop structure and the **conformal antennas** that are designed to wrap up along the shape of the capsule [JP06; Wan+12]. For wire antennas, a very common allocation method is through spirals. A research group from Yonsei University, Korea, devoted to improving the performance of small spiral antennas for WCE devices by constructing the spirals into various

planar and spatial structures [KCY05; LCY07; Lee+08; Lee+11]. The concept to better utilize the space inside the capsule has led to the development of conformal antennas. Merli et al. presented their efforts to evaluate several typologies of conformal antennas for an implant capsule[Mer+11]. More recently, an in-depth study on a conformal antenna that works at ISM 433 MHz band was conducted by Nikolayev et al. [Nik+17]. In this part, some of these antenna typologies are reviewed.

1. Wire loop antennas in planar and spatial spiral structures

As concluded in [Wan+12], four different structures of spiral antennas that resonate around 400 MHz to 500 MHz and suitable for cylindrical capsules were proposed. Figure 2.3 shows the antenna models in CEM tools. All of these antennas have employed the single-arm Archimedean spiral structure and a round ground plane. Antenna (a) and (b) are backed by dielectric materials, which is not the case in antenna (c) and (d). The researchers targeted on increasing the electrical length of the wires through utilizing the space. Return loss and azimuth radiation pattern of these antennas were examined respectively, which exhibited an orderly improvement. However, to the author's knowledge, only antenna (a) and (d) were fabricated.

According to the measurement results obtained with the same bio-equivalent phantom, antenna (a) has reached a return loss of -30 dB at 470 MHz with a bandwidth of 70 MHz at -10 dB [KCY05]; while antenna (d) resonated at 500 MHz with S_{11} = -25 dB and the bandwidth was increased to 104 MHz at -10 dB [Lee+11]. The fat-arm structure of antenna (d) was designed to further increase the bandwidth to cope with the impedance detuning from the movement of the WCE device through different gastrointestinal tract tissues [Nik+17]. However, increasing the bandwidth would be repaid by reduced radiation efficiency [Bes06]. A balance between the bandwidth and radiation efficiency should be obtained.

2. Conformal antennas

The second group is the conformal antenna. Merili et al. studied four antenna typologies for an implant device at both MICS band and 2.4 GHz as shown previously in Figure 2.2. Three out of these four antenna models were of conformal structure. After comparison of the antennas' performances, the non-conformal one was selected since it has the best directivity and the highest radiation efficiency [Mer+11], which reflects the different considerations in antenna performance between implant and ingestible devices.

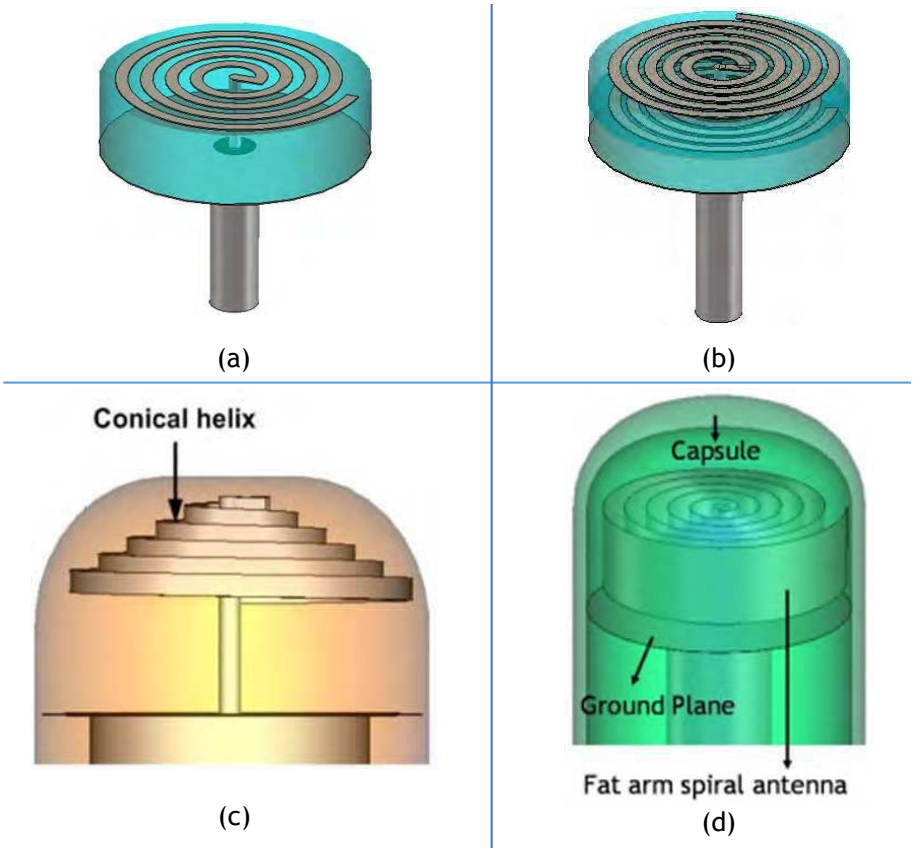

Fig. 2.3: Example spiral antennas for cylindrical capsules: (a) sing-arm planar spiral antenna [KCY05] (b) dual layered single-arm planar spiral [LCY07] (c) single-arm conical spiral antenna [Lee+08] (d) fat single-arm spiral antenna [Rom+14]

Nikolayev et al. designed and implemented a conformal antenna that works at 433 MHz as shown in Figure 2.4. This antenna shows better performances than all the aforementioned antennas. First of all, it was more closely matched to 50 Ohm, which provides higher chance of not being dependent on the PCB. Next, it was examined with capsules of different diameters and the frequency shift was acceptable. Besides, it has a more omnidirectional radiation pattern than the wire antennas [Nik+17].

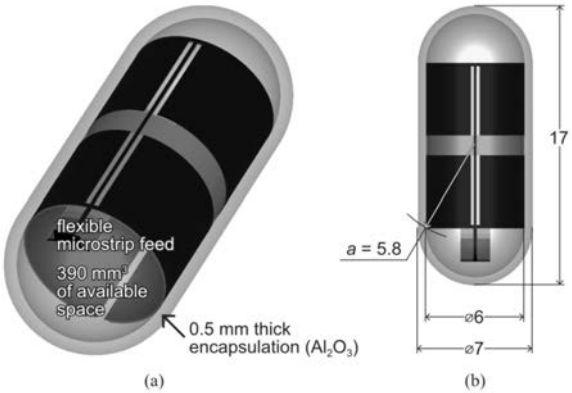

Fig. 2.4: Conformal antenna proposed in [Nik+17] (a) Antenna within an alumina capsule. (b) Capsule dimensions and antenna circumradius

2.3 Theoretical channel studies

2.3.1 Introduction

As it has been revealed in the previous sections, in-body wireless communications will undergo severe signal decay when propagating in the in-body environment [Wan+12; Gar+18]. The received signal is the superimposition of several replicas of the transmit signal with different levels of attenuation, delay, and distortion. Moreover, the dominant channel characteristics would vary for different wireless transmission scenarios [WW12]. Therefore, a proper prediction of the radio channel's characteristics is essential, since it helps to understand the influence from in-body environment and the incurred energy loss during propagation [Kur+11; Sta+16; Gar+18]. Channel study is considered the first step to explore the body area communications and to investigate on an adequate communication system [WW12].

Theoretical studies of the channel, which could trace back to fundamental EM theories would permit a explicit modelling of the channel in a specific scenario [YS10]. Usually, one of the channel output parameters, such as the received signal level, is selected as the channel index, whose probability level is studied in a given scenario [CDO14]. PL models are thus derived from studying the probabilities of the received signal level. Such models can

reflect the dielectric properties of the transmission channel, the separation distance between TX and RX (denoted as TX-RX in this thesis), and antenna positions and orientations etc. [WW12]. Meanwhile, it should be noted that the channel statistics in theoretical PL modelling is considered as "wide sense stationary" [CDO14]. An adequate PL model can help to calculate the link budget, which testifies the link viability of the target transmission channel. Theoretical channel study is indispensable and crucial before system installation or experiment with a living object, which is of special importance for WBAN applications that involve in-to-out body transmissions.

In this section, the theoretical channel studies are generated into two parts: PL modelling and link budget calculation. The review of theoretical channel studies corresponds to Chapter 4 of the thesis.

2.3.2 PL modelling

Both numerical analysis and laboratory measurement with bio-equivalent phantoms are the common research methodologies for PL modelling. Human 3D heterogeneous models have been widely used in CEM simulations to investigate on PL between an implant and ingestible devices and a wearable receivers [AH09; Rom+14; Sta+16; Nik+17]. Besides an accurate representation of the anatomic structures and dielectric properties of various tissues, different models are developed to emulate human beings of different genres, ages, and body sizes etc. [Rom+14]. The results from numerical analysis are usually compared with those obtained from laboratory measurements. 3D animal models that could be adopted by CEM tools are very limited. To the author's knowledge, there is no adequate model for either big or small ruminant.

Laboratory evaluation with bio-equivalent phantoms are also prevalent [YH10; SCQ16; Wan+17; Nik+17], even though most of these phantoms are homogeneous Garcia et al. reported that some researchers might have a different opinion over using tissue-simulating phantoms [Gar+16], who questioned the reliability of the measured results. In the author's opinion, both numerical method and measurement with phantom should be performed if possible.

The computed and measured PL data are both plotted against TX-RX. Some

of the results were fitted in a semi-log plot [SAH09; Wan+17] while others were fitted in a linear plot [Rom+14; Sta+16; SCQ16]. In the author's opinion, such difference might be originated from system setup, measurement environment, as well as different materials and components. According to See et al., divergence between simulated and measured result could be reduced by adding more objects that exist in the measurement environment to the simulation environment [SCQ16]. They also pointed out that using network analyzer for laboratory measurements might lead to inaccurate results since the network analyzer would take into account more noises in the measurement environment. As a result, they changed to spectrum analyzer in their work [SCQ16]. Similar situation has been encountered by the author in the research work of [Wan+17].

2.3.3 Link budget

As explained in [Ara08], link budget is to balance the power levels for a minimum system performance. A list of all the power levels, noise components, gains, and losses in the system is the foundation for link budget. Depending on system design goals and requirements, the items in the same physical model could have different values.

In the work of Stango et al. about the in-to-out body MICS link for upper limb prostheses [Sta+16], they evaluated the link budget between an implant antenna and an on-body receiver using FDTD methods. Taking reference from International Telecommunication Union (ITU) standard and recommendations on MICS applications [Rem98][Ass+08][YS10], the effective isotropic radiated power, the noise figure, and the signal-to-noise ratio were set to be -16 dBm, 10 dB, and 5 dB respectively, from which the receiver sensitivity was derived. The resulted link margin was 11 dB. To further improve the link viability, they pointed out that increasing transmit power might not be the desired solution since it would raise concerns about biosafety under radiation and increase battery consumption. Instead, they suggested that the link margin could be improved by optimizing the gain of both TX and RX antennas, such as altering their orientations, and changing modulation scheme.

In the work of Sani et al. on in-to-out body MICS link [SAH09], they chose the noise power to be 20 dB above the thermal noise level, as suggested in ITU's standard [Rem98]. As a result, the other noise component, such

as signal-to-noise ration and noise figure, were not needed for link budget calculation.

In the work of Johansson et al., budget for both the uplink and downlink were analyzed. Even though the items in the system were more or less the same, they were attributed with different characteristics in the two directions of data transmission. Besides, in their work, they suggested a noise figure of 4 dB and a fade margin of 10 dB for implant applications at MICS band [Joh04].

2.4 WBAN channel studies considering time-variant characteristics

2.4.1 Introduction

For both WCE devices and ruminal boluses, composition of the in-body environment is more complicated than that of implant devices: besides various layers of body tissues, contents inside the digestive organs should also be considered. In addition, this in-body environment is time-variant since: 1) the ingestible device is moving inside the digestive organs [Sat+12; Nik+17]; 2) body movements of the target object in the normal status would alter the radio transmission paths inside the in-body environment [WW12]; and 3) digestive processes would bring in changes of dielectric properties inside the organs [AH09]. As a result, besides the parameters employed in theoretical channel studies for static scenarios, more time-variant features are needed to describe the channel's dynamic behaviors. To the author's knowledge, a majority of the reported work in this area are only for on-body wireless transmissions, which might have different focus and methodologies from in-body transmissions. However, it is believed that the concepts elaborated in the research work of on-body dynamic channel would be helpful to investigate the dynamics of the in-body environment. Moreover, understanding the time domain characteristics of the digestive processes is also crucial for a proper design and analysis of in vivo investigations.

2.4.2 Dynamic channel studies for WBAN radio links

1. Characterization of dynamic WBAN channels through measurements

David et al. provided an in-depth and forward-looking review of propagation models in WBAN [Smi+13]. They pointed out the limitations of the static channel models. First of all, the static channel models solely relying on propagation distance and PL exponent to describe channel behaviors. However, body postures, and amount of body movements, in "everyday activities" would be varying, and would result in different transmission scenarios. In addition, considering the transmission channel dynamically would also break the commonly accepted viewpoint of categorizing the WBAN channels to be either line-of-sight (LOS) or non-line-of-sight (NLOS), which would lead to stereotyped channel modelling. They argued that the more appropriate way is to obtain the rate of the major changes in the radio link, conduct measurement-campaigns accordingly, and describe PL in the time domain using statistical methods. They also introduced second-order statistics to describe the channel's behaviors, including **power delay profile**, **average fade duration**, **coherence time**, and **cross-correlation**. In the case of characterizing the in-body channels, they commented that there are fewer canonical models for in-body communications than for the on-body and off-body wireless transmissions. In terms of describing the dynamic features of the in-body wireless transmission environment, the methodologies used in external body channel modelling might not be applicable since the in-body environment would include various additional components [Smi+13]. However, the concept of estimating the speed of changes in the target environment, and introducing time-variant parameters to statistically model dynamic channels enlightened the in vivo investigations of this thesis work.

2. Characterization of dynamic WBAN channels through numerical methods

Some researchers demonstrated the propagation characterization of dynamic communication channels through numerical simulation.

Gallo et al. combined the animation software and CEM simulation tools to

characterize channel fading in the on-body WBAN channel at 2.45 GHz when the body posture is changing. They pointed out that channel fading, caused by body movements in a scattering environment, can be categorized into long-term fading and short-term fading [Gal+11]. The former one originates from changes of the relative position of different body parts while the latter one is caused by the multipath interference. They used animation tools to extract dozens of frames for a single body movement and performed CEM analysis to all of these frames respectively with considerable repetitions. In this way, small changes of the on-body channel in a dynamic scenario could be approximately obtained, from which Gallo et al. deduced long-term fading characteristics. It should be noted that the human body models used in their research work are homogeneous models and the dielectric parameters of the skin tissue at 2.45 GHz were assigned to the model. Comparisons between homogeneous models and heterogeneous models with the same posture in static scenarios were made, which revealed that the internal structure of the human body would make a difference of 8 dB in PL for some of the on-body transmission scenarios [Gal+11]. However, it would take extra effort to export heterogeneous body models to animation tools for frame extraction. Since the 3D heterogeneous models of ruminant animals either for animation or for CEM analysis are still at a very primitive stage, it is not realizable to analyze the dynamic channel numerically.

2.4.3 In vivo investigations of WBAN radio links with animals

In vivo characterization of WBAN radio links is widely considered the most effective method to understand the channel's behaviors [Hu+07; WW12; Smi+13; Flo+15]. For in-to-out body communications, measurements with animals are usually performed, in which the animals could either be substitute of human body [Lee+11; Flo+15] or the targets for the studies [Sat+12; Nog+17]. In this part, the focus is more on the measurement setup and execution rather than the channel study methodologies.

1. Using animals as surrogates of human beings in WBAN channel studies

Considering the similarities in tissue's dielectric properties[GGC96], some

researchers chose to use small sized living pigs as surrogates of human bodies for in vivo studies of the WCE devices [Lee+11; Flo+15; Gar+16]. The work of Lee et al. focused on antenna design and evaluation for WCE devices at around 500 MHz. They integrated a proposed antenna to a small WCE prototype device, and inserted it to both the stomach and the intestine of an anesthetized pig through the mouth or the anus. The receiving antenna was placed on the surface of the pig's body. Return loss and received power were examined with a network analyzer, which showed various differences compared with the laboratory measurement results with a homogeneous phantom[Lee+11]. The exact locations of the WCE prototype device were not mentioned. Nor did the measurement environment, where the influence from the surrounding objects and ground were thus undetermined.

Garcia et al. developed PL models of ultra wideband communications from 3.1 GHz to 10.6 GHz via in vivo measurements with a pig under a general anesthesia. Laparotomy was performed to fix the implant device at desired locations inside the abdominal cavity. Two scenarios were considered: in-to-out body and in-to-off body. The receiving antenna in the in-to-out body scenario was moved along the body surface; while in the in-to-off body scenario it was moved away from the body. Electromagnetic tracking device was used to calibrate the TX-RX, which ranged between 3 cm and 10 cm for in-to-out body and between 5 cm to 50 cm for in-to-off body. PL was measured with a network analyzer and plotted against TX-RX for both scenarios. In the case of in-to-out body, PL was fitted by linear approximation; while in in-to-off body case, a log-distance model was developed [Gar+16].

Although derived from in vivo studies, these models could hardly demonstrate the dynamic features of the in-to-out body radio channels since the pigs were in anesthesia. If the pigs were in their normal status, using network analyzers to assess the PL might not be realizable since the cables would affect body movements. In addition, in a real in vivo situation, obtaining accurate TX-RX values would not only be less possible but also of less significance, since it would give way to other time-variant parameters as the dominant channel characteristics [WW12].

3. Animal targeted WBAN channel studies

Benaissa et al. investigated the off-body radio channels with dairy cows wearing commercial devices in a farm [Ben+16]. They built up a log-distance PL model for analyzing large-scale fading. In addition, they performed intensive measurements for 10 minutes to generate a statistical distribution of

the temporal fading. Even if off-body scenarios are usually more predictable than in-body wireless transmissions, their research could be regarded as a good example for in vivo investigations of the in-body wireless channels using dairy cows in a farm.

H. Nogami et al. also designed a wireless ruminal bolus and tested it with a cannulated cow in a barn [Nog+17]. The RX was placed in front of the cow about 2 meters away for continuous recording of the rumen temperature, bolus movement, and packet reception rate. Significant differences in the bolus movement between active and idle modes of the digestive system have been discovered. Moreover, they reported that the packet reception rate was greatly worsened when the cow was in sitting position in its stall, which accounted for less than one-quarter of time during their three-day continuous observation. Although it is widely believed that cows would normally spend much more time in sitting posture [Limb], the research of H. Nogami et al. has reminded us that digestive activities and body posture might have certain impacts on the in-body radio channels between a ruminal bolus and an external receiver.

2.5 Summary

This chapter provides extensive reviews of a majority of the involved topics in this doctoral thesis. Through analyzing existing research work and solution, research direction of this thesis became clearer. Devising a small antenna for UAB bolus'17 was the primary task and meeting dimensional requirements was considered more crucial than improving antenna performance. With this small antenna, research work to characterize the in-to-out body channel between UAB bolus'17 and an on-body receiver could be launched. Theoretical channel studies could provide an estimation of the radio channel's behaviors, in terms of signal attenuation profile, and the required power level for a minimum system requirement. In vivo channel studies observed the channel's time-variant features in an original scenario, in which random changes take place and make the channel more variable. A concise and practical channel model that could account for various channel features is the desired radio solution that this doctoral thesis pursued.

3 Implementation of the bolus antenna

> *An error does not become truth by reason of multiplied propagation, nor does truth become error because nobody sees it.*
>
> **— Mahatma Ghandi**

This chapter presents the implementation of the small spiral antenna for UAB bolus'17, including antenna modelling, parameterization, fabrication, and verification. The aim of devising this antenna was to give life to UAB bolus'17, the foundation of a series of research work on small ruminal boluses for sheep and goats. The antennas integrated in previous UAB bolus were neither customized for use in in-body environment nor able to meet the dimensional requirements. Achieving compact design was therefore of primary concern. Besides, the vicinity environment, as well as fabrication requirements, were taken into account during antenna design. The design goal was achieved after two fabrications.

3.1 Introduction

The antenna is a crucial component for ingestible devices. First of all, it must comply with the strict dimensional requirement, which would limit the radiation performance. Moreover, multiple factors would need to be considered in antenna design, such as the in-body environment, the bandwidth versus radiation efficiency, the directivity, and the matching etc. Besides, when the research work leads to production, the antenna would need to be "fabrication friendly", so that all the desired geometric parameters could be implemented accurately. In addition, more challenges would be brought in when the target electronic circuitry is not a standard product, which is very common in real application cases. In short, repetitions in design and fabrication are indispensable to obtain an adequate antenna [SA16].

For this doctoral thesis, the primary task was to seek a suitable antenna

for UAB bolus'17, so that studies of the radio transmission channel based on ruminal boluses for small ruminants, which used to be a blind field, could commence. Therefore, the desired antenna should be compact in size, suitable for ingestible application, and easy to be fabricated. Besides the strict constraints in dimension, the radiation environment, which consists of compound mediums, need to be characterized properly. Utilizing the computational electromagnetic (CEM) methods, both geometric parameters and dielectric parameters for each of the component in the antenna's vicinity were specified in the most accurate possible way. The numerical tool FEKO was highly engaged throughout antenna modelling, parameterization, and optimization. For antenna verification, a tissue-simulating liquid was used to estimate antenna performance in an in-body environment.

This chapter is divided into 6 sections. Besides the current introductory one, the others involve antenna implementation, fabrication and assembly, verification, and discussions. A summary is provided in the end of the chapter.

3.2 Antenna implementation

Implementation of the antenna was divided into four parts: typology, modelling, parametric sweep and optimization. Antenna typology was decided combining space planning and experiences from others' research. Antenna modelling involved adding all the components and mediums in its vicinity, as well as requirements from manufacturer. Parametric sweep examined influences from the manageable parameters to antenna performance. The optimum set of parameters were generated through optimization algorithms provided by FEKO.

3.2.1 Antenna typology

Space planning

According to the definitions of UAB bolus' dimension, the external diameter of the cylindrical capsule is around 22 mm and the external length is around 80 mm, which gives an internal diameter of around 17 mm since the bio-

compatible material for packaging would be over 2 mm thick [Oli+18]. All of the components are of small form-factor: the microcontroller unit (MCU), the RF transceiver module, and the battery were already selected for UAB bolus'17, which left a cylindrical space to the bolus antenna. Figure 3.1 demonstrates the top view and side views of the bolus prototype and placement of its component, with the available area for the antenna marked. The original spring antenna could not fit in unless compressed axially, which would affect its performance and bring in more uncertainties to the radio channel.

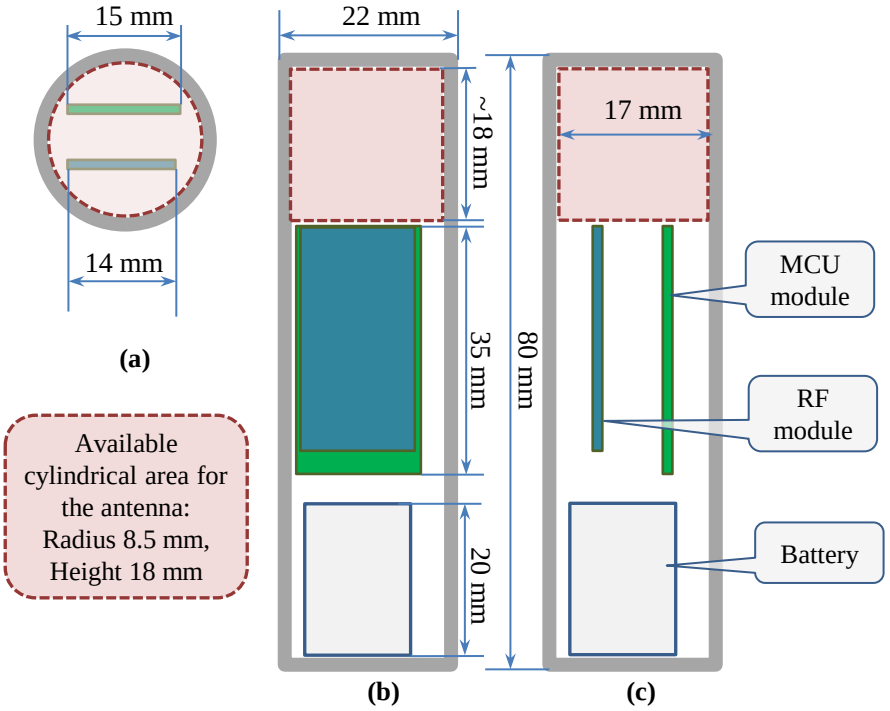

Fig. 3.1: Space plan for the bolus antenna in (a) Top view, (b) Front view, and (c) Left view of the desired bolus

Antenna selection

Single-arm Archimedean spiral antenna in a planar structure, presented and fabricated in [KCY05], was selected as the antenna to start with, taking into account the following factors:

- From the literature review in Section 2.2.3, there are substantial research work based on planar spiral antennas, which have been

integrated to electronic circuits for in vivo measurements at similar radio bands [Sam+90] [KCY05] [Lee+11].

- No special material or industrial procedure would be needed for antenna fabrication, which could limit the cost.
- Its simple geometry makes it easier for space planning inside the capsule.
- Its rigid structure makes its performance more predictable for long-term indwelling applications, compared to spring antenna and conformal antenna.

3.2.2 Antenna modelling

Adding vicinity components and mediums in the in-to-out body channel

As elaborated in Section 2.2.2, mediums and components in the in-to-out body channel would have various influences to the radio propagation, which need to be characterized and modelled for CEM simulations. Table 3.1 provides a summary of these substances in the target radio channel and their corresponding attributes in FEKO. The RF transceiver module was modelled by a PCB sheet with a dimension of 27mm $\times$ 13.5 mm $\times$ 0.8 mm, made of FR-4 dielectric material and two PEC layers. Location of the antenna pin on the RF transceiver board was also specified in the FEKO model. The digestive contents were considered together with the body tissues since verified dielectric parameters for rumen contents were not available. The

Tab. 3.1: Substances and their FEKO attributes in the in-to-out body radio channel

Substances	Dielectric characteristics	Influence to antenna	Attributes in FEKO
Spacer medium inside the capsule	air	adding loss (due to dramatic change in permittivity)	dielectric media
Adjacent electronic components	cuboid of FR4 with 2 metal layers	changing impedance, adding heat	dielectric media
Capsule	lossy medium	adding loss	plastic
Digestive contents	lossy medium	detuning, absorption	lossy medium
Body tissues	lossy medium	detuning, absorption	lossy medium

resulted antenna model and its simulated S_{11} are shown in Figure 3.2.

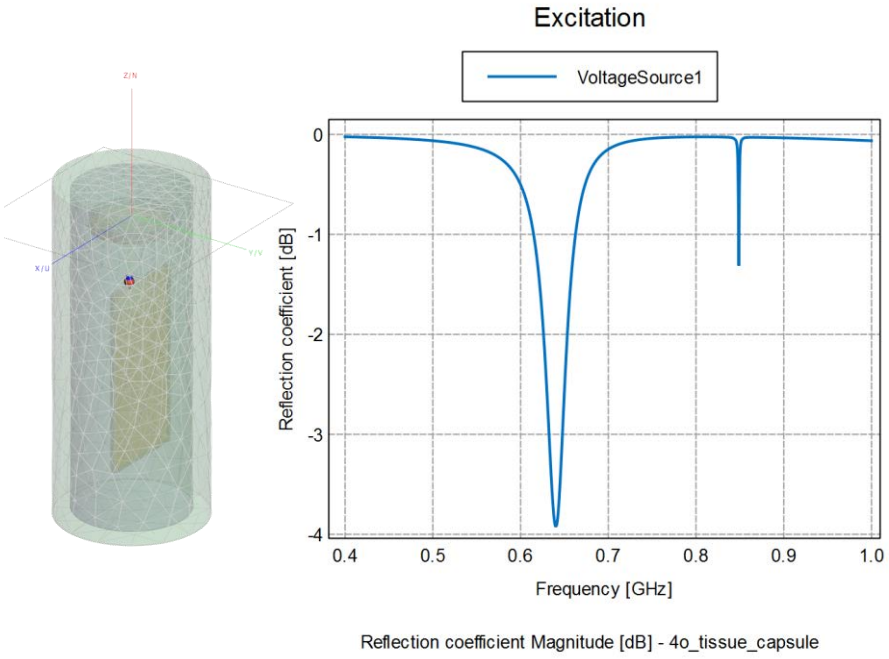

Fig. 3.2: Antenna model with vicinity substances (a) Antenna 3D view and (b) Simulated S_11

Adding manufacturer-defined parameters

"Naked proto PCB" service provided by Eurocircuits (PCB prototyping, Belgium) was selected, which allows for fast prototyping of PCB design on 2-layer boards without mask or legend. The cost of such service is also relatively low than fully finished PCBs. Therefore, it is ideal for component prototyping in the primary design stage, which was the case of this doctoral thesis. As advised by the manufacturer, it is of great benefit to understand and integrate the manufacturing rules to the design so that the production could interpret the original design with minimum changes.

The materials and industrial process adopted by the manufacturer also play an important role in antenna parameterization. The actual dielectric parameters of the substrate material are usually defined by a range, rather than a determined value. A one percent difference in the value would result in a considerable deviation in both resonant frequency and magnitude of the

return loss.

Other requirements from the manufacturer that would affect the antenna design are the industrial precision, such as the minimum width of copper, the minimum separation, and the minimum diameter of the vias etc. Table 3.2 lists a number of the requirements on PCB design from EuroCircuits and their correspondences in the antenna model. As a result, small changes were made to the antenna model: the feeding line was moved to the center of the spiral while a small portion of arm (around 0.5 mm) was added to connect the starting point of the spiral to the feed.

Tab. 3.2: Service parameters from EuroCircuits and their correspondences in the antenna model

Parameters	Value	Correspondence in antenna model
Base material thickness	1.55 mm	substrate height
Min. track width	0.150mm	spiral arm width
Min. track spacing	0.175mm	space between adjacent turns
Min. finished hole size	0.25 mm	diameter of the drill
Min. copper to board-edge clearance	0.25 mm	difference between the substrate radius and spiral's outer radius, considering spiral arm width

3.2.3 Parametric sweep

As stated by Slawomir et al. in [SA16], sweeping of the parameters, when well-combined with engineering experience, has been considered the fundamental approach for designing antenna with CEM simulations. Usually, it is believed that satisfactory results could be expected from parametric sweep, as long as the researchers or designers of the antenna make sensible sweeping configurations, such as the choice of parameters, their priorities, and ranges etc. Nevertheless, it should also be aware that interdependence may exist among some of the antenna parameters, especially those antennas with complicated geometries [SA16], which would reflect the insufficiency of a sole reliance on parametric sweep for the optimum result.

Parametric sweep was performed on the geometry of the spiral antenna. A list of the involved parameters, their reference values and their ranges for sweeping was prepared, as shown in Table 3.3. For each sweep, only one parameter was examined while the others were set to typical values. The

Tab. 3.3: Geometric parameters of the spiral antenna for parametric sweep

Parameter	Explanation	Reference value	Sweep range
width	spiral arm width	0.6 mm	0.3–0.8 mm
r_{in}	spiral inner radius	0.5 mm	0.4–2.4 mm
r_{out}	spiral outer radius	6.1 mm	5.0–7.0 mm
r_{sub}	antenna substrate radius	6.1 mm	6.5–8.0 mm
h_{sub}	antenna substrate height	1.55 mm	1.55–3 mm

results are shown in Figure 3.3. It could be summarized that spiral inner radius, turn numbers, and substrate height are more significant to antenna performance while spiral outer radius, spiral arm width, and substrate radius are less influential. Among these parameters, the substrate height had to be 1.55 mm, which was the only solution for "Naked Proto PCB" service. As a result, the other parameters were prepared for optimization.

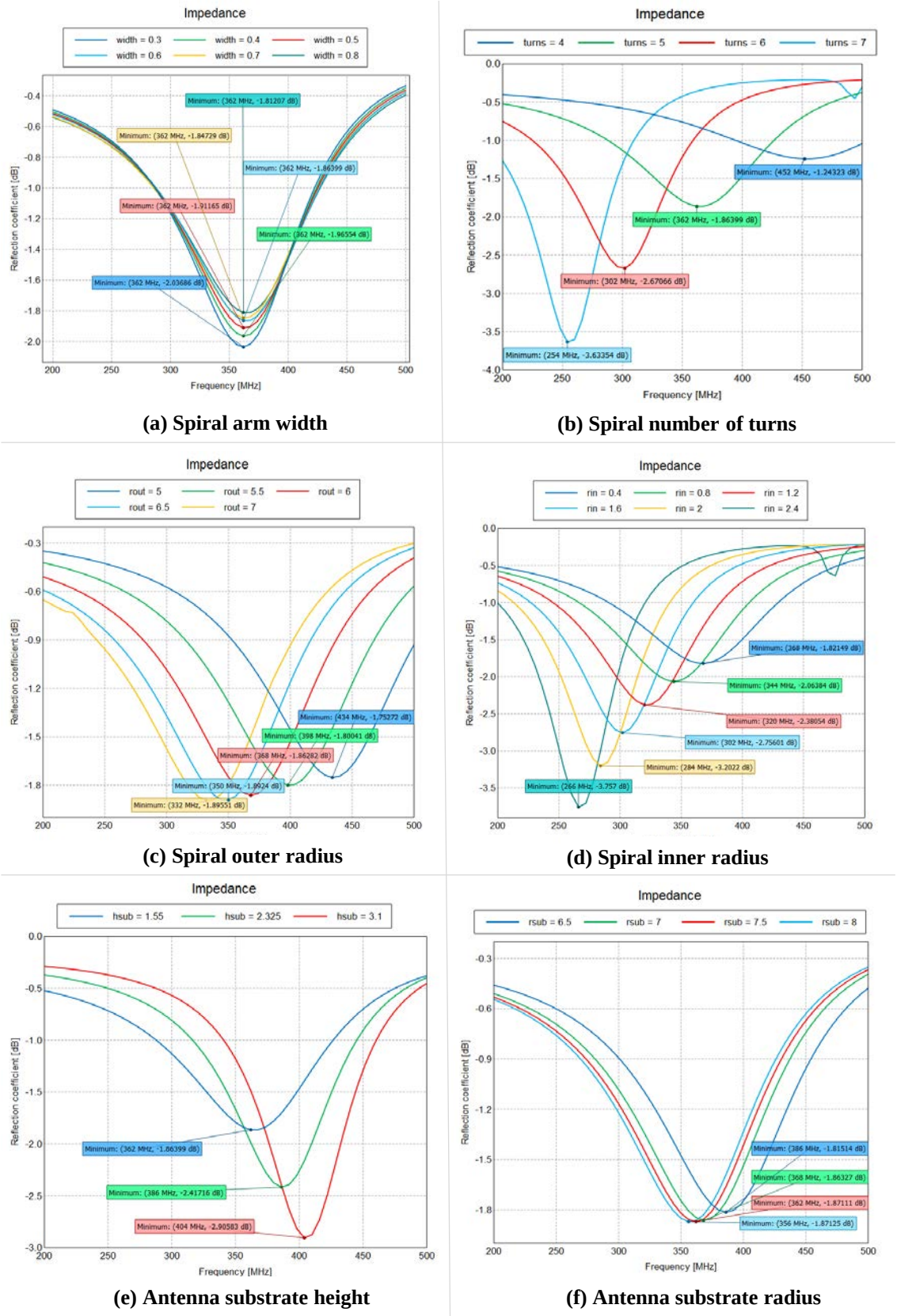

Fig. 3.3: Parametric sweep 1: spiral geometries: (a) Spiral arm width, (b) Spiral number of turns, (c) Spiral outer radius, (d) Spiral inner radius, (e) Antenna substrate height, and (f) Antenna substrate radius

3.2.4 Design optimization

With FEKO's optimization tool, the key parameters derived from previous part were set as optimization parameters and the return loss was selected as the optimization goal. A series of models were generated in order, whose return loss was extracted from the single frequency simulation. They were then compared with the optimization goal to determine the next model permutation. Dozens of iterations were made until the goal was met or the optimum solution was found within the defined number of iterations.

It should be noted that the target frequency was intentionally set higher since a deviation of 20 MHz was observed between the original design and measurement with the fabricated antenna from the first fabrication.

The resulted antenna geometry from optimization and the planned mounting to the PCB are shown in Figure 3.4.

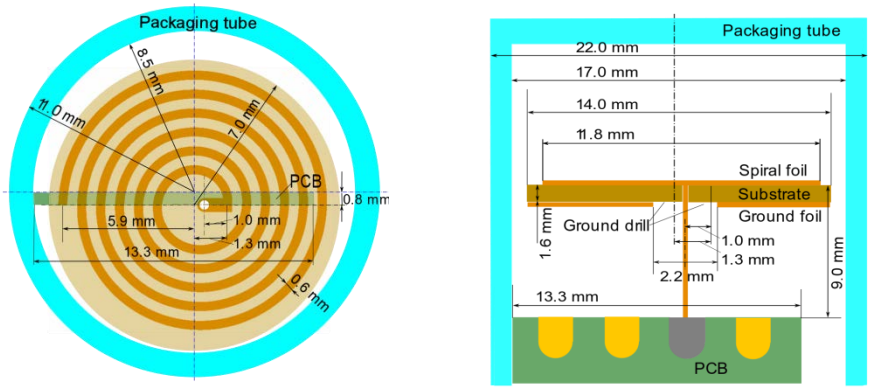

(a) **(b)**

Fig. 3.4: Antenna model with the optimized parameters for UAB Bolus'17: (a) Top view, and (b) Front view

3.3 Antenna fabrication and assembly

3.3.1 Artwork preparation

"Artwork" refers to the file sent for fabrication. EAGLE (Electronic design automation, AutoDesk, California) was used to generate the desired production file from FEKO models. Figure 3.5 shows the top views of the

spiral antenna in FEKO and EAGLE respectively. Special cautions are needed when transforming the antenna geometry between these tools.

Two fabrications were performed during the internship in UGENT, Belgium. In the first fabrication, the spiral was built up with the parameterized geometry tool in EAGLE. Even though all of the parameters were set as they were defined in FEKO, the fabricated antenna turned out to have a frequency deviation of over 100 MHz. The cause was found out to be the different handling of spiral geometries in FEKO and EAGLE. In the second fabrication, the spiral was imported to EAGLE as a wire (as shown in Figure 3.5 (b)), whose width was assigned in EAGLE. The central part to connect the drill and the spiral's starting point was built up in EAGLE as well, since the geometry was simple.

In EAGLE, cutouts were firstly created to facilitate detachment from the stencil board (shown as the light blue trails in Figure 3.5 (c)). Next, the layers were well aligned, with the drills, in the form of an axial and non-plated through hole, marked on all of the layers. Last but not least, geometries were well labelled. The generated BRD file was generated with EAGLE and acceptable by Eurocircuits.

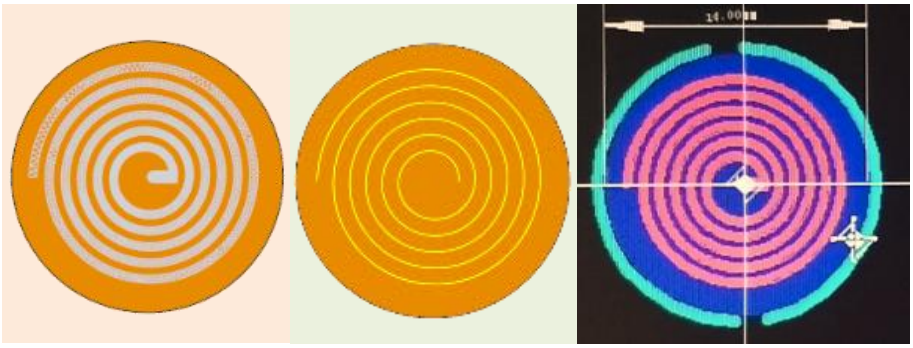

(a) (b) (c)

Fig. 3.5: Top views of the spiral antenna in FEKO and EAGLE: (a) The original spiral antenna, (b) The model for export to EAGLE, and (c) The model in EAGLE for fabrication

Eurocircuits provides a fully automated interactive online tool— PCB visualizer, which allows a fast and detailed review of the submitted board data before cost calculation and order placement. It consists of two parts: PCB configurator and PCB checker, to analyze the design data and report all detected rule-violation issues. The whole process could be divided into three stages: 1) PCB design data analysis, 2) Single image preparation, and 3) Panelization. In the first stage, format, completeness, and part definitions of the artwork are examined before being converted to an internal data format.

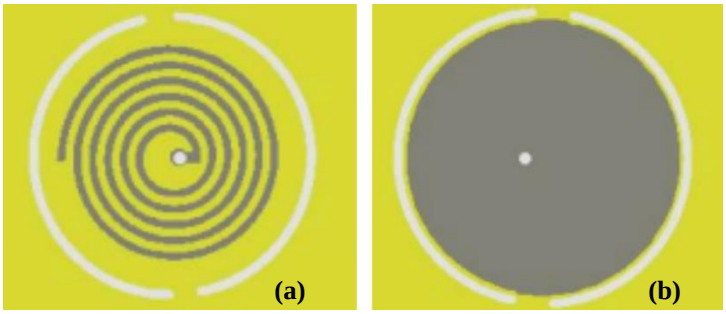

Fig. 3.6: PCB images of the spiral antenna model prepared by Eurocircuits : (a) Top view, and (b) Bottom view

Then, more detailed scrutiny is performed to find out violations to design rules. In the second stage, drill data, copper layers, and other layers are checked and prepared to have the design adapted to the plating and drilling process. In the third stage, the production panel is automatically generated, rechecked and optimized before sending for manufacturing. The final report from Eurocircuits is shown in Figure 3.6.

3.3.2 Assembly of antenna model

The manufactured spiral antennas are shown in Figure 3.7. Good agreement was achieved between the original design models and the fabricated models. Engineering work was needed to assemble the fabricated spiral antennas to

Fig. 3.7: Top view of the fabricated antenna and its designed model

certain connectors and boards for further verification. Overall, two models were prepared: a standalone antenna and a spiral antenna with a PCB sheet. The PCB sheet, with the same dimension as the RF transceiver PCB (28 mm $\times$ 13.5 mm $\times$ 0.8 mm), was used as a substitute of the latter. The spiral

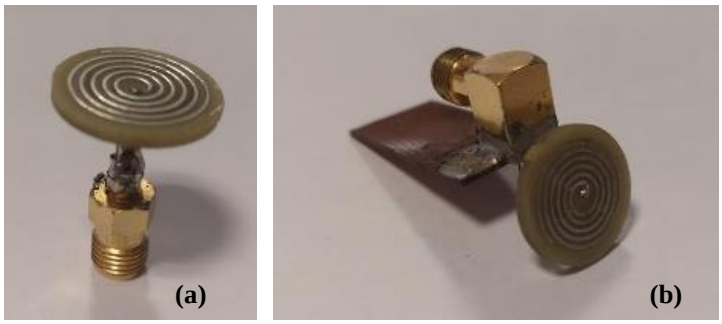

Fig. 3.8: Assembled spiral antenna models for further verification: (a) Standalone spiral antenna, and (b) Spiral antenna and a PCB sheet

antenna was mounted on the PCB sheet in the same way as it was designed to be mounted on the transceiver PCB. Coaxial cables and SMA connectors were used, which have matched geometries with the fabricated spiral antenna: diameter of the coaxial cable's inner conductor could penetrate the drill of the spiral antenna, while diameter of the coaxial cable's outer conductor could be soldered to the SMA connectors. The assembled models are shown in Figure 3.8.

3.4 Antenna verification

3.4.1 Laboratory measurement setup

1. Vector network analyzer

A Rohde& Schwarz ZNC vectro network analyzer was used to measure the return loss of the antenna models. Calibration of the instrument and the coaxial cable is indispensable before each measurement. Besides, it is very important to use the same cable for all of the measurements.

2. Tissue-simulating liquid

Around 40 liters of tissue-simulating liquid HSL450V2 from SPEAG (EM test equipment, Switzerland) that has similar dielectric properties of head tissues at 450 MHz was poured into a container to form a bio-equivalent phantom. Such liquid is based on a mixture of water and sugar, with small portions of NaCl (to increase the conductivity), cellulose (to keep the sugar solved), and preservatives (to suppress the growth of bacterial and fungal). It should be noted that the actual dielectric parameters of the tissue-simulating liquid would change over time and usages. Thereby, before each measurement,

it is crucial to examine the relative permittivity and conductivity of the tissue-simulating liquid [SA]. 85070E Dielectric probe kit from Keysight (RF instrument, United States) was used to perform the impedance measurement of the target liquid, which was compared with that of the reference liquid—saline solution. The relative permittivity and conductivity were deduced using the methods described in [Oli17].

Maintenance and adjustment of the tissue-simulating liquid are discussed in Chapter 4, in which such liquid was more intensively used for characterizing the in-to-out body transmission channel.

3.4.2 Measurement results

Standalone spiral antenna in the free space

The measurement was performed with a longer and a shorter cable (both calibrated before measurements) respectively. The results were compared with the simulation result of the original design in FEKO, as shown in Figure 3.9. The S_{11} curves have the same shape, while around 20 MHz deviation in resonant frequency, which was from the experience in the first fabrication. The S_{11} plot reveals how much power is reflected across the spectrum; minimum reflection occurs at the resonant frequency where S_{11} is the lowest. Since the spiral antenna was designed to be mounted on a small PCB, encapsulated in a small container, and to be used in an in-body environment, the standalone spiral antenna demonstrated different resonant frequency and S_{11} magnitude when verified in the free space.

Spiral antenna and PCB sheet in tissue-simulating liquid

A plastic cylindrical tube, with a diameter of 2.5 cm and a length of 8 cm, was used to package the spiral antenna and the PCB sheet. The tube was placed inside the tissue-simulating liquid vertically. Through the SMA connector on the PCB sheet, the model was connected to the vector network analyzer for verification. Figure 3.10 shows the reflection loss (S_{11}) over the frequency spectrum between 350 MHz and 550 MHz from measurement with the assembled model (the red solid line) and simulation of the original design (green dashed line). The red solid curve is the measured S11 of the fabricated

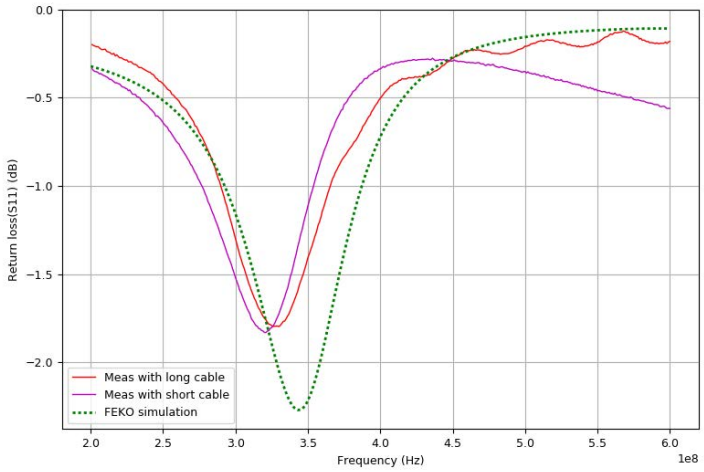

Fig. 3.9: Return loss for the standalone spiral antenna in free space

spiral antenna mounted on the PCB sheet. Since the deviation in resonant frequency was concerned when assigning antenna optimization goals, the assembled antenna model can resonate around the target frequency, 433 MHz, with a return loss of -10.5 dB. The bandwidth at S_{11} = -10 dB is around 7.5 MHz, which could cope with antenna detuning within a limited range. As indicated in [Nik+17], for ingestible antenna that works at 433 MHz band, a bandwidth of 17 MHz at S_{11} = -10 dB could be considered sufficient. Overall, the fabricated antenna works as anticipated.

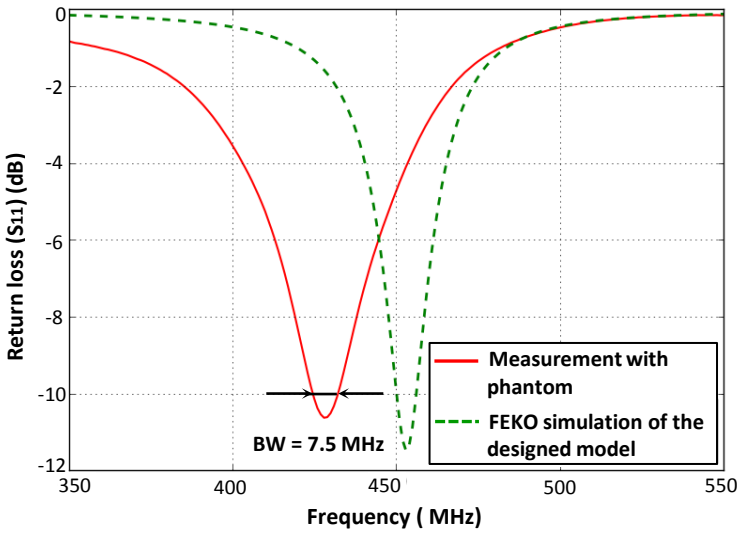

Fig. 3.10: Return loss for the spiral antenna + PCB sheet in tissue-simulating liquid

3.5 Discussions

3.5.1 Medium influence to antenna performance

Influence from the capsule size

Size of the capsule decides the volume of the air spacer around the antenna. Several more parametric sweep were designed to find out the influence from the radius and the length of the capsule to the antenna model. Figure 3.11 shows the results from this series of parametric sweep. The radius of the capsule has a much more profound influence on antenna performance, both in the resonant frequency and in the magnitude of return loss. The length of the capsule, on the contrary, has a very limited influence to antenna performance.

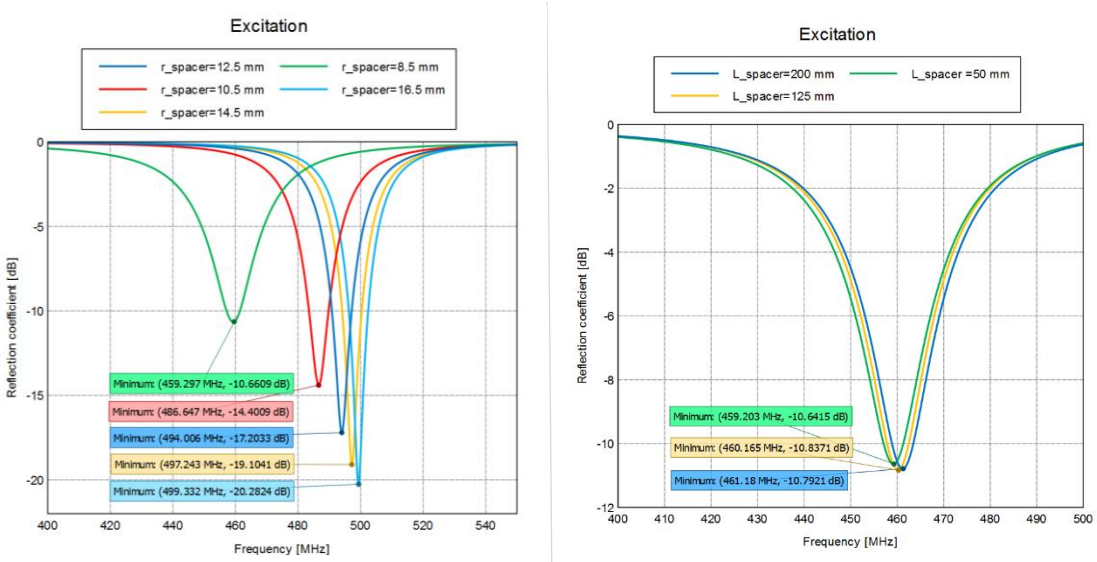

(a) Capsule radius **(b) Capsule length**

Fig. 3.11: Parametric sweep 2: Influence from capsule dimension: (a) capsule radius, and (b) Capsule length

Such results are consistent with the radiation pattern of the antenna model in free space, which is in the shape of a doughnut with the axis of the antenna passing through the hole in the centre of the doughnut (as shown in Figure 3.12). The antenna model is therefore considered omnidirectional.

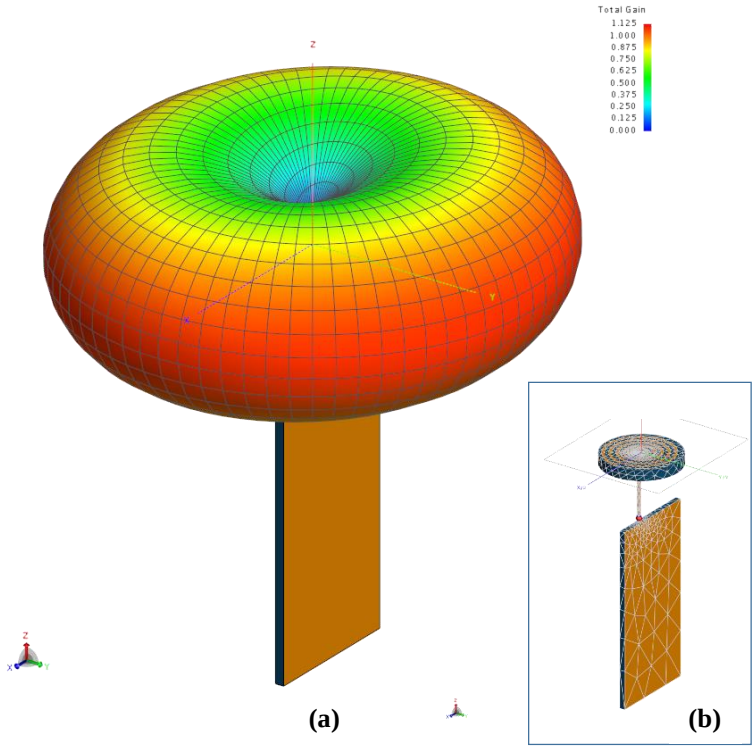

Fig. 3.12: Radiation pattern of the antenna model in free space: (a) 3D Far-field, and (b) 3D meshed antenna model

Influences from the lossy medium

Dielectric parameters of the background medium in FEKO model were set to be the values of the tissue-simulating liquid HSL450V2 from SPEAG, which were relative permittivity $\epsilon_r = 45$ and conductivity $\sigma = 0.78$ S/m. However, the actual dielectric characteristics of the in-body medium would be different from these ones. To examine the influence from different lossy mediums to antenna performance, another series of parametric sweep were performed, taking the most common values of both relative permittivity and conductivity for implant and ingestible applications listed in Table 1.1 of Chapter 1. The results are shown in Figure 3.13. Meanwhile, antenna frequency resposnce in the most lossy (such as small intestine) and least lossy (such as fat) body tissues were plotted together.

The results of the antenna model's resonance response in tissues of different dielectric parameters indicate that the best matching is in the predefined medium. Besides, limited variations in either relative permittivity or conductivity would mainly affect antenna matching (the magnitude of the S_{11} curve), rather than frequency detuning. However, much more obvious

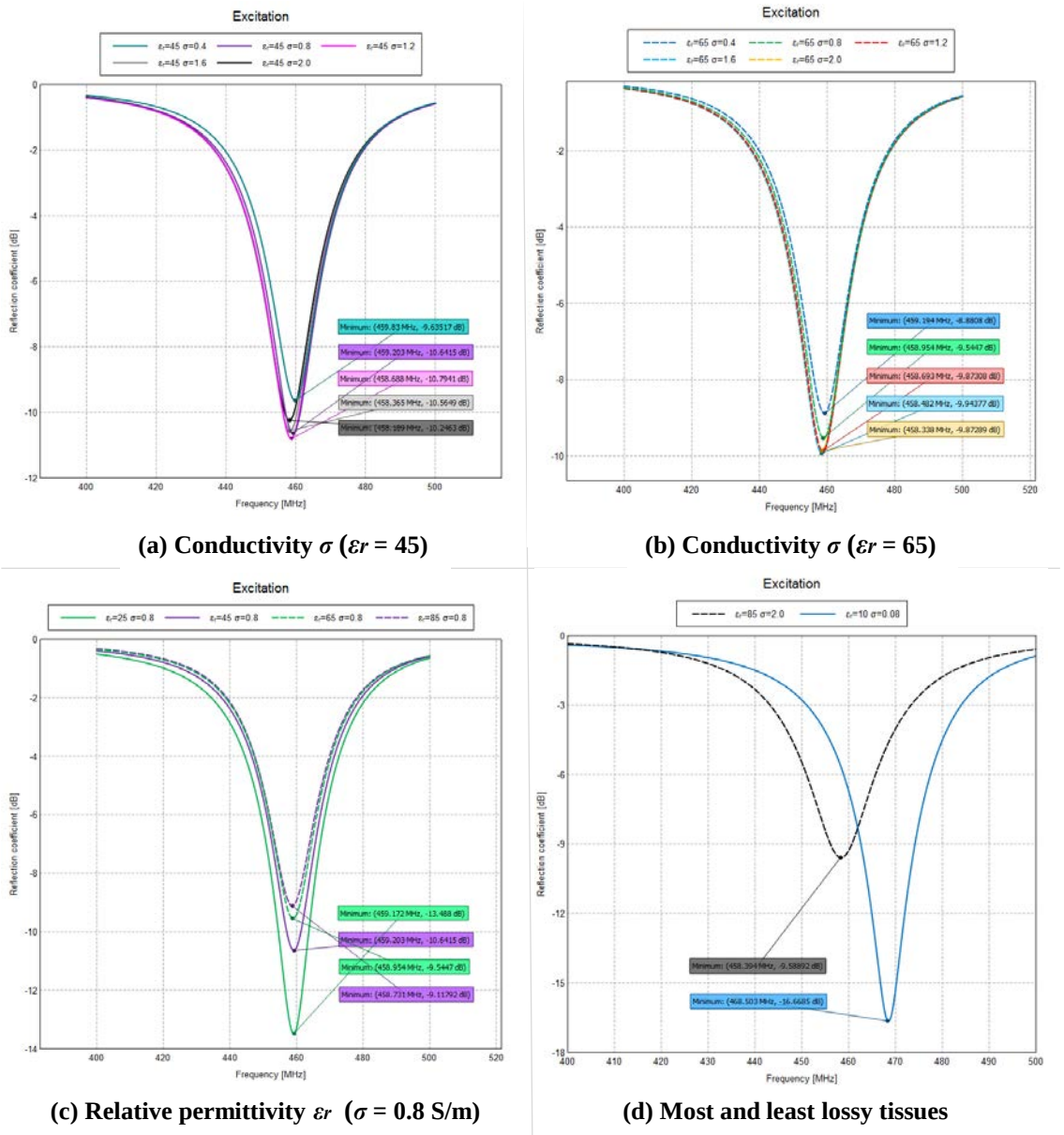

(a) Conductivity σ (εr = 45)

(b) Conductivity σ (εr = 65)

(c) Relative permittivity εr (σ = 0.8 S/m)

(d) Most and least lossy tissues

Fig. 3.13: Parametric sweep 3: influences from tissue's dielectric parameters: (a) Conductivity σ (ϵ_r = 45), (b) Conductivity σ (ϵ_r = 65), (c) Relative permittivity ϵ_r (Conductivity σ = 0.8 S/m), and (d) Most and least lossy tissues

deviations exist between the most and the least lossy tissue, in both resonant frequency and S_{11} magnitude.

Such a result implies the importance of a reliable body model for CEM analysis, whose dimension, structure, and dielectric properties should be close to the target object.

3.5.2 Differences between the designed model and the fabricated model

It was observed that 20 MHz difference in resonant frequency existed between the antenna model from experimental fabrication and its simulated model. Even though there was no difference in geometry. As a result, a deviation was considered when setting optimization goals for the second production of the spiral antenna. Unsurprisingly, such difference was also discovered in antenna verification. A number of reasons are conceivable, which may include:

- Inaccurate configurations of the feeding wire, such as, its location, length, wire thickness etc.
- Influence from the SMA connector, which was not modelled in simulation.
- Tolerances of material properties [Mül+16]

3.5.3 Characterization of non-standard products

In many electronic design projects, especially those at their primary stage, it is inevitable to employ some non-standard commercial components whose actual parameters might not be fully traceable or consistent with the disclosed data. For a small antenna used in a scaled-down electronic system, a minor difference in one of the parameters, either of its own geometry or of its surrounding environment, could bring in much larger divergence from the predicted antenna performance. As illustrated in Section 3.3.2, the actual dielectric parameters of the FR 4 material used by the manufacture should be scrutinized, since it could bring in considerable shift in resonant frequency. It is the researchers' responsibility to solve the problems during

the investigations and fill the gap. Nonetheless, it is also vital to prioritize the problems and seek a balance between the efforts and the outcome. Bearing this principle in mind, we should be flexible in looking for workaround solutions.

One example of non-standard products causing problems in this doctoral thesis is the radio transceiver module used in UAB boluses. This module is observed to have a matching network for the original spring antenna, which was recommended by the vendor of the module. However, details of the circuitry were kept confidential by the designers. After consulting experts in antenna design, we got to learn that the required resources, time and experiences to characterize some active components on a non-standard transceiver module would exceed the scope of this doctoral thesis. First of all, the significance of revealing the matching network would be limited since neither the spring antenna nor the transceiver module is a representative component in WBAN research and application. In addition, it is unknown how "well" they were matched, which makes it less promising to devise the substitute antenna through benchmarking the original spring antenna. Moreover, rather than digging into the matching network on the transceiver module, it is of higher priority to characterize signal attenuation in the target in-to-out body wireless transmission channel, which would shed light in design improvement of the bolus and its components. Therefore, in this thesis work, we decided to model the RF transceiver as a double-layered PCB sheet regardless of the active component, and not to pore over the spring antenna either. However, in Chapter 5, we would compare signal reception in the in vivo scenario, with UAB bolus'15 and UAB bolus'17 respectively.

3.6 Summary

A small spiral antenna was devised for use in UAB bolus'17. Besides its small form-factor, this spiral antenna was designed to resonate at 433 MHz in a compound environment of air spacer, PCB board, capsule, and body tissues. The PCB was added to the antenna model, which is usually omitted in antenna design work but actually affects both the resonant frequency and the magnitude of the return loss. Besides, requirements from the antenna manufacturer were also considered during antenna implementation. Parametric sweep and optimization provided by FEKO were performed to

generate the optimum antenna model for fabrication. The fabricated antenna was proved to work as expected when assembled with a small PCB sheet and verified in the tissue-simulating liquid.

4 Theoretical studies of the in-to-out body radio transmission channel

> *We must revisit the idea that science is a methodology and not an ontology.*
>
> — **Deepak Chopra**

This chapter discusses theoretical study of the channel between the UAB bolus'17 and a reference receiver. The spiral antenna devised in Chapter 3 was integrated into UAB bolus'17. Both 3D numerical simulations and laboratory measurements with a bio-equivalent phantom were employed, aiming at discovering how radio signal would attenuate in tissue-simulating mediums. Mathematical models of path loss against separation distance between the bolus and the receiver were developed. Link budget analysis was performed to examine the link viability when noises at receiver side were considered. Although details regarding the ruminal composition and internal body structures were not involved due to the limitation on accessible resources, such efforts are considered the first step to characterize the in-to-out body radio transmission channel and also a pioneer in the research of WBAN for animals.

4.1 Introduction

In wireless communications, channel models are used to obtain the profile of a transmit signal from the received signal [Sta+16]. Theoretical channel study refers to using mathematical channel models to characterize the radio link of a specific situation. These models are usually originated from the fundamental EM propagation principles, which require comprehensive depiction of the propagation environment and the involved antennas. Even though a single theoretical channel model may not be sufficient to describe the radio channel in macro environments, it is widely considered the first step towards building

up a good communication link, which could ensure lower latency and higher reliability [Ara08; YS10; WW12; Sta+16].

For in-to-out body wireless communications used by implant or ingestible medical devices, it is of crucial importance to characterize the profile of signal attenuation in the in-body radio propagation environment, which is an intrinsic lossy and heterogeneous medium [YH10]. EM wave propagation in such a medium would be different from that in free space. Higher attenuation to transmit power is expected due to signal absorption, reflection, and refraction etc. PL models are therefore developed to account for signal attenuation in the target channel with respect to the environment, the frequency, the antennas, and TX-RX etc.

Generally speaking, PL models can be obtained by CEM simulations as well as physical measurements with bio-equivalent phantoms. 3D heterogeneous human models have been widely used in CEM simulation for WBAN research, which are believed to have reduced the gaps between simulation results and authentic application scenarios [AH09; SAH09; Rom+14; Sta+16]. However, for evaluation of the PL between a ruminal bolus and an on-body receiver, there is no adequate 3D heterogeneous animal models for numerical analysis. Consequently, homogeneous models are usually used for CEM simulation while homogeneous tissue-simulating liquids are used as phantoms for laboratory measurements [Wan+17].

Once PL models of the typical application scenarios are developed, link budget is performed to evaluate basic capabilities of the wireless communication system, such as, cell range, minimum transmit power, and channel capacity etc. Link budget provides a systematic examination of the robustness of the radio link [Ara08; WW12]. For in-to-out body wireless communications in WBAN research, link budget has its special significance in system evaluation before the installation of implant or ingestible devices on living subjects.

4.2 Path loss modelling

Theoretical PL models can be applied to various scenarios. However, it is vital to understand the components in the model, as well as their corresponding physical objects in the target application scenarios.

4.2.1 The principles

The path loss, usually expressed in decibels, is defined as the ratio of the transmit power to the received power. It accounts for the losses incurred during EM wave propagation in the radio link between TX and RX antennas. Figure 4.1 shows an example physical model of a radio link [Cam]. As suggested in [Ara08], PL can be expressed as

$$PL = P_{TI} - P_{RI} = P_T + G_T + G_R - P_R - L_T - L_R \tag{4.1}$$

where P_{TI} and P_{RI} are the transmit and received powers in terms of Effective Isotropic Radiated Power (EIRP), which are regarded as the actual amount of power leaving the TX antenna and arriving at the RX antenna [Ara08]. It should be noted that P_T and P_R are the power levels at the output of the TX circuitry and at the input of the RX circuitry respectively, which usually do not equal to P_{TI} and P_{RI}. The differences come from the feeder losses, L_T and L_R, and antenna gains, G_T and G_R, at both ends of the radio link. Special attentions would be needed to the antenna gains, which are also referred to an isotropic antenna, and expressed in decibels relative to isotropic (dBi). As a rule of thumb, the gain of an isotropic radiator is 2.15 times higher than that of a half-wave dipole, whose gain is usually provided in decibels related to dipole antenna (dBd) [Ara08]. To relate PL to the channel characteristics,

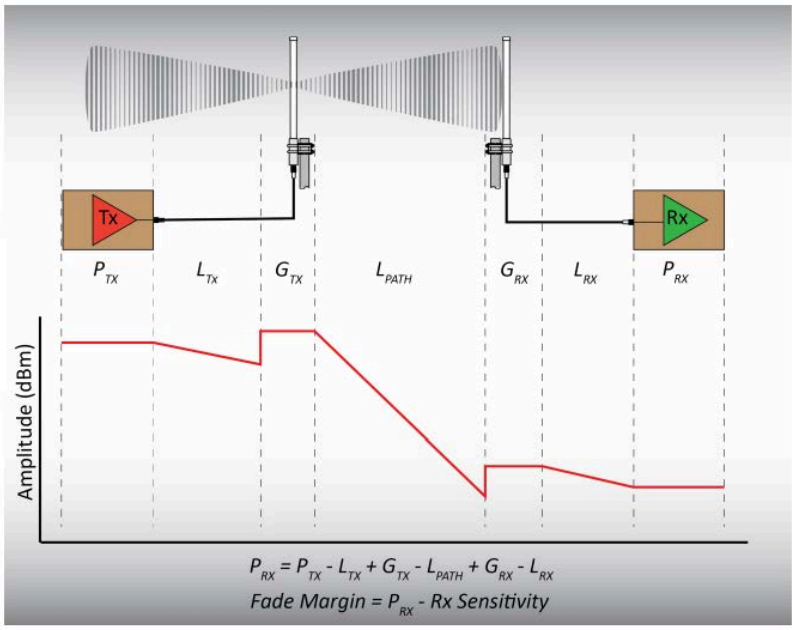

Fig. 4.1: Example physical model of a wireless transmission system [Cam]

such as TX-RX and its attenuation indices, PL of the in-to-out body wireless transmissions is usually modelled as [SAH09] [YS10]

$$PL = P_{TI} - P_{RI} = PL_0 + 10n \log 10 \frac{d}{d_0} + X_g \tag{4.2}$$

where d represents TX-RX, n stands for the path loss exponent of a specific propagation scenario, which implies how fast the signal decreases with distance [MAF07], PL_0 signifies PL at the reference distance d_0, which is considered being in the far-field of TX antenna, and X_g denotes a zero-mean random variable that accounts for shadow fading in the channel.

4.2.2 Laboratory measurements

Measurement setup

1. The laboratory environment

Laboratory measurements were conducted in the basement laboratory of iGent building in Ghent, Belgium, during August 2017. The laboratory is around 2.5 meters high, 5 meters wide, and over 15 meters long. Rather than an ideal anechoic chamber, there are metal shelves and computers in the laboratory. To improve measurement condition, acoustic wedge foams were installed vertically in a region of $1 \times 2\text{m}^2$.

2. The bio-equivalent phantom

Inside the wedge foam region, a bio-equivalent phantom was built with a tank and around 40 liters of the tissue-simulating liquid HSL450V2 from SPEAG (the same as mentioned in Chapter 3 for antenna verification). Top view of the tank is an ellipse, whose major and minor axes are 60 cm and 40 cm respectively. The depth of the tank is around 40 cm. It was placed 1 meter above the floor. Level of the liquid, when completely poured into the tank, is around 18 cm measured from the bottom of the tank.

The tissue-simulating liquid was prepared in advance, and left in stationary several hours before the measurements to let the air bubbles dissipate. Besides, its dielectric properties were verified and compared with the standard values before each measurement as changes would take place during both the usage and the storage. As suggested by the manufacturer SPEAG in [SA], adding water could increase the relative permittivity and

slightly decrease the conductivity, which can be reversed by adding sugar. Adding NaCl will mainly increase the conductivity.

3. TX and RX

A prototype of the UAB bolus'17 was prepared as the TX in the measurements. The fabricated spiral antenna was soldered to the antenna pin of the radio transceiver board, which was programmed to send a packet every second. Such a short transmission interval was chosen for the purpose of facilitating signal detection during the measurements. The system was powered by a lithium-ion battery. All these components were sealed inside a cylindrical tube, with a diameter of 2.5 cm and a length of 8 cm.

The RX in the measurements consisted of three parts: a broadband biconical antenna, a coaxial cable, and a spectrum analyzer. The biconical antenna (Schwarzbeck UBA 9116), which has similar gain and antenna factors as half-wave dipoles while having its merit of broadband features, is reported to have isotropic gain of 0.4 dBi at 425 MHz and 0.1 dBi at 450 MHz [Mes]. The loss in the cable was measured to be around 0.9 dB. The spectrum analyzer (FSL3, Rhode& Schwarz) was configured to have a resolution bandwidth of 100 kHz and a sweep time of 2.5 ms, which was proved to be sufficient to capture the received signal.

4. Cartesian coordinate robot

A Cartesian coordinate robot was used to manipulate movements of the bolus inside the phantom. Through interfaced control, the robot can make linear displacement with steps as small as 0.5 cm. Besides, calibration of the coordinates were necessary after each power-off and power-on of the control system since drifting was discovered.

Measurements execution

The tube that contained UAB bolus'17 was sunk vertically into the phantom, and moved horizontally by the robotic arm along the major axis of the phantom. The vertical distance between the bottom end of the tube and the bottom of the tank was around 8 cm, which made spiral antenna be placed at the mid-depth of the liquid level in the phantom. Horizontally, the tube was moved by the robot along the major axis of the phantom tank with a step of 2 cm, starting from 2 cm and ending at 42 cm to the phantom's vertical border,

outside of which the RX was fixed at the same height as the spiral antenna, and aligned to the major axis of the phantom tank. Figure 4.2 demonstrates the measurement setup and execution. At each TX location, 5 readings of the received signal levels were recorded.

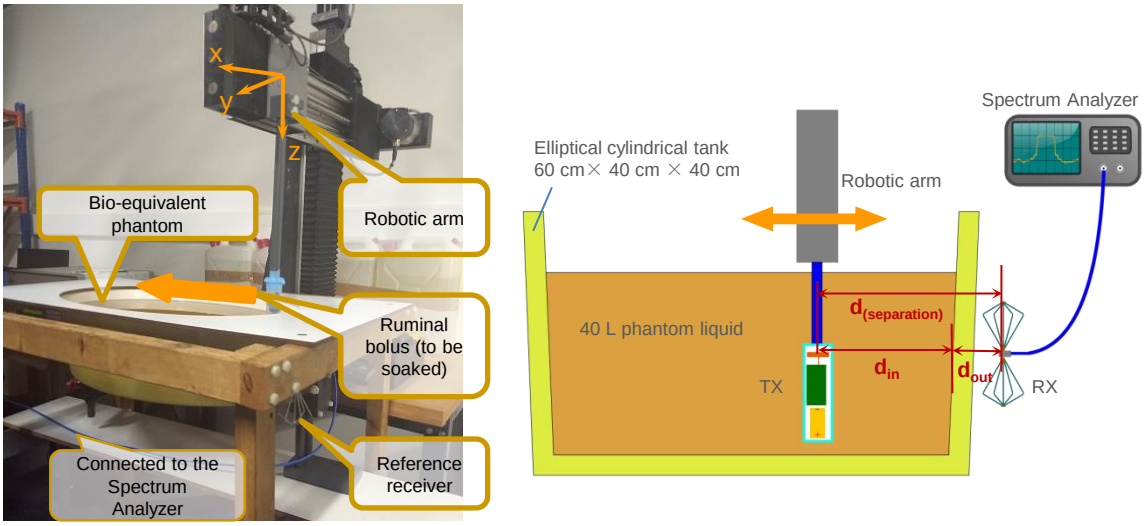

Fig. 4.2: Laboratory setup and the illustration in front view for PL examination

4.2.3 FDTD simulations

The laboratory measurement setup illustrated in Section 4.2.2 was explicitly modelled in Sim4Life v3.2, including all of the objects and mediums, their dimensions, dielectric properties, and locations. Table 4.1 shows the list of objects and their grid settings for simulation. Besides manual setting of all the parameters, it is possible to configure the simulation via Python scripting and submit to the server for series of simulations.

Even with accelerators, simulations of the developed Sim4Life models turned out to be very time-consuming. This is partially because FDTD is a time-domain method, whose simulation time is inversely related to the frequency band of the excitation. Besides, very small grids for objects with delicate geometry were applied extensively to the whole space. As a result, objects that did not require fine grid had to adopt very small grids in the intersection regions, which increased the computational cost dramatically. For example, the spiral arm of the antenna required for 0.15 mm $\times$ 0.15 mm grids in XY plane (as shown in Figure 4.3) while the grid size for tissue liquid was

Tab. 4.1: Sim4Life model and configurations for theoretical channel studies

Object	Materials	Min. grid size	Voxel priority
Spiral antenna + wire	PEC	0.15mm	
Antenna ground	PEC	0.15 mm	
Antenna substrate	FR-4	0.5 mm	prioritized
PCB	FR-4	0.5 mm	prioritized
PCB metal foils	PEC	1 mm	
Tube	plastic	1 mm	
Spacer	air	2 mm	
Tissue-liquid	body tissue	50 mm	
Tank	resin	2 mm	
Background medium	air	N/A	

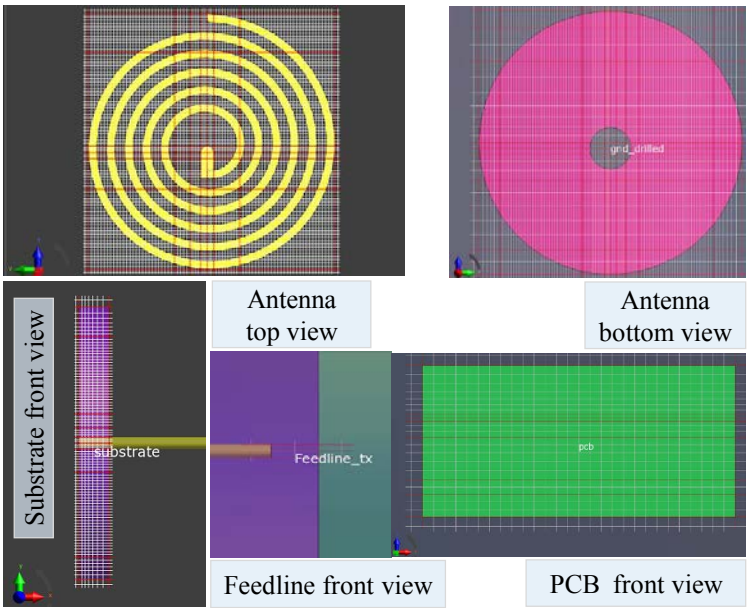

Fig. 4.3: Grid settings of the spiral model in Sim4Life

50 mm $\times$ 50 mm. At their intersection plane, all of the tissue liquids were converted to small square grids of 0.15 mm $\times$ 0.15 mm. Additional toolbox from Sim4Life that could define regions where only small grids are required was not available during the internship period in UGENT.

4.2.4 Results

The reference TX-RX d_0 was selected to be 150 mm considering: 1) the thickness of thoracic wall [BBB10], and 2) the RX being in the far-field

of the spiral antenna in UAB bolus'17. PL from laboratory measurements and numerical analysis are plotted into a semi-log coordinate and fitted respectively, as shown in Figure 4.4. The resulted parameters of the PL model: path loss exponent (n), reference PL (PL_0), and standard deviation of X_g (noted as σ_s) are provided in Table 4.2 with reference TX-RX was chosen to be 150 mm. The difference between the two PL models are discussed in Section 4.

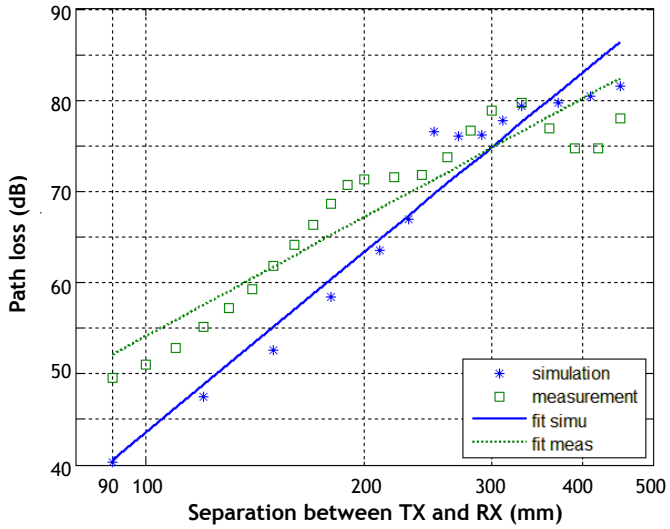

Fig. 4.4: PL fitted as logarithmic functions of TX-RX from both measurement with phantom and numerical analysis

Tab. 4.2: Parameters of PL models from measurement and simulation

Item	Measurement	Simulation
n	4.31	6.51
PL_0	61.81	52.57
σ_s	1.51	1.97

4.3 Link budget calculation

4.3.1 The principles

As defined in the book [Ara08], link budget is the "calculation of signal powers, noise powers, and/or signal-to-noise ratios for a complete communication link". It involves all the gains and losses between the TX and

RX, which are derived from various individual parameters of the system [Mob][Cam]. As a handy approach to the basic design of a complete communication system, link budget examines the feasibility of the radio link, which requires that the power level at RX should be sufficient to support a minimum level of system performance. The minimum level of system performance can be interpreted by desired cell range, the maximum allowed bit-error rate, and the minimum data rate etc.

Link budget can serve different design purposes, depending on the given parameters of the system and the design goals. However, the essence is always to examine if the transmitted power at RX is no less than the required power for the desired system performance. The gains and losses (all in dB) are components in the link budget, which build up different power levels (in dBW) at both TX and RX to denote system characteristics. In this doctoral thesis, link budget is used to estimate the cell range of the in-to-out body wireless transmission link, on condition that the minimum detectable signal, also defined as receiver sensitivity, is required on RX. On the one hand, the maximum acceptable path loss (MAPL) can be estimated as the difference between the transmit power and minimum detectable signal. On the other hand, with a reasonable fade margin, MAPL can be used to deduce the cell range (denoted as d_{max}, the maximum TX-RX), employing the PL models developed in Section 4.2.4.

4.3.2 Components in link budget

Receiver sensitivity

Receiver sensitivity is quantified as minimum detectable signal level at RX. It signifies the RX ability to demodulate and get useful information from a weak signal [Lay]. It is the sum of background noise, the noise figure, and the signal to noise ratio (SNR). These components can be obtained by calculations with system parameters, as well as from regulations or references of similar research work.

1. Background noise

The background noise can be theoretically estimated from the thermal noise

[Joh04], assuming that additive white Gaussian noise is the only noise at RX side [WW12]. It can be calculated as

$$N_{T,\mathrm{dB}} = 10\log_{10}(kTB) \tag{4.3}$$

where $k = 1.38 * 10^{-23}$ J/K is the Boltzmann's constant in Joules/K, T is the temperature in Kelvin, and B is the bandwidth of the channel selective filtering in RX [Lay]. In this doctoral thesis, T was assigned to be 38.6°C (and 311.75 K) for the RX on the ruminants' body [AB97] while $B = 300$kHz [Sta+16] [See].

2. Noise figure

The noise figure (NF) is the amount of noise power added by the electronic circuitry of RX, such as amplifiers and mixers, to the thermal noise power from the input of the receiver [Lay]. For implant applications at MICS bands, the noise figure of an uplink is estimated to be 4 dB [Joh04] [Rem98], which can be related to ISM 433 MHz band due to their similarity.

3. Signal-to-noise ratio

Signal-to-noise ration (SNR) is defined as the ratio of signal power to the noise power at RX, often expressed in decibels. The bit error rate of a digital communication system could become intolerable below a certain SNR, which thereby limits the performance of the system. As suggested in [Sta+16], SNR was assigned to be 5 dB for an on-body receiver, as the minimum acceptable value of SNR.

Maximum acceptable path loss

Maximum acceptable path loss (MAPL) not only serves as a culmination of other components in link budget, but also a bridge to relate them with one another. When minimum detectable signal is calculated, MAPL can be obtained through a subtraction from the effective isotropic transmit power. Meanwhile, MAPL consists of predicted loss and fade margin, which are also important indices of the communication system. The predicted loss is derived from PL model, and could be used to predict cell range. Since both PL model and minimum detectable signal have been explained in previous sections, only effective isotropic transmit power and fade margin are discussed here.

1. Effective isotropic transmit power

The effective isotropic transmit power is more commonly known as the effective isotropic radiated power (EIRP), and is an important component in both PL modelling (as mentioned previously in Section 4.2.1 as P_{TI}) and link budget analysis. As defined in [Ara08], it is calculated as

$$\text{EIPR}_{(\text{dB})} = P_{TI,\text{dB}} = P_{T,\text{dB}} + G_{T,\text{dB}} - L_{T,\text{dB}} \tag{4.4}$$

where P_T is the transmit power, G_T is the TX antenna gain, and L_T is the feeder loss at TX.

2. Fade margin

The fade margin denotes the degree of system resilience against unpredictable system fading. The greater the fade margin, the more reliable the system. However, it should be noted that a larger fade margin would also limit the system range [Ara08]. For implant sub-G Hz applications, a fade margin of 10 dB is recommended [Joh04] [Rem98].

4.3.3 Results

Applying the parameters discussed in Section 4.3.2, the link budget for the in-to-out body radio link is shown in Table 4.3. The estimated system range based on PL model from laboratory measurements is 2.2 meters; while 1.2 meters for that from CEM simulations.

4.4 Discussions

4.4.1 Differences between simulated and measured PL models

As shown in Figure 4.4, the differences between the two fits can be divided into two parts: slope difference and magnitude difference. The slope difference mainly comes from the lack of environmental influences in the simulation model. In the laboratory environment, influences, such as reflections from the ground, the ceiling, the wall, and other objects to the transmit signal were also captured by RX. However, in the simulation model, only the absorption loss and some reflections from the phantom tank were

Tab. 4.3: Link budget from theoretical channel studies

	Item	Explanation	Value
(a)	P_T	Transmit power	-10 dBW
(b)	L_T	TX feeder loss	0
(c)	G_T	TX antenna gain	-9.62 dBi
(d)	P_{TI}	Effective isotropic transmit power (a-b+c)	-19.62 dBW
(e)	MAPL	Maximum acceptable propagation loss	L dB
(f)	G_R	RX antenna gain	2.15 dBi
(g)	Minimum signal power transmitted to RX input = (d-e+f)		-17.47-L dB
(h)	NF	RX noise figure	4 dB
(i)	Background noise	$10\log_{10}(kTB)$ $T = 311.75$ K B = 300 kHZ	-148.85 dBW
(j)	RX noise power referred to input = (h+i)		-144.86 dBW
(k)	SNR	Required signal-to-noise ratio	5 dB
(l)	Receiver sensitivity	Required input signal power = (j+k)	-139.86 dBW
(m)	MAPL	by solving g=l	122.39 dB
(n)	Fade margin		10 dB
(o)		Maximum predicted loss = (m-n)	112.39 dB
(p)	$d_{max,meas}$	Cell range from measured PL model	2.2 m
(q)	$d_{max,simu}$	Cell range from simulated PL model	1.2 m

considered. As implied by their path loss exponents, radio signal in the simulation scenario would attenuate faster than in the measurement scenario, which would result in a shorter cell range in link budget.

The magnitude difference is more obvious when TX-RX is between 90 mm and 230 mm: an average of 8 dB more in PL is observed from measured PL. From 230 mm to 450 mm, the difference between simulated and measured PL becomes much less evident. In the author's opinion, there are several possible causes: 1) configurations of the simulation model were not fully consistent with the real objects in the laboratory, which include differences in both dielectric properties and dimensions; 2) the emitted power from TX antenna was less than expected; 3) influences from laboratory environment added more loss to the channel. It could be predicted that there would be less divergence between simulated and measured PL if the measurement were carried out in an anechoic chamber.

4.4.2 RF instrument for laboratory measurement

As suggested by many existing research work [SAH09] [Kur+11] [Flo+15] [Gar+16], laboratory measurement of PL in WBAN research were performed with a network analyzer. However, it is discovered that network analyzer might not be the proper instrument for measuring transmission parameters of ISM 433 MHz band signals inside tissue-simulating liquids in a non-anechoic laboratory. See et al. also reported that more reasonable results were obtained for modelling PL in lossy mediums at sub-G Hz band with a spectrum analyzer [SCQ16]. This could be related to performance and capability of individual instrument. However, it should also be noted that measuring the transmission parameters (S_{12} and $\S_{21}$) with the network analyzer would require more precise operations and anechoic environment since it is very sensitive to the ambient.

4.4.3 Link viability

The estimated cell range from link budget analysis varies between laboratory measurement and CEM simulation, which are 2.2 m and 1.2 m respectively. Such difference comes from the derived path loss exponents of the two methods of theoretical study. When using the smaller cell range for system examination, 1.2 m is sufficient for in-to-out body radio transmission based

on a small ruminant animal. According to Haenlein et al., the top line length usually would not exceed 1.8 m [Hae01]. Since the reticulo-ruminal chamber is in the middle part of the body, a system range of 1.2 m would be adequate for the radio transmission initiated by a ruminal bolus.

It should also be mentioned that the link budget was made based on laboratory settings rather than live conditions of the ruminants. For theoretical channel studies, this is adequate since the developed PL model is also theoretical. In addition, there are no proper 3D models for either the ruminants or the environment where the ruminants live. The actual cell range through in vivo studies will be introduced in Chapter 5.

4.5 Summary

Theoretical characterization of the in-to-out body radio transmission channel between UAB bolus'17 and a reference receiver was carried out. Utilizing both a bio-equivalent phantom and a 3D numerical model, PL data were obtained through laboratory measurement with a spectrum analyzer and a FDTD simulation tool, Sim4Life, respectively. Two log-distance PL models were developed, as difference in path loss exponent was observed between the results from the two methods. Link budget was analyzed using both PL models, which indicated that the estimated cell ranges would be adequate for radio transmissions in small ruminant animals. Even though the research work in this part was limited by the large computational cost, the available instrument, and the experiment environment, applying a canonical theoretical PL model and link budget analysis to investigate radio transmissions from a ruminal bolus to an on-body receiver is still a notable progress in the research of WBAN for animals. The gap among the measurement phantom, the simulation model, and the real scenario, would need to be filled through future research.

5 In vivo studies of the in-to-out body radio transmission channel

> *An experiment is a question which science poses to nature, and a measurement is the recording of nature's answer.*
>
> **— Max Planck**

This chapter presents in vivo studies of the radio transmission channel between the UAB bolus'17 and an body receiver through measurements with a cannulated cow in its normal status. Rather than to capture and report received signal level through some random measurements, the experiment campaigns designed in this doctoral thesis focused on discovering the radio channel's dependence on biological behaviors of the animal. Moreover, dynamic features of the channel's variables, many of which have been defined in theoretical channel studies, were identified and analyzed. Optimum settings of the configurable variables were suggested and applied in a continuous channel observation campaign, which aimed at developing a diurnal PL pattern, associated with the digestive activity routines of the ruminant animals. Such a novel PL pattern, as the outcome of multidisciplinary research work, could contribute to system optimization and power-saving design of ruminal boluses. Moreover, the methodologies explored through these in vivo studies are expected to induce more comprehensive future research in WBAN for animals.

5.1 Introduction

Channel studies with both numerical methods and bio-equivalent phantom in a static scenario, as elaborated in Chapter 4, have suggested that the in-to-out body radio link between UAB bolus'17 and an on-body receiver is theoretically feasible. However, the internal structure and movements of

either the ruminant's body or its digestive contents cannot be interpreted solely through theoretical studies of a single static channel model. Due to the lack of adequate 3D models and animations to simulate the ruminant animals and their behaviors, discovering the channel's dynamic features through CEM simulations is not yet realizable. The most effective method for channel study is thus through in vivo observations of the received signal level, which can directly reflect authentic channel behaviors. Moreover, under professional guidance with bolus placement and retrieval through the rumen canula, both the animal and the research staff could benefit from the expedited operational processes.

As one of the primary in vivo investigations on radio channels of WBAN, developing a mathematical channel model was not the goal of this doctoral thesis, since it would rely on abundant and extensive research work. However, defining and observing certain channel variables, making use of the concepts and principles from both theoretical and empirical channel modelling, and rumen physiology, are essential for understanding channel behaviors in its original scenes. Consequently, a practical PL model that could include general channel behaviors is desired, which not only could demonstrate the implemented radio link on the application level but also could be used to examine configurations of the system, including both time related parameters and power settings.

This chapter involves measurement design, channel modelling, and more essentially, the combination of multidisciplinary knowledge and experiences. It begins with principles of conducting in vivo channel studies, which consists of conducting experiments with animals, the digestive profile of the ruminant animals, and features of the target radio channel. Design of measurement campaigns and execution are then introduced, followed by results and discussions. Specially, a power saving plan is provided based on findings from the in vivo studies. At last, a short summary is provided.

5.2 Principles of in vivo channel studies

5.2.1 Code of conduct for experiments with animals

As suggested by Festing et al., laboratory experiments with animals should firstly be ethically acceptable [FA02]. They elaborated some guidelines to help with the design, execution, and presentation of the measurements with laboratory animals based on the "Three Rs" principles (as replacement, refinement, and reduction) proposed by Russell and Burch in [RBH59], which include:

- Refinement of the experiment protocols is always necessary to reduce adverse effects, both physically and psychologically, for the animals under observation. The animals should be protected from pathogens and all kinds of infection, if surgical intervention is involved. Operation staff should receive sufficient training. The housing for the on site experiments should be in compliance with established standards.
- Experiment design should involve as few animals as possible, provided that requirements from efficient statistical analysis could be met.

In this doctoral thesis, all the measurement procedures and materials were approved by the Ethics Committee on Animal and Human Experimentation of the Autonomous University of Barcelona (reference CEEAH 11/1166) and the codes of recommendations for the welfare of livestock of the Ministry of Agriculture, Food and Environment of Spain.

5.2.2 Diurnal profile of ruminal digestive activities

Various research work have suggested that the ruminants generally spend around 6 hours eating, 7 to 8 hours ruminating, and the rest hours relaxing. In addition, the ruminants usually eat or forage between sunrise and sunset and spend most of the night time ruminating and taking rest [Bow; SBR13; SPC13]. Once in a familiar and stable environment with regular feeding, the digestive activities would become regular and are synchronized among the

herd members [Chu88]. As a result, studying the pilot animal's daily digestive behaviors can be considered representative to the entire group. In this section, the normal diurnal pattern is firstly presented through observations of the target cow's digestive activities. Next, a temporary pattern is proposed based on a fasting protocol, which targeted on compressing the diurnal pattern into daytime in the purpose of not disturbing the rumination and relaxation hours at nighttime.

Normal diurnal pattern of digestive activities

In dairy farms, the ruminants usually have two major feedings everyday: one in the morning and one in the afternoon. To illustrate the time distribution in feeding, rumination, and relaxation across the day, a simplified diurnal pattern of these three digestive activities is shown in Figure 5.1.

To differentiate digestive statuses within a day, five time blocks TB_1 to TB_5 were assigned, whose correspondences are shown in Table 5.1. TB_1 to TB_4 are daytime activities that account for 12 hours with a total feed intake of 94%. During TB_5, the ruminants eat very few and spend qualified time ruminating and relaxing.

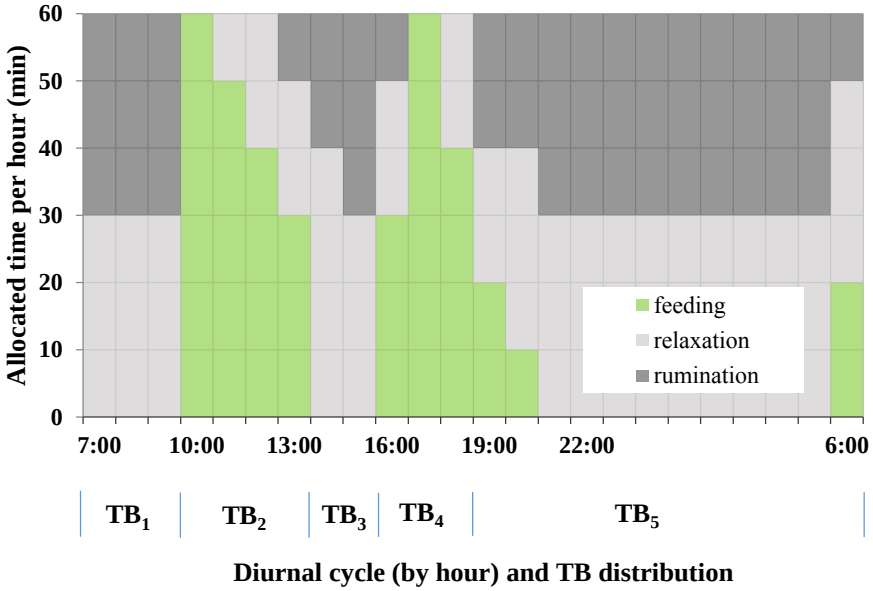

Fig. 5.1: Simplified diurnal pattern of digestive activities

Tab. 5.1: Correspondences of the time blocks (TB)

TB#	Duration	Definition	Feed%
TB_1	7h-10h	Before morning feeding	0%
TB_2	10h-14h	Morning feeding	50%
TB_3	14h-16h	Before afternoon feeding	8%
TB_4	16h-19h	Afternoon feeding	34%
TB_5	19h-7h^{+1d}	Ruminating and relaxing	8%

Temporary pattern of digestive activities based on a short fasting protocol

In the livestock industry, short-term fasting, which usually lasts from several hours up to two days, has been proved to be a safe technique to assist nutrition experiments [KS82; DL13; ONe+18]. To avoid disturbing the cow's nighttime relaxation and rumination, a short fasting protocol was thus developed to squeeze the diurnal digestive activities into an 8-hour time window during daytime.

On the day prior to the measurement, both the morning and the afternoon feedings were brought forward so that a 18-hour fasting period could be applied to the target cow, which started at 17:00 and lasted till 11:00 on the day of the measurement. Drinking water was always accessible. Such temporary feeding protocol changed the habitual feeding schedule; however, the total amount of feed intake should be maintained as much as possible. A temporary digestive pattern based on the short-term fasting protocol is shown in Figure 5.2.

Next, five predefined time blocks from a normal diurnal pattern were assigned to the temporary pattern, considering their similarities in digestive status and accumulated feed intake. The five time blocks in the temporary pattern are marked with an apostrophe, for example, TB_1'. Particularly, TB_5' of the previous day is represented by the early morning hours on the measurement day, assuming that digestive activities are less active during the fasting period, which would result in a relatively stable PL over TB_5'. In this way, it is possible to obtain approximate channel behaviors in the normal diurnal pattern through observations of the radio channel while the cow is arranged with the temporary pattern. It should be noted that the allocated ruminating

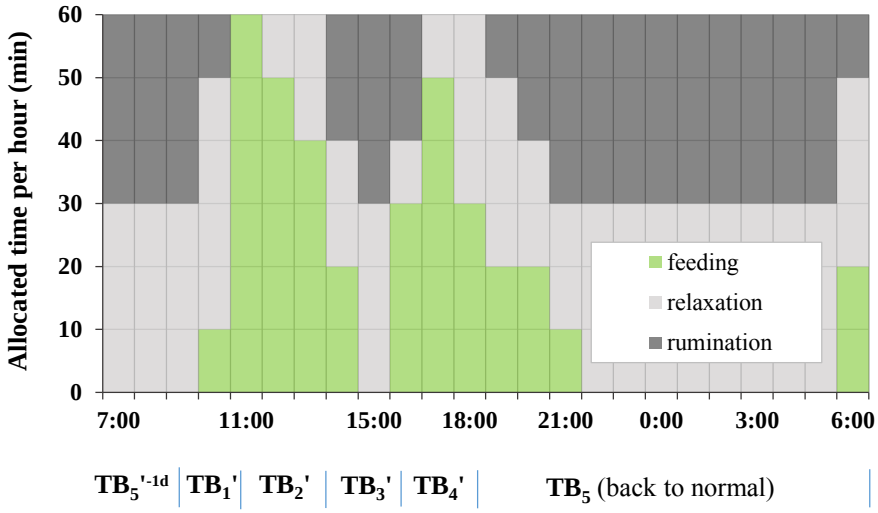

Fig. 5.2: Temporary digestive pattern from a fasting protocol

time and relaxing time in the temporary pattern were estimated based on observations and experiences with the cow's habitual behaviors.

5.2.3 Features of the target radio channel

Channel variables

The theoretical channel model developed in Section 4.2 suggested that PL is related to the separation distance between the transmitter and the receiver (TX-RX), as well as the dielectric characteristics of the channel, which refers to the path loss exponent for a specific radio transmission scenario. However, these parameters can hardly be quantified in the in vivo investigations presented in this chapter. This is because: 1) dielectric parameters of the in-body environment are not available; 2) more complicated mathematical models are needed to represent the changes in reticulo-ruminal composition driven by rumen motility; and 3) the exact location and orientation of the bolus are not observable. As a result, the channel could only be characterized with perceptible variables through evaluating their respective influences to PL.

1. Bolus location

As illustrated in Section 1.2.2, the rumen could be simplified into a 3-layer

model Mottram [Mot], with distinct dielectric properties. The location of the bolus in these layers would affect the observed PL. Although the exact location of the bolus cannot be obtained with the available resources, it is possible to control its accessible region through the retrieval rope attached to it. One end of the retrieval rope entered the cannula with the bolus, while the other end was remained outside of the animal body. By varying the length of the part inside the cannula, the bolus would reach to the designated layer inside the rumen chamber driven by rumen motility.

In this doctoral thesis, volume of the target cow's rumen chamber is estimated to be 180 liters. A simplified 3-layer cuboid model was developed to estimate the residing layer of the bolus with regard to the length of the retrieval rope. The rumen chamber is approximately represented by an cuboid of 45 cm $\times$ 60 cm $\times$ 70 cm, with the 60 cm edge along the ventral-dorsal axis and the 70 cm edge along the cranial-caudal axis. The location of the cannula is usually at the intersection region of gas cap and fiber mat. When a shorter portion of the retrieval rope is left inside the cannula, the bolus could be restricted from sinking to fluid layer. On the contrary, with longer retrieval rope, the bolus would be able to soak in the fluid layer. In this case, extra weight could be added to the bolus so that it would be more likely to stay in the fluid layer. An estimation of the retrieval rope's internal length related to its accessible layer is given in Figure 5.3. Two lengths L_1 =25 cm and L_2 = 90 cm were defined based on the structure of the bolus, which enable the bolus residing in fiber mat and fluid layer respectively. To examine the received signal level with the bolus residing at different layers, it is advised to record the received signal level with sufficient indwelling time.

2. Receiver location

In WBAN for animals, neck collars are usually used to fix the wearable sensors as well as the on-body receivers since they have shown benefits in animal comfort, device maintenance and human manoeuvre [Alz+07; Mot; Min+18]. The receiver (RX) for UAB bolus'17 was also placed on the neck collar. In this doctoral thesis, RX location was considered a channel variable to study signal reception at different parts of the collar. Four RX candidate locations were defined: on the top (N_1), left (N_2), bottom (N_3), and right (N_4) of the neck collar to examine which location would bear the least signal attenuation. Theoretically, when the bolus is at the same location, different PL should be observed from these RX locations since they correspond to different TX-RX. In reality, the bolus would keep changing its location and orientation, driven by rumen motility. To evaluate these candidate RX

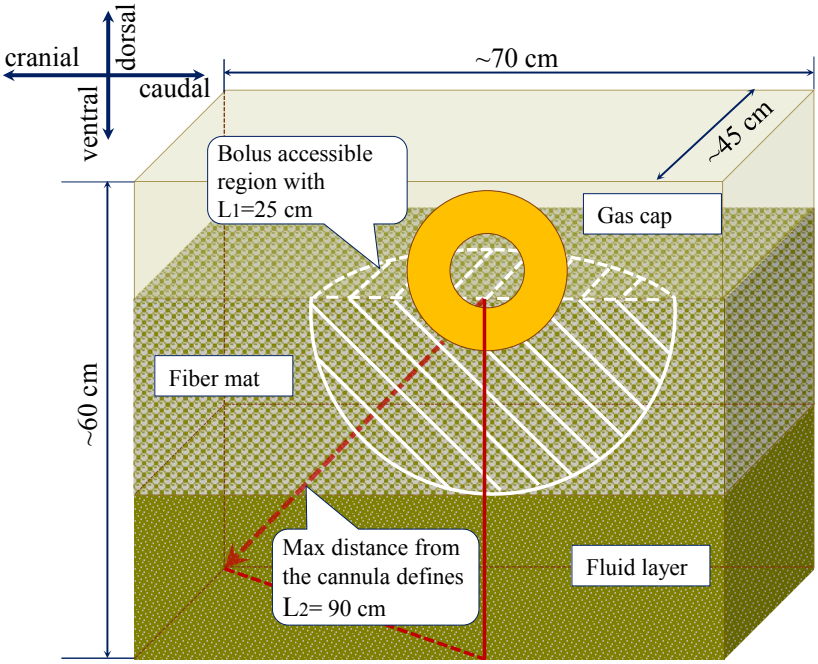

Fig. 5.3: Simplified model of the rumen chamber for evaluating bolus location versus length of the retrieval rope

locations and compare their signal reception, it is important to have other channel variables be "identical" during the measurement, in other words, with the minimum possible variances. Thereby, "instant" readings of the received signal level are desired at all of these candidate RX locations, assuming that the bolus and the in-body environment are considered stationary during these readings. Moreover, it is crucial to discover the period of time in which changes in the in-body channel could be neglected. This topic involves concepts in dynamic channel modelling and will be discussed in later part of this section.

3. Bolus orientation

The orientation of the bolus is aligned with the orientation of the spiral antenna. In this doctoral thesis, the bolus could rotate almost freely inside the rumen chamber. Thereby, this parameter cannot be used to observe PL. However, in real applications, it is always preferred to have the bolus be limited to axial rotation [Zos+10; Sat+12], so that some biosensors, such as the pH probe, could always have good contact with the ruminal fluid.

4. RX orientation

Once the RX location is decided, it would be fixed on the neck collar and the RX antenna is unlikely to be rotated, especially when the animal is relatively stable. Instead, it is the bolus antenna that would keep changing

its orientation in a much less perceptible way. Since antenna alignment concerns the angular difference between TX antenna and RX antenna, it is possible to characterize it through a conversion of the scenario, in which the bolus antenna is considered stable while the RX antenna is rotating. At each RX candidate location, parallel to the surface of the collar, two orthogonal directions were considered: one being parallel to the cranial-caudal axis (OX) while the other being perpendicular to it (OY for N_1 and N_3, OZ for N_2 and N_4). Same as the measurements to decide RX location, comparisons of RX orientations are only valid when the in-body environment could be considered unchanged. Unlike those for RX locations, the measurements with RX orientations focused on the distribution of PL difference related to antenna alignment rather than specific PL values for any RX orientation.

5. Body postures

As mentioned in Chapter 2, the in vivo investigation on a ruminal bolus working at 315 MHz, carried out by Nogami et al., discovered that signal reception degenerated significantly when the cow under observation was in the sitting posture: the signal reception rate dropped from 90% in standing posture to less than 50% [Nog+17]. In their work, a wire antenna that resonates at 315 MHz in free space was integrated to the bolus. As explained in Chapter 3 of this doctoral thesis, antennas would be detuned by organ contents and body tissues. Besides, depending on the location of the bolus, the severity of such detuning effect would be different: in fluid layer, it is supposed to be more significant than in fiber mat due to the higher conductivity caused by increased water content [SF80]. In short, antennas for the bolus application need to be tuned to radiate properly in the in-body environment; otherwise the link viability might be affected.

Since the ruminants would usually lie down around 14 hours per day [Lava], it is crucial to have a reliable radio link in regardless of body posture. When the cow is seated, either on left side or right side, the abdomen would lay on the ground. As a result, reflections from the ground would take place, which further affect signal reception. Therefore, considered as a channel variable, it is indispensable to examine the influence from body posture.

6. Digestive status

As presented in Section 1.4, the ruminant would be in one of the three typical digestive statuses: feeding, rumination, and relaxation. Principles of rumen physiology indicates that the ruminal contents would be in different velocities and directions of movements during these three statuses [LMH57]. As a

result, it is believed that digestive status is an important criterion to describe radio channel's behaviors.

Estimation of the coherence time

Coherence time is a concept in dynamic channel modelling that denotes how fast the channel changes. For in vivo channel studies, the coherence time could be estimated through continuous observations of PL over a certain amount of time, and at a designated time interval. Firstly, rumen physiology could provide a general idea on the time magnitude: 1) the reticulo-ruminal contraction takes place every 60 to 90 seconds, and 2) the time for rumination per hour would not exceed 30 minutes during the non-eating hours in a normal diurnal pattern [SBR13]. Next, the transmission interval of UAB bolus'17 in this work was set to emit one packet every second for research purpose. Therefore, sampling rate of the received signal level was chosen to be 10 seconds while the duration of measurement would be from 10 to 30 minutes, depending on the duration of a certain digestive status.

With the aforementioned scheme, the expected PL against time would exhibit fluctuations among contiguous sampling points. However, through reasonable grouping of a certain number of adjacent individual measurements, the channel could be considered "coherent" during the corresponding period. More significant changes in PL would be observed among different groups rather than within the same group. The length of the group is therefore estimated to be the coherence time of the channel.

5.3 In vivo measurements

5.3.1 Materials and preparations

1. Transmitter and Receiver

UAB bolus'17 served as the transmitter (TX), in which the electronic control platform devised in [Oli+18], the fabricated spiral antenna as described in Chapter 3, and a Lithium battery (SAFT, 3.6 V, 14 250 mAh) were integrated. All of these components were sealed inside a cylindrical plastic tube of 2.5 cm in diameter and 8 cm in length. Radio transmission time interval, data

rate, as well as the transmit power level are configurable. In this work, for the convenience of signal capture, the bolus was programmed to transmit a data packet every second with a data rate of 15 kbps and an emitted power of 20 dBm.

On the RX side, a quarter-wave whip antenna (MW433, Embedded Antenna Design Ltd.) with a flexible main shaft was selected as the on-body receiving antenna. It has an operation frequency centred at 433 MHz and a bandwidth of 70 MHz for a Voltage Standing Wave Ratio of 1.9. A 3-meter flexible coaxial cable was used to connect the whip antenna and a spectrum analyzer (EXA N9010A, Keysight), which was configured to measure the received signal level.

2. Cannulated cow

UAB boluses are designed for small ruminants and it would be more appropriate to conduct in vivo investigations with a cannulated sheep or goat. However, only cannulated cows were available at the time of the in vivo studies of this thesis. The objective of the in vivo study is not only to obtain PL in the authentic channel but also to discover the connections between channel behaviors and specific digestive activities, such as rumination, which are shared by both big and small ruminants. Therefore, we decided to use the cannulated cow to conduct in vivo studies.

A 3-year-old rumen-cannulated Holstein cow was selected for the measurements. The cannula acts as a port from the rumen to the outside and is sealed by a tightly fitted rubber plug. The plug in the center fit tightly into the cannula. Key body dimensions of the cow are shown in Figure 5.4. The cow weighted around 800 kg, whose rumen chamber was estimated to have a capacity of 180 liters.

The target cow is from a small herd that has close bonds among the members. The herd usually spend daytime in the barn for feed intake and evening time in the ranch. To avoid inducing psychological stress to any of the herd members, the entire herd was kept together during all of the measurements. Moreover, the operation staff should be familiar with the herd. In addition, duration of the measurements should not affect their ranch time so that the cows could relax and ruminate with no disturbance.

3. Accessories

In order to protect the target cow, as well as the devices, several accessories were prepared for both the bolus and the RX antenna. A flexible plastic rope

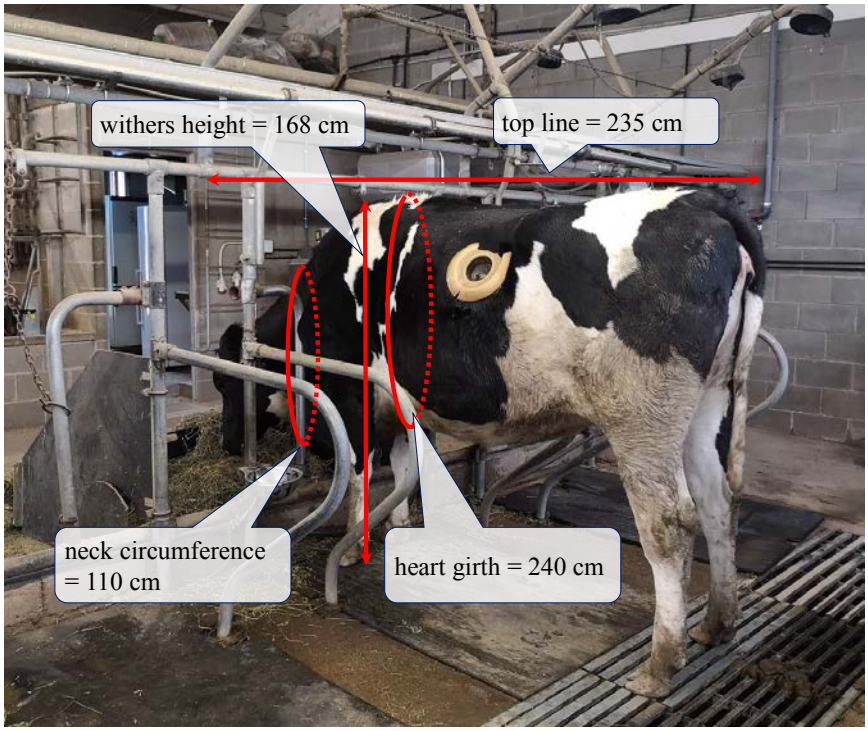

Fig. 5.4: Target cow for in vivo channel studies

was bound to the bolus tube leaving an open end of 120 cm long for the convenience of bolus recollection. It was therefore named the "retrieval rope", and was also used to control the residing layer of the bolus inside the rumen. Around 100 grams of rice were filled into the tube to prevent it from floating on top of the fiber mat.

To fix the RX antenna at certain location and orientation around the cow's neck, a piece of elastic cohesive bandage was made into a temporary neck collar and two small pockets of orthogonal orientations were sewed to hold the RX antenna.

5.3.2 Measurement setup

All of the in vivo channel studies were conducted in the multi-functional barn of the Experimental Farm of the Autonomous University of Barcelona in Bellaterra, Spain (41°34'N 2°6'E, 245 m above sea level). Equipped with thermostat system, the barn can maintain an internal temperature between 15°C and 25°C. It has nine standard stalls for the small herd of dairy cows. The measurements were carried out in the spring season from April to May 2018.

As shown in Figure 5.5, the target cow was maintained in the stall on the right while a folding table made of resin was placed in the vacant stall on the left to hold the equipment. The RX antenna was fixed on the cow's neck and connected by the coaxial cable to the spectrum analyzer. The operation staff could enter the gaps between the stalls in case of unexpected behaviors of the cows.

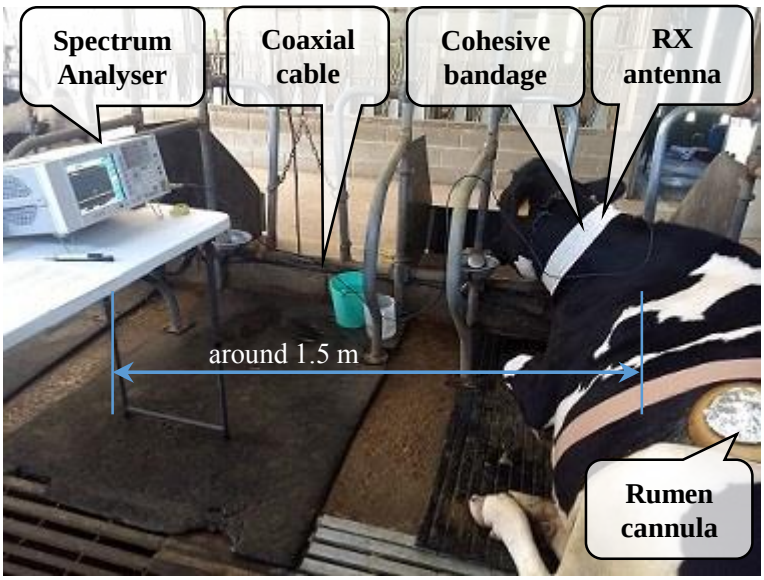

Fig. 5.5: Setup of the in vivo measurement in the barn

5.3.3 Measurement executions

Overall, the measurements were organized into 3 series of campaigns. Basic campaigns aimed at discovering basic features of the channel, including the coherence time and the relation between body posture and digestive status. Short-term repetitive campaigns examined the influences from the placement of TX and RX. Continuous observation campaign targeted to discover the diurnal PL pattern.

1. Basic campaigns: coherence time

As stated in previous sections, deciding the coherence time of the target channel was considered the foundation for all of the other measurements,

since it provides a general idea of the time duration in which the channel is considered relatively constant. Typical values of the channel variables were utilized in this series of measurements, which are bolus location= fluid layer, RX location= N_2 and aligned to OX. The digestive statuses and body postures cannot be controlled and thereby, all of the possible cases were considered. The received signal level was sampled every 10 seconds and recorded continuously until the animal changed digestive status or body posture, which usually lasted 10 to 30 minutes. Calculated as the difference between the transmitter power and the received signal level, the resulted PL would be a series of scattered points that represent individual measurements every 10 seconds. The estimated coherence time is 2 minutes. Details of data analysis are provided in Section 5.4.

2. Short-term repetitive campaigns: body postures and digestive statuses

While conducting measurement 0a to estimate coherence time, certain connections were discovered between body posture and digestive statuses during the measurements: the cow, as well as other members of the herd, would always be standing while eating; a majority of the rumination time is spent in sitting posture; both sitting and standing postures are involved for relaxation. Consequently, these two variables could be combined in the following measurements. **Short-term repetitive campaign a: bolus location**

This series of measurements evaluate PL when the bolus is maintained at fiber mat and fluid layer respectively, controlled by the length of the retrieval rope inside the cannula. However, it is impossible to manipulate bolus location without pulling it out entirely for a reinsertion, with desired length of the retrieval rope. Due to the large capacity and density of ruminal contents, it would take a certain time (for example, several minutes or even longer) for the bolus to reach to fluid layer, as well as to be retrieved from fluid layer. Especially, to retrieve the bolus from a deeper location, it is advised to take out several kilograms of the ingesta in fiber mat so that the exposure time of the cannula in the open air could be limited to protect the internal microbes. Therefore, comparison of received signal level with the bolus in fiber mat and fluid layer respectively cannot be accomplished within the channel's

coherence time.

To ensure that the cow's feed intake was at a similar level for different bolus locations, this series of measurements were carried out at certain hours, 10:00 to 12:00 and 15:00 to 17:00, across different days, assuming that the cow followed the normal diurnal pattern. Besides, the aforementioned hours could guarantee that different digestive statuses be sampled. All of the RX candidate locations and RX orientations were measured, since the results could be shared with other series of measurements. Besides, the body postures across all the measurements were recorded. **Short-term repetitive campaign b: RX location**

As mentioned in previous part, this series of measurements were included in Measurement 1a that evaluated bolus location. For each bolus location, within the estimated coherence time, RX antenna was first placed at N_2 and aligned to OX for reference measurements. Right after 20 samples, the RX antenna was moved to the other three candidate locations, where 20 samples were recorded at each location. Such steps were repeated several times in the same day and across different days. **Short-term repetitive campaign c: antenna alignment**

The alignment measurements were also included in the bolus location measurements. The RX location was chosen to be its typical value, N_2. Within the estimated coherence time, the antenna was first aligned to OX for 20 samples and immediately rotated 90 degrees for another 20 samples. Such procedures were repeated several times. Observed PL difference with RX antenna at the two orthogonal orientations were used to determine the influence from antenna misalignment.

3. Continuous observation campaign: PL pattern

Prior to this measurement, the target cow was maintained with normal feeding pattern for at least 3 days, during which time no other ruminal study was conducted. The day before the measurement, the cow was fasted after 17:00 with only water supply being accessible. During the preparation period, no irregular behavior was detected.

On the day of the measurement, feeding protocol developed for the temporary pattern in Section 5.2.2 was applied to the target cow. Typical values were assigned to the channel variables: The bolus was placed in fluid layer; The RX

was fixed at N_2 and oriented as OX. The estimated coherence time was set as the sampling interval of the spectrum analyzer. Besides the three digestive statuses, other digestive activities of the target cow, such as drinking and defecation, were also recorded. Professional veterinarian consultancy was maintained available.

5.4 Results and discussions

5.4.1 Basic campaign: coherence time

Results from intensive PL observation are shown in Figure 5.6. The diamond markers indicate individual measurements, while dotted smooth lines are added to demonstrate how PL varied between adjacent individual measurements. It is discovered that around 80% of the PL differences between adjacent individual measurements are relatively small in scale: 3 dB for feeding phase, 3.8 dB for relaxation phase, and 2 dB for rumination phase. In the rest 20% cases, the larger PL differences between adjacent individual measurements are discovered to exhibit periodical attributes: they tend to take place every 7 to 15 individual measurements with smaller PL differences. This serves as a foundation for discovering the coherence time of the in-body radio channel.

To make the PL pattern more distinguishable, moving average trend lines, marked as dashed lines in Figure 5.10, are employed to smooth out the valleys and the peaks in the PL plots. The differences between the adjacent valleys and peaks (which include both peak to adjacent valley and valley to adjacent peak) are discovered to be varied from 8 dB to 15 dB in magnitude, and from 2 to 5 minutes in time domain, containing from 12 to 30 individual measurements.

With the aforementioned data, the most tilted moving average trend line are identified, in the purpose of dividing the individual measurements around them into two groups: one with the valley around its centre and another with the peak around its centre. The width of the groups, displayed in time, are set to be 2 minutes, which could be applied to partition the PL plots for all of the three digestive phases. The groups are circled with red dotted ovals throughout the entire plots as shown in Figure 5.6. These ovals are identical and continuous in time domain, with a width of 2 minutes and an amplitude

of 7.5 dB. Therefore, the coherence time of the channel is estimated to be 2 minutes, within which time PL fluctuations are smaller than 7.5 dB.

5.4.2 Short-term repetitive campaigns

a & b. Bolus location and RX location

The two campaigns that evaluated influences from bolus location and RX location were combined during measurement executions. The results are demonstrated in Figure 5.7, in which the same number of samples were obtained for each possible combination of bolus location and RX location. It could be discovered that PL at N_1 and N_2 were less than N_3 and N_4 for bolus in either fiber mat or fluid layer. Between N_1 and N_2, the latter has shown slightly better signal reception. Such a result is consistent with ruminant anatomy, which indicates that the reticulo-ruminal chamber of an adult ruminant would occupy almost all of the left part of abdominal cavity. Consequently, when RX is placed at the left side of the neck, TX-RX for N_2 would be shorter than other cases with RX on the other three candidate locations. Besides better signal reception, N_2 has its benefits in device maintenance and easier operation, especially when compared to N_1 and N_3. In short, it is proved with in vivo investigation that left side of the neck is an optimum location for RX.

On the other hand, comparisons between fiber mat and fluid layer as bolus residing layers revealed the existence of up to 16 dB difference in average PL, out of the collected data at designated hours across different days, as shown in Figure 5.7. This could be explained by the different medium compositions and different TX-RX when the bolus was at these two layers. As water content increases with depth inside the reticulo-ruminal chamber, the corresponding channel medium in ventral sac, which belongs to the fluid layer would be lossier than that of fiber mat. As a result, higher PL is expected when the radio signal is emitted from the fluid layer than from fiber mat. In reality, ruminal boluses that are integrated with bioclimatic sensors would normally reside in the fluid layer to sample the ruminal liquid. When studying the in-to-out body radio channels with cannulated ruminants, it is very important to leave the bolus at a sufficient depth. In addition, using retrieval rope demonstrated its benefits in such in vivo measurements.

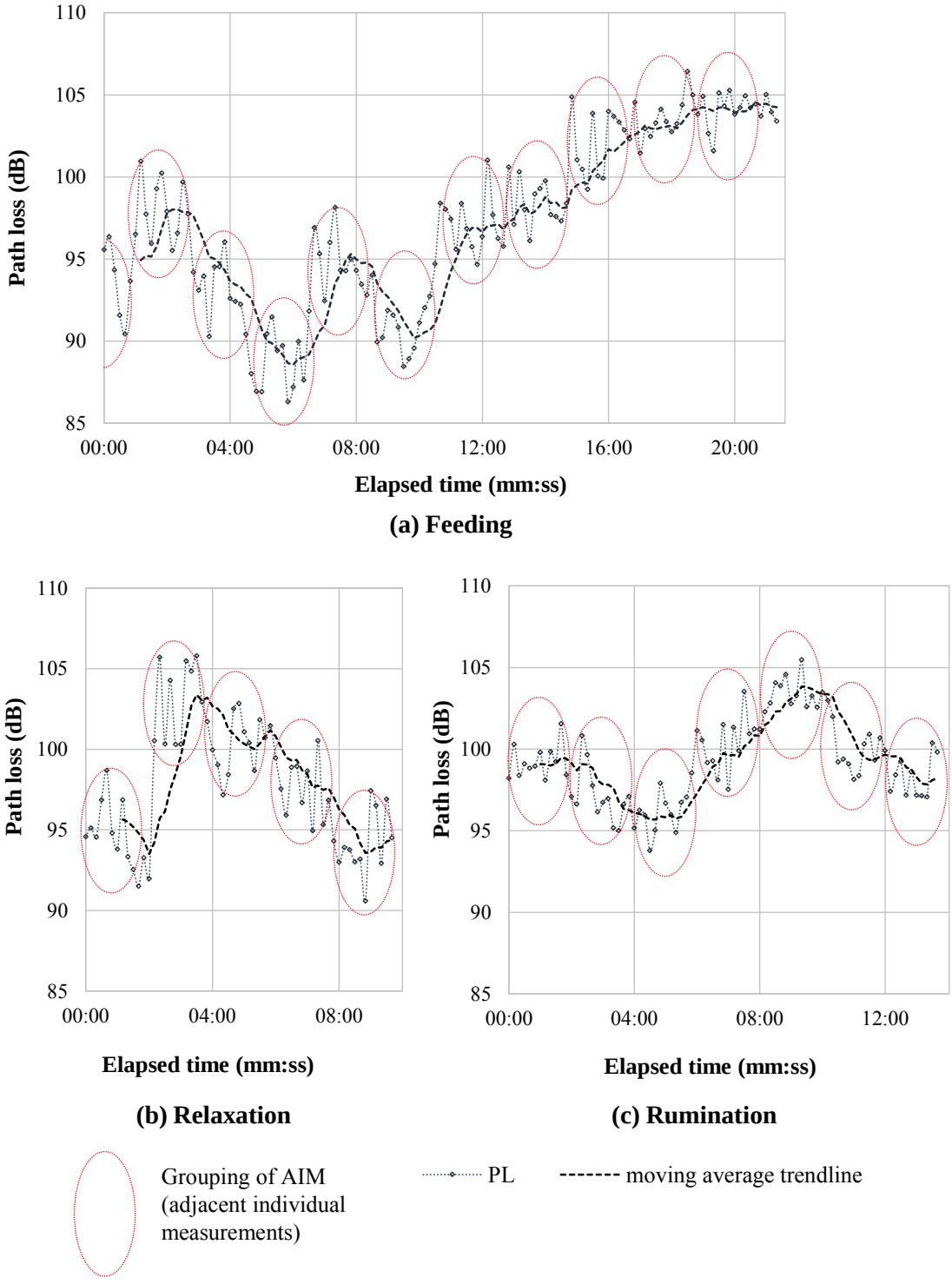

Fig. 5.6: Intensive PL observations for coherence time estimation in (a) feeding, (b) relaxation, and (c) rumination statuses

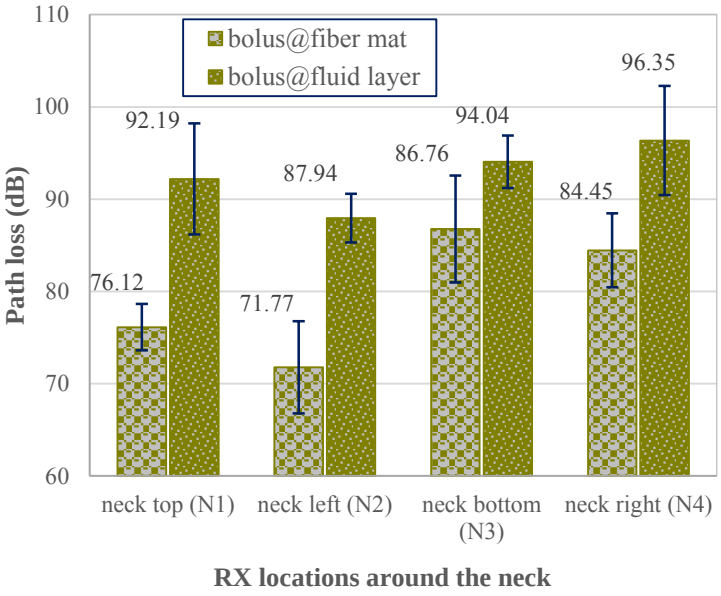

Fig. 5.7: Comparison of path loss with the bolus at different depths and the RX at different locations around the neck

c. Antenna alignment

Following the measurement schemes, 38 pairs of comparisons were recorded for evaluating the changes of PL caused by different antenna orientations. The detected difference varied between 0 and 21 dB, which are divided equitably into three groups as shown in Figure 5.8. Out of these 38 comparisons, 28 pairs showed a difference below 7 dB, seven pairs in between 8 and 14 dB, and three pairs in between 15 and 21 dB. Such results could imply that an abrupt change of antenna orientation, which could be generated either on the RX side (for example, the cow tossing its head) or on the bolus side (for example, propelled by rumen motility), is unlikely to cause a dramatic change in PL. When considering the orientation of the bolus antenna as a time-variant parameter of the in-body channel, we could also conclude that antenna alignment would have limited effect on signal reception and the PL, provided that there are few restrictions on the movement and rotation of the bolus. This is because antenna alignment would be changed constantly by the bolus, even if RX antenna remains stationary. Therefore, as long as both the bolus antenna and the RX antenna could adapt orientation changes, in other words, not being unidirectional, the impact from antenna alignment on PL would be limited.

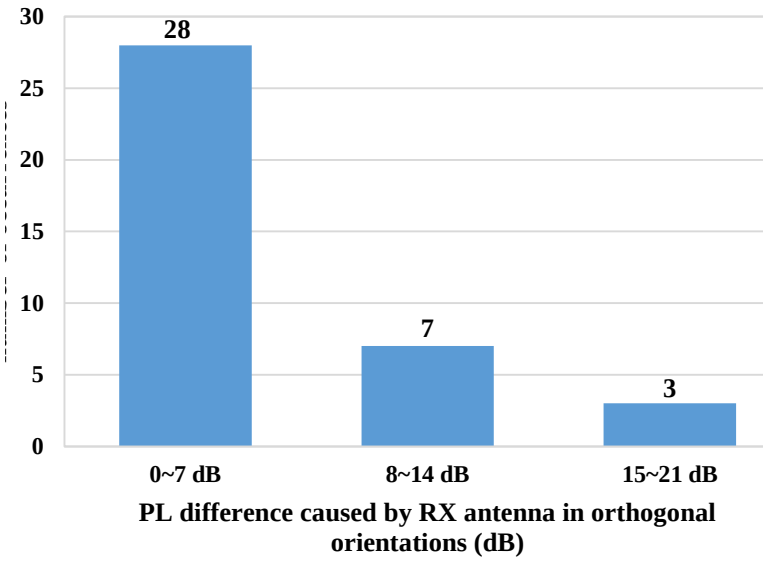

Fig. 5.8: Distributions of PL differences caused by RX antenna orientation

5.4.3 Continuous observation campaign

This campaign was the last in sequence of the in vivo investigations of this doctoral thesis. The bolus location, RX location and orientation were set to their default and optimum values, which were: fluid layer, N_2, and OX respectively. The estimated coherence time, 2 minutes, was set as the sampling frequency of the spectrum analyzer. Based on the temporary feeding protocol suggested in Section 5.2.2, the cow was fasted for 18 hours prior to the campaign. On the day of the campaign, the measurement started at 9:40 in the morning and lasted for 8 hours, during which time the cow was in its normal status. The first feeding was finished at around 15:00 and by 17:30, the second feeding was 80% finished. An intensive rumination phase took place at noon. The PL and its related digestive statuses, as well as other digestive activities across the eight-hour observation are plotted in Figure 5.9. The diamond markers denote the individual measurements which took place every 2 minutes. The dotted smooth lines show the transition between adjacent individual measurements.

According to the previous distribution of TB_1' to TB_5' in the temporary pattern, the 8-hour PL plot was partitioned into the five corresponding time blocks with their average PL marked in horizontal lines. TB_3' was brought forward for about one hour compared to the planned temporary pattern, which could be the cow's reaction to adapt the temporary feeding protocol. The observed

PL patterns in each of the time blocks in the temporary pattern correspond to their namesakes in the normal diurnal pattern, and are explained below in time sequence.

In TB_5', preserved from the day prior to the campaign, two relaxation phases and one rumination phases were captured with an average PL around 104 dB. Higher PL, as well as obvious peaks and valleys, are found in the rumination phase. On the other hand, different PL patterns are demonstrated in the two relaxation phases: when fitted linearly, the one prior to rumination has smaller ascending slope while the one after rumination descends notably. Further investigations on PL variances during relaxation phases are needed.

In TB_1', which corresponds to the 3 hours before morning feeding in a normal diurnal pattern, the fasting period terminated and the cow started to eat the feed. Following the descending trend in the second relaxation phase of TB_5', it is noticed that TB_1' has the lowest average PL, about 92 dB. In both normal pattern and the temporary pattern, this time block comes after long-time rumination and would have relatively smaller volume of rumen content.

Morning feeding period is defined as TB_2', during which time the cow would consume half of its daily feed. With the accumulation of ingesta, the PL plot in TB_2' is observed to increase gradually and the average PL turn out to be 95 dB, 3 dB higher than that of TB_1'.

Intensive rumination phase is defined as TB_3'. Similar to the rumination phase in TB_5', PL in TB_3' is observed to reach its peak values and later followed by a descending. Since there was no other digestive activities accompanied, the average PL in this time block is found to be the highest, about 108 dB.

Following the intensive rumination, in TB_4', the cow was basically engaged in afternoon feeding, as well as certain relaxation. Average PL in TB_4' has decreased 6 dB from that of TB_3', as 102 dB.

The largest difference is around 16 dB, between TB_1 (before morning feeding) and TB_3 (midday intensive rumination). Besides, higher PL are observed in rumination phases than that in adjacent feeding and relaxation phases. Such results could be related to rumen physiology. Firstly, the reticulo-ruminal contractions in rumination phases propel the ingesta as well as the bolus into different regions all over the reticulo-ruminal chamber, whose dielectric properties would vary a lot due to the difference in water content of each region. On the contrary, a different type of reticulo-ruminal contractions take place in feeding phases, which mainly mix up the newly ingested

feed and would only involve the upper level of fiber. As a result, the PL is unlikely to increase dramatically. Secondly, in rumination phases, the esophagus would be full of boluses of digesta for regurgitation and later redeglutition. Meanwhile, large amount of salive is mixed with the digesta, which is not secreted in feeding phases. The participation of saliva would make a difference to the dielectric properties of the medium in the channel. Therefore, it could be concluded that different types of reticulo-ruminal contractions and the secretion of saliva are the main causes for distinct PL patterns in rumination and feeding phases. As for the PL in relaxation phases, various patterns have been observed. According to Nogami et al., no motion of the bolus has been detected when the cow is in relaxation status [Nog+17]. It is suggested that more efforts would be needed to investigate PL in relaxation phase. This topic is therefore left for future research.

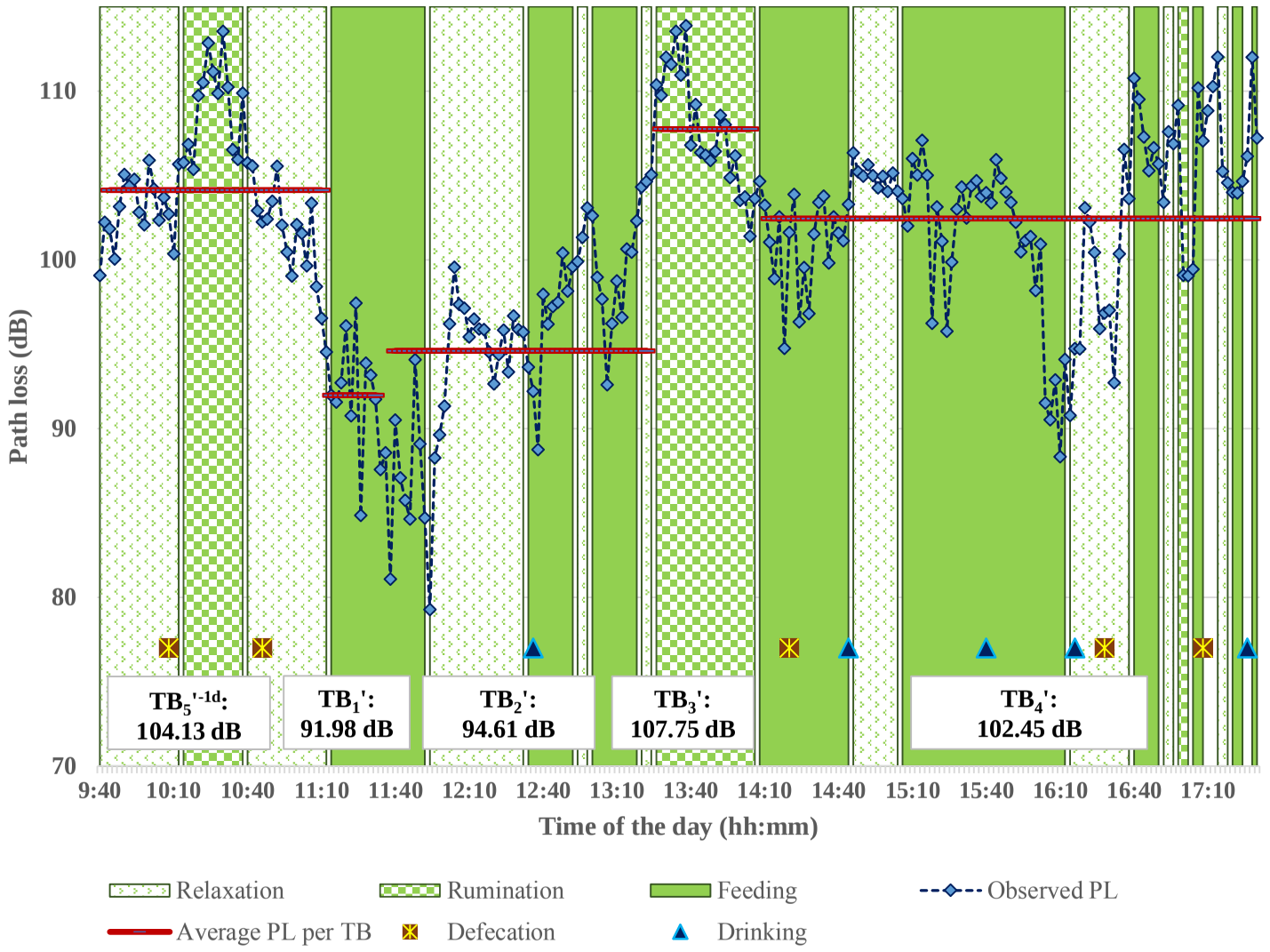

[hbt]

Fig. 5.9: Continuous PL observation with a temporary feeding protocol

5.4.4 Example application: power-saving plan for UAB bolus'17

The discovered diurnal PL pattern suggested that during certain hours of the day, such as TB_1: 7:00—10:00 and TB_2: 10:00—14:00, less PL would be exhibited in the channel. Consequently, it is possible to optimize the power supply plan during these hours. An example power profile of UAB bolus'17 is given in Figure 5.10. Throughout the in vivo studies, maximum power supply (+20 dBm) was provided, whose current is about 86 mA. Assuming that maximum power supply is required for TB_3, TB_4, and TB_5, then the transmit power could be stepped down to +8 dBm (as defined in [See]) for TB_1 and TB_2, considering the differences in observed average PL. The current for +8 dBm transmit power is around 31 mA.

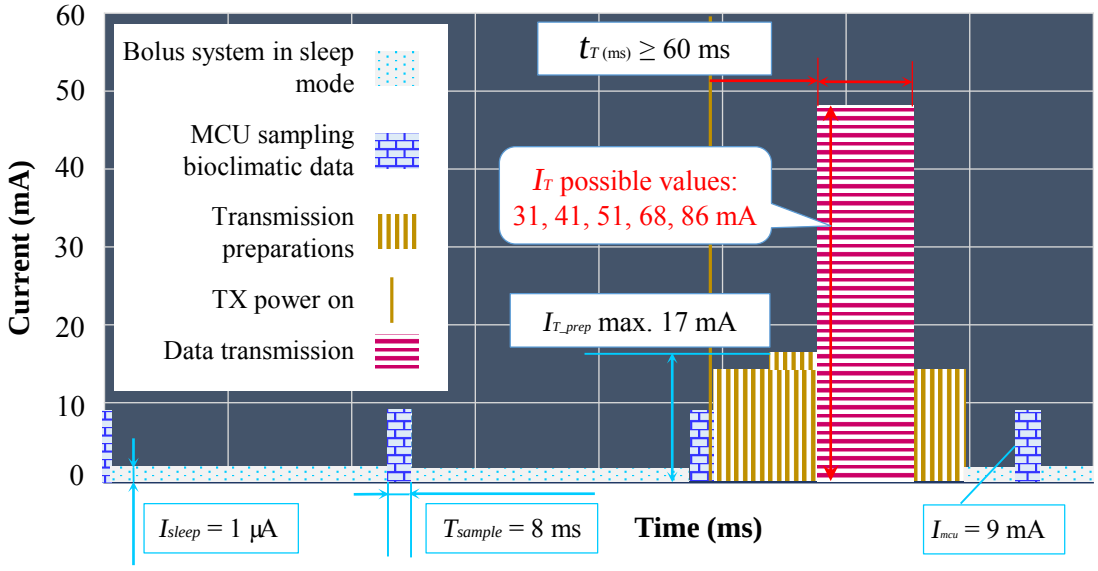

Fig. 5.10: Example power profile of UAB bolus'17

Analyzing power profile requires taking into account all of the power consuming components in the system, demonstrated as rectangles filled with different patterns in Figure 5.10. For example, duration of the data transmission is set to 80 ms, excluding the transmission preparation time. Power consumed during transmission is calculated by multiplying the current I_T and time t_T, which is the manageable part. Time length of transmission preparation can be estimated as 120 ms, with an average current of 15 mA, both of which are fixed. Assuming one transmission takes place every 10 minutes, during which time the MCU performs 5 samplings. Thereby, when

the transmit power is at its maximum, power consumed for data transmission would account for around 71.4% of the total power consumption of the bolus system, by calculating the sum of areas of all of the rectangles in Figure 5.10. Reducing the transmit power from +20 dBm to +8 dBm would bring in 45.6% power reduction in the bolus system. Combined this result with the diurnal PL pattern, there are 7 hours assigned in TB_1 and TB_2, which could benefit from the proposed power-saving plan. As a result, the diurnal power consumption could be reduced by 13.3%. Accordingly, the battery life would be prolonged by 15.3% from the original power setting.

5.5 Summary

The in-to-out body wireless channel between UAB bolus'17 and an on-body receiver was investigated in its original scenarios with a cannulated dairy cow. In vivo experiment campaigns that focused on different aspects of channel behaviors were designed and executed under professional veterinarian guidance. Considering the periodical reticulo-ruminal contractions, feed accumulations, as well as random body movements, the channel could be considered "coherent" within 2 minutes. With this time-domain feature, PL was examined under different TX and RX configurations. Due to the different compositions inside the rumen, different bolus residing layer would result in obvious difference in PL. Besides, the optimum location for RX was proved to be on the left side of the neck. Since the bolus antenna is not unidirectional, the influence from antenna misalignment was discovered to be limited. In the continuous PL observation, a diurnal PL pattern was developed which suggested that PL is associated with digestive behaviors across the day. Accordingly, applying the diurnal PL pattern to the power consumption profile of the bolus system, the battery life is expected to be prolonged by over 15% when the transmit power is reduced before and during morning feeding hours.

Conclusion

6

> *The best way to have a good idea is to have lots of ideas.*
>
> **— Linus Pauling**

This doctoral thesis has been focused on providing a radio solution for a wireless ruminal indwelling sensing node (UAB bolus'17) designed for small ruminants. The designated goals for this radio solution have been achieved. A small antenna has been implemented and verified in the original application scenario. The radio channel has been characterized both with theoretical models and through in vivo investigations. The discovered channel characteristics imply its lossy nature, and the time-varying features of its parameters. The findings have been applied to generate a power-reduction plan for UAB bolus'17, which has suggested over 15% prolongation of battery life.

The spiral antenna, whose implementation is elaborated in Chapter 3, has its merits in matching with the surrounding environment, both in dimension and in performance. Even though antenna design and matching are not the focus of this thesis, implementation of this spiral antenna has followed a meticulous process. The major components and mediums in its vicinity —some of which are seldom considered but have considerable impacts on antenna performance—have been modelled for numerical analysis. Fabrication requirements have also been applied. Parametric sweep and optimization provided by FEKO were performed to generate the optimum antenna model for fabrication. The resulted spiral antenna was proved to work as planned.

Theoretical channel characterization was launched after the spiral antenna was integrated to UAB bolus'17 and encapsulated in a small tube. As presented in Chapter 4, laboratory measurements with a tissue-simulating phantom were performed to obtain the PL pattern against TX-RX. In addition, FDTD methods were used to simulate the same transmission scenario. Discrepancies have been found between the measured and calculated PL patterns. When applied with the canonical log-distance path loss model, two sets of parameters were obtained, which further generated different

predictions of cell ranges through link budget calculation. A minimum system performance could be achieved when applying the shorter predicted range on a general small ruminant animal. Although facing great challenges in adequate models and computational costs, using canonical channel models and link budget analysis to theoretically investigate the radio transmission channel from a ruminal bolus to an on-body receiver is still a notable progress in animal-targeted WBAN.

In vivo channel investigation campaigns were carried out by placing UAB bolus'17 into the rumen of a cannulated cow, and a reference receiver antenna around its neck to observe received signal level. Dynamic features of the channel were simplified utilizing an estimated channel coherent time. Considerable differences in PL have been observed when the bolus was at different composition layers of the rumen: the lower it resides, the higher the PL. Left side of the neck has been proved to be the optimum location for RX. Besides, limited influence on PL has been discovered from TX antenna and RX antenna misalignment. Through continuous observation, a diurnal PL pattern has been developed suggesting the impact of digestive statuses on PL: low level of PL has been discovered before and during morning feeding hours while highest PL has been found in intensive ruminating phases. Accordingly, applying the finding to the system power profile, the battery life is expected to be prolonged by over 15% when the transmit power is reduced during the low PL hours.

Future work

7

> *Look up at the stars and not down at your feet. Try to make sense of what you see, and wonder about what makes the universe exist. Be curious.*
>
> **— Stephen Hawking**

In this doctoral thesis, a radio solution designed to balance dimension restriction and system performance has been provided for a ruminal bolus designed for small ruminants. The thesis is finished, but research never ends. For this reason, a list of topics that could be investigated in future works is given:

Improvement in bolus antenna performance

For the spiral antenna, much improvement could be achieved through changes to the substrate: either using other dielectric materials or increasing the thickness of the current one. Furthermore, other antenna typologies will also yield improved radiation performance, such as the conformal antenna.

Customized design for receiver antenna

The receiver antenna would also be detuned due to its proximity to lossy tissues. With similar design methodologies as the bolus antenna while less constraints on dimension, a customized receiver antenna will improve the robustness of the radio link.

Materials for bolus filling and packaging

The surrounding environment of the antenna also brings in signal attenuation due to the large difference in permittivity from digestive contents. Using high permittivity and low loss solid material, in the form of particles, to fill in the bolus will alleviate the situation. Meanwhile, materials of similar characteristics is desired for bolus packaging.

Adequate 3D animal models for numerical analysis

3D heterogeneous human models have played an important role in human-targeted WBAN research. For animal-targeted WBAN, applying numerical

methods on adequate animal models that include key biological portraits and behaviors will elevate the research work to another class.

Dedicated study of the radio channel when the ruminants are in relaxation status

Since the ruminant animals would spend much time in relaxation, there is a further chance to reduce transmit power through a more specified PL pattern during relaxation phases.

Wireless power transfer

More and more implant or ingestible WBAN devices will be recharged through wireless power transfer, which is becoming a game changer to the research and development work in WBAN. Consequently, the involved antennas are preferable to support both data transmission and power transfer. Moreover, the coexistence of different electromagnetic radiation systems is among the top research topics.

Bibliography

[AB97] GW Atkenson and B Bickert. „Open holding pens: A need for summertime shade“. In: *Michigan Dairy Review* 2.3 (1997) (cit. on p. 58).

[AH09] Akram Alomainy and Yang Hao. „Modeling and characterization of biotelemetric radio channel from ingested implants considering organ contents“. In: *IEEE Transactions on Antennas and Propagation* 57.4 (2009), pp. 999–1005 (cit. on pp. 2, 16, 17, 22, 24, 50).

[Alz+07] Ousama Alzahal, B Rustomo, NE Odongo, TF Duffield, and BW McBride. „A system for continuous recording of ruminal pH in cattle“. In: *Journal of animal science* 85.1 (2007), pp. 213–217 (cit. on pp. 2, 69).

[Ara08] Alejandro Aragon-Zavala. *Antennas and propagation for wireless communication systems*. John Wiley & Sons, 2008 (cit. on pp. 23, 50, 51, 56, 59).

[Ass+08] IEEE Standards Association et al. *IEEE 802.15: WPAN™ task group 6 (TG6) body area networks*. 2008 (cit. on p. 23).

[Aug09] Robin Augustine. „Electromagnetic modelling of human tissues and its application on the interaction between antenna and human body in the BAN context“. PhD thesis. Université Paris-Est, 2009 (cit. on p. 18).

[BBB10] S Buczinski, C Bourel, and AM Belanger. „Ultrasonographic determination of body wall thickness at standing left laparotomy site in dairy cows“. In: *Veterinary Record* 166 (2010), pp. 204–205 (cit. on p. 55).

[Ben+16] Said Benaissa, David Plets, Emmeric Tanghe, et al. „Experimental characterisation of the off-body wireless channel at 2.4 GHz for dairy cows in barns and pastures“. In: *Computers and Electronics in Agriculture* 127 (2016), pp. 593–605 (cit. on p. 27).

[Bes06] Steven R Best. „Bandwidth and the lower bound on Q for small wideband antennas“. In: *Antennas and Propagation Society International Symposium 2006, IEEE*. IEEE. 2006, pp. 647–650 (cit. on p. 19).

[C+97] M Chenost, C Kayouli, et al. „Roughage utilization in warm climates.“ In: *FAO animal production and health paper* 135 (1997) (cit. on p. 6).

[Caj+99] G Caja, C Conill, R Nehring, and O Ribó. „Development of a ceramic bolus for the permanent electronic identification of sheep, goat and cattle“. In: *Computers and electronics in agriculture* 24.1-2 (1999), pp. 45–63 (cit. on pp. 11, 13).

[Car+10] S Carne, G Caja, MA Rojas-Olivares, and AAK Salama. „Readability of visual and electronic leg tags versus rumen boluses and electronic ear tags for the permanent identification of dairy goats“. In: *Journal of dairy science* 93.11 (2010), pp. 5157–5166 (cit. on p. 11).

[CCK16] Gerardo Caja, Andreia Castro-Costa, and Christopher H Knight. „Engineering to support wellbeing of dairy animals“. In: *Journal of Dairy Research* 83.2 (2016), pp. 136–147 (cit. on p. 2).

[CDO14] Simon L Cotton, Raffaele D'Errico, and Claude Oestges. „A review of radio channel models for body centric communications“. In: *Radio Science* 49.6 (2014), pp. 371–388 (cit. on pp. 21, 22).

[Chu88] David Calvin Church. *The Ruminant animal: digestive physiology and nutrition*. 1988 (cit. on p. 66).

[CLF94] G Caja, M Luini, and PD Fonseca. „Electronic identification of farm animals using implantable transponders“. In: *FEOGA Research Project (Contract CCAM 93-342), Final Report* 1 (1994) (cit. on p. 11).

[DL13] Garland R Dahlke and Daniel D Loy. „Estimating Beef Cow Maintenance Efficiency with a Fasting Protocol“. In: *Animal Industry Report* 659.1 (2013), p. 20 (cit. on p. 67).

[Duf+04] T Duffield, JC Plaizier, A Fairfield, et al. „Comparison of techniques for measurement of rumen pH in lactating dairy cows“. In: *Journal of dairy science* 87.1 (2004), pp. 59–66 (cit. on p. 2).

[EJ01] JMD Enemark and RJ Jørgensen. „Nutrition: Subclinical rumen acidosis as a cause of reduced appetite in newly calved dairy cows in Denmark: Results of a poll among Danish dairy practitioners“. In: *Veterinary quarterly* 23.4 (2001), pp. 206–210 (cit. on p. 2).

[FA02] Michael FW Festing and Douglas G Altman. „Guidelines for the design and statistical analysis of experiments using laboratory animals“. In: *ILAR journal* 43.4 (2002), pp. 244–258 (cit. on p. 65).

[FFC16] João M Felıcio, Carlos A Fernandes, and Jorge R Costa. „Comparing liquid homogeneous and multilayer phantoms for human body implantable antennas“. In: *Antennas and Propagation (APSURSI), 2016 IEEE International Symposium on*. IEEE. 2016, pp. 1049–1050 (cit. on p. 9).

[Flo+15] Pål Anders Floor, Raúl Chávez-Santiago, Sverre Brovoll, et al. „In-body to on-body ultrawideband propagation model derived from measurements in living animals“. In: *IEEE journal of biomedical and health informatics* 19.3 (2015), pp. 938–948 (cit. on pp. 9, 26, 27, 61).

[Gal+11] Michele Gallo, Peter S Hall, Qiang Bai, et al. „Simulation and measurement of dynamic on-body communication channels“. In: *IEEE Transactions on Antennas and Propagation* 59.2 (2011), pp. 623–630 (cit. on p. 26).

[Gar+16] Concepcion Garcia-Pardo, Alejandro Fornes-Leal, Narcıs Cardona, et al. „Experimental ultra wideband path loss models for implant communications“. In: *Personal, Indoor, and Mobile Radio Communications (PIMRC), 2016 IEEE 27th Annual International Symposium on*. IEEE. 2016, pp. 1–6 (cit. on pp. 22, 27, 61).

[Gar+18] Concepcion Garcia-Pardo, Carlos Andreu, Alejandro Fornes-Leal, et al. „Ultrawideband Technology for Medical In-Body Sensor Networks: An Overview of the Human Body as a Propagation Medium, Phantoms, and Approaches for Propagation Analysis“. In: *IEEE Antennas and Propagation Magazine* (2018) (cit. on p. 21).

[GGC96] Camelia Gabriel, Sami Gabriel, and y E Corthout. „The dielectric properties of biological tissues: I. Literature survey“. In: *Physics in Medicine & Biology* 41.11 (1996), p. 2231 (cit. on pp. 7, 16, 17, 26).

[GLG96a] Sami Gabriel, RW Lau, and Camelia Gabriel. „The dielectric properties of biological tissues: II. Measurements in the frequency range 10 Hz to 20 GHz“. In: *Physics in medicine & biology* 41.11 (1996), p. 2251 (cit. on p. 7).

[GLG96b] Sami Gabriel, RW Lau, and Camelia Gabriel. „The dielectric properties of biological tissues: III. Parametric models for the dielectric spectrum of tissues“. In: *Physics in Medicine & Biology* 41.11 (1996), p. 2271 (cit. on p. 7).

[Hae01] GFW Haenlein. „Past, Present, and Future Perspectives of Small Ruminant Dairy Research1“. In: *Journal of Dairy Science* 84.9 (2001), pp. 2097–2115 (cit. on p. 62).

[Han76] J Hanton. „Rumen implantable method of electronic identification of livestock“. In: *Pages I1–10 in Proc. Verslag van een symposium gehouden. Univ. Wageningen, Wageningen, the Netherlands*. 1976 (cit. on p. 11).

[HS10] TJ Hackmann and JN Spain. „Invited review: ruminant ecology and evolution: perspectives useful to ruminant livestock research and production“. In: *Journal of dairy science* 93.4 (2010), pp. 1320–1334 (cit. on p. 1).

[Hu+07] Zhen H Hu, Yuriy I Nechayev, Peter S Hall, Costas C Constantinou, and Yang Hao. „Measurements and statistical analysis of on-body channel fading at 2.45 GHz“. In: *IEEE Antennas and Wireless Propagation Letters* 6 (2007), pp. 612–615 (cit. on p. 26).

[Idd+00] Gavriel Iddan, Gavriel Meron, Arkady Glukhovsky, and Paul Swain. „Wireless capsule endoscopy“. In: *Nature* 405.6785 (2000), p. 417 (cit. on p. 15).

[Ito+01] Koichi Ito, Katsumi Furuya, Yoshinobu Okano, and Lira Hamada. „Development and characteristics of a biological tissue-equivalent phantom for microwaves“. In: *Electronics and Communications in Japan (Part I: Communications)* 84.4 (2001), pp. 67–77 (cit. on p. 9).

[Joh04] Anders J Johansson. „Wireless communication with medical implants: antennas and propagation“. In: (2004) (cit. on pp. 24, 58, 59).

[JP06] Lars Josefsson and Patrik Persson. *Conformal array antenna theory and design*. Vol. 29. John wiley & sons, 2006 (cit. on p. 18).

[KCY05] Sang il Kwak, Kihun Chang, and Young Joong Yoon. „Ultra-wide band spiral shaped small antenna for the biomedical telemetry“. In: *Microwave Conference Proceedings, 2005. APMC 2005. Asia-Pacific Conference Proceedings*. Vol. 1. IEEE. 2005, 4–pp (cit. on pp. 19, 20, 31, 32).

[Kou+06] Stavros Koulouridis, Gullu Kiziltas, Yijun Zhou, Derek J Hansford, and John L Volakis. „Polymer–ceramic composites for microwave applications: fabrication and performance assessment“. In: *IEEE Transactions on Microwave Theory and Techniques* 54.12 (2006), pp. 4202–4208 (cit. on p. 17).

[KS82] KR King and CR Stockdale. „Fasting as a technique for use in dairy cattle nutrition experiments“. In: *Proceedings of the Australian Society of Animal Production*. Vol. 14. 1982, p. 621 (cit. on p. 67).

[Kur+11] Divya Kurup, Maria Scarpello, Günter Vermeeren, et al. „In-body path loss models for implants in heterogeneous human tissues using implantable slot dipole conformal flexible antennas“. In: *EURASIP Journal on Wireless Communications and Networking* 2011.1 (2011), p. 51 (cit. on pp. 21, 61).

[LCY07] Sang Heun Lee, Kihun Chang, and Young Joong Yoon. „A dual spiral antenna for wideband capsule endoscope system“. In: *Microwave Conference, 2007. APMC 2007. Asia-Pacific*. IEEE. 2007, pp. 1–4 (cit. on pp. 19, 20).

[Lee+07] Sangyong Lee, Jin-Gul Hyun, Hyungsoo Kim, and Kyung-Wook Paik. „A Study on Dielectric Constants of Epoxy/SrTiO3 Composite for Embedded Capacitor Films (ECFs)“. Undetermined. In: *IEEE Transactions on Advanced Packaging* 30.3 (2007), pp. 428–433 (cit. on p. 17).

[Lee+08] Sang Heun Lee, Kihun Chang, Ki Joon Kim, and Young Joong Yoon. „A conical spiral antenna for wideband capsule endoscope system“. In: *Antennas and Propagation Society International Symposium, 2008. AP-S 2008. IEEE*. IEEE. 2008, pp. 1–4 (cit. on pp. 19, 20).

[Lee+11] Sang Heun Lee, Jaebok Lee, Young Joong Yoon, et al. „A wideband spiral antenna for ingestible capsule endoscope systems: Experimental results in a human phantom and a pig“. In: *IEEE Transactions on Biomedical Engineering* 58.6 (2011), pp. 1734–1741 (cit. on pp. 2, 9, 15, 17–19, 26, 27, 32).

[LGX14] Changrong Liu, Yong-Xin Guo, and Shaoqiu Xiao. „Circularly polarized helical antenna for ISM-band ingestible capsule endoscope systems“. In: *IEEE Transactions on Antennas and Propagation* 62.12 (2014), pp. 6027–6039 (cit. on pp. 16, 17).

[Lin09] Xiaoxiao Lin. „Evaluation of Kahne rumen sensors in fistulated sheep and cattle under contrasting feeding conditions: a thesis presented in partial fulfilment of the requirements for the degree of Master of Science in Agriculture at Massey University, Palmerston North, New Zealand“. PhD thesis. Massey University, 2009 (cit. on p. 12).

[LJ13] E Lezar and U Jakobus. „GPU-acceleration of the FEKO electromagnetic solution kernel“. In: *Electromagnetics in Advanced Applications (ICEAA), 2013 International Conference on*. IEEE. 2013, pp. 814–817 (cit. on p. 8).

[LKW05] Matthew Loy, Raju Karingattil, and Louis Williams. „ISM-band and short range device regulatory compliance overview“. In: *Texas Instruments* (2005) (cit. on pp. 5, 13).

[LMH57] GP Lofgreen, JH Meyer, and JL Hull. „Behavior patterns of sheep and cattle being fed pasture or soilage“. In: *Journal of Animal Science* 16.4 (1957), pp. 773–780 (cit. on pp. 6, 71).

[MAF07] Guoqiang Mao, Brian DO Anderson, and Barış Fidan. „Path loss exponent estimation for wireless sensor network localization“. In: *Computer Networks* 51.10 (2007), pp. 2467–2483 (cit. on p. 52).

[Mer+11] Francesco Merli, Léandre Bolomey, Jean-François Zürcher, et al. „Design, realization and measurements of a miniature antenna for implantable wireless communication systems“. In: *IEEE Transactions on Antennas and propagation* 59.10 (2011), pp. 3544–3555 (cit. on pp. 15–19).

[Min+18] Ben Minnaert, Bart Thoen, David Plets, Wout Joseph, and Nobby Stevens. „Wireless energy transfer by means of inductive coupling for dairy cow health monitoring“. In: *Computers and Electronics in Agriculture* 152 (2018), pp. 101–108 (cit. on pp. 15, 69).

[Mot+08] Toby Mottram, John Lowe, Michael McGowan, and Nancy Phillips. „A wireless telemetric method of monitoring clinical acidosis in dairy cows“. In: *computers and electronics in agriculture* 64.1 (2008), pp. 45–48 (cit. on pp. 12–14).

[Mot16] TTF Mottram. „Is monitoring rumen pH a routine tool or a seasonal adjustment to new forage quality?“ In: *Proceedings of the 7th Nordic Feed Science Conference*. 2016 (cit. on p. 12).

[Mül+16] Simon Müller, Rene Thull, Maximilian Huber, and Andreas R Diewald. „Microstrip patch antennas on EUROCIRCUITS process“. In: *Antennas & Propagation Conference (LAPC), 2016 Loughborough*. IEEE. 2016, pp. 1–5 (cit. on p. 46).

[Nik+17] Denys Nikolayev, Maxim Zhadobov, Laurent Le Coq, Pavel Karban, and Ronan Sauleau. „Robust ultraminiature capsule antenna for ingestible and implantable applications“. In: *IEEE Transactions on Antennas and Propagation* 65.11 (2017), pp. 6107–6119 (cit. on pp. 7, 13, 15–22, 24, 42).

[Nog+17] Hirofumi Nogami, Shozo Arai, Hironao Okada, Lan Zhan, and Toshihiro Itoh. „Minimized Bolus-Type Wireless Sensor Node with a Built-In Three-Axis Acceleration Meter for Monitoring a Cow's Rumen Conditions“. In: *Sensors* 17.4 (2017), p. 687 (cit. on pp. 2, 12, 13, 17, 26, 28, 71, 84).

[NRR07] Mark Norris, J-D Richerd, and Deborah Raynes. „Sub miniature antenna design for wireless implants“. In: (2007) (cit. on p. 15).

[Oli+18] Joan Oliver, C Ferrer, Alejandro Peralta Alzate, et al. „Temperature rumen bolus able to record intake and drinking behavior for dairy small ruminants“. In: *Fifth DairyCare Conference*. DairyCare, 2018. Mar. 2018 (cit. on pp. 3, 13, 31, 72).

[Oli17] Bartomeu Oliver Riera. „Permittivity measurements using coaxial probes“. B.S. thesis. Universitat Politècnica de Catalunya, 2017 (cit. on p. 41).

[ONe+18] HA O'Neill, Edward Cottington Webb, L Frylinck, and PE Strydom. „Effects of short and extended fasting periods and cattle breed on glycogenolysis, sarcomere shortening and Warner-Bratzler shear force“. In: *South African Journal of Animal Science* 48.1 (2018), pp. 71–80 (cit. on p. 67).

[Pis+13] Davy Pissoort, Mehdi Mechaik, Henry Zeng, et al. „Influence of the interaction between antenna currents and return currents on the coupling between digital interfaces and on-board antennas“. In: *Electromagnetic Compatibility (EMC), 2013 IEEE International Symposium on*. IEEE. 2013, pp. 1–6 (cit. on p. 17).

[Poo+15] Carmen CY Poon, Benny PL Lo, Mehmet Rasit Yuce, Akram Alomainy, and Yang Hao. „Body sensor networks: In the era of big data and beyond“. In: *IEEE reviews in biomedical engineering* 8 (2015), pp. 4–16 (cit. on p. 12).

[PT15] Tapan Pattnayak and Guhapriyan Thanikachalam. „Antenna design and RF layout guidelines“. In: *Cypress Semiconductor AN91445; Cypress Semiconductor: San Jose, CA, USA* (2015) (cit. on p. 17).

[RBH59] William Moy Stratton Russell, Rex Leonard Burch, and Charles Westley Hume. *The principles of humane experimental technique*. Vol. 238. Methuen London, 1959 (cit. on p. 65).

[Rem98] ITU-R Remote Sensing 1346. „Sharing between the meteorological aids services and medical implant communication systems (MICS) operating in the mobile service in the frequency band 401–406 MHz“. In: (1998) (cit. on pp. 15, 23, 58, 59).

[RF16] Stefan Rosenkranz and Mario Fallast. *Device for the measurement of individual farm animal data*. US Patent 9,504,231. Nov. 2016 (cit. on pp. 12–14).

[Rom+14] Karen Lopez-Linares Roman, Günter Vermeeren, Arno Thielens, Wout Joseph, and Luc Martens. „Characterization of path loss and absorption for a wireless radio frequency link between an in-body endoscopy capsule and a receiver outside the body“. In: *EURASIP Journal on Wireless Communications and Networking* 2014.1 (2014), p. 21 (cit. on pp. 17, 20, 22, 23, 50).

[RTR97] Raquel F Reinoso, Brian A Telfer, and Malcolm Rowland. „Tissue water content in rats measured by desiccation“. In: *Journal of pharmacological and toxicological methods* 38.2 (1997), pp. 87–92 (cit. on pp. 7, 16).

[SA16] Koziel Slawomir and Bekasiewicz Adrian. *Multi-objective design of antennas using surrogate models*. World Scientific, 2016 (cit. on pp. 29, 34).

[SAH09] Andrea Sani, Akram Alomainy, and Yang Hao. „Numerical characterization and link budget evaluation of wireless implants considering different digital human phantoms“. In: *IEEE Transactions on Microwave Theory and Techniques* 57.10 (2009), pp. 2605–2613 (cit. on pp. 16, 17, 23, 50, 52, 61).

[Sam+90] TV Samulski, P Fessenden, ER Lee, et al. „Spiral microstrip hyperthermia applicators: technical design and clinical performance“. In: *International Journal of Radiation Oncology• Biology• Physics* 18.1 (1990), pp. 233–242 (cit. on p. 32).

[Sat+12] Shigeru Sato, Atsushi Kimura, Tomoaki Anan, et al. „A radio transmission pH measurement system for continuous evaluation of fluid pH in the rumen of cows“. In: *Veterinary research communications* 36.1 (2012), pp. 85–89 (cit. on pp. 2, 12, 14, 17, 24, 26, 70).

[SBR13] AJ Sheahan, RC Boston, and JR Roche. „Diurnal patterns of grazing behavior and humoral factors in supplemented dairy cows“. In: *Journal of Dairy Science* 96.5 (2013), pp. 3201–3210 (cit. on pp. 65, 72).

[SCQ16] Terence Shie Ping See, ZhiNing Chen, and Xianming Qing. „IMPLANTED ANTENNAS AND RF TRANSMISSION IN THROUGH-BODY COMMUNICATIONS“. In: *Electromagnetics of Body Area Networks: Antennas, Propagation, and RF Systems* (2016), p. 159 (cit. on pp. 18, 22, 23, 61).

[SF80] Jonathan L Schepps and Kenneth R Foster. „The UHF and microwave dielectric properties of normal and tumour tissues: variation in dielectric properties with tissue water content“. In: *Physics in Medicine & Biology* 25.6 (1980), p. 1149 (cit. on pp. 7, 16, 71).

[Smi+13] David B Smith, Dino Miniutti, Tharaka A Lamahewa, and Leif W Hanlen. „Propagation models for body-area networks: A survey and new outlook“. In: *IEEE Antennas and Propagation Magazine* 55.5 (2013), pp. 97–117 (cit. on pp. 25, 26).

[SPC13] N Soriani, G Panella, and LUIGI Calamari. „Rumination time during the summer season and its relationships with metabolic conditions and milk production“. In: *Journal of dairy science* 96.8 (2013), pp. 5082–5094 (cit. on p. 65).

[Sta+16] Antonietta Stango, Kamya Yekeh Yazdandoost, Francesco Negro, and Dario Farina. „Characterization of in-body to on-body wireless radio frequency link for upper limb prostheses“. In: *PloS one* 11.10 (2016), e0164987 (cit. on pp. 2, 21–23, 49, 50, 58).

[Wan+12] Zhao Wang, Eng Gee Lim, Tammam Tillo, and Fangzhou Yu. „Review of the wireless capsule transmitting and receiving antennas“. In: *Wireless Communications and Networks-Recent Advances*. InTech, 2012 (cit. on pp. 15, 17–19, 21).

[Wan+17] Lu Wang, Günter Vermeeren, Marta Prim, Wout Joseph, and Carles Ferrer. „Characterization and Implementation of in-to-out Body Wireless Sensor Data Transmission for Smaller Ruminants“. In: *Multidisciplinary Digital Publishing Institute Proceedings* 1.8 (2017), p. 847 (cit. on pp. 12–14, 17, 22, 23, 50).

[WW12] Jianqing Wang and Qiong Wang. *Body area communications: channel modeling, communication systems, and EMC*. John Wiley & Sons, 2012 (cit. on pp. 17, 21, 22, 24, 26, 27, 50, 58).

[YH10] Kamya Yekeh Yazdandoost and Kiyoshi Hamaguchi. „Antenna polarization mismatch in body area network communications“. In: *Antennas and Propagation (EuCAP), 2010 Proceedings of the Fourth European Conference on*. IEEE. 2010, pp. 1–4 (cit. on pp. 22, 50).

[YS10] K Yazdandoost and K Sayrafian-Pour. „TG6 channel model ID: 802.15-08-0780-12-0006“. In: *IEEE submission, Nov* (2010) (cit. on pp. 21, 23, 50, 52).

[Zos+10] J Zosel, H Kaden, G Peters, et al. „Continuous long-term monitoring of ruminal pH“. In: *Sensors and Actuators B: Chemical* 144.2 (2010), pp. 395–399 (cit. on pp. 2, 4, 12, 70).

Online references

[Bow] Richard Bowen. *Rumen Physiology and Rumination*. URL: http://www.vivo.colostate.edu/hbooks/pathphys/digestion/herbivores/rumination.html. (accessed: 2011) (cit. on p. 65).

[Cam] Inc. Campell Scientific. *The Link Budget and Fade Margin*. URL: https://s.campbellsci.com/documents/us/technical-papers/link-budget.pdf (cit. on pp. 51, 57).

[DeL] Jean-Jacques DeLisle. *What Are the Differences between Various EM-Simulation Numerical Methods?* URL: https://www.mwrf.com/software/what-are-differences-between-various-em-simulation-numerical-methods. (accessed: 2014-11-10) (cit. on p. 8).

[Gmb] smaXtec animal care GmbH. *Inside monitoring*. URL: https://www.smaxtec.com/en/inside-monitoring/. (accessed: 2018) (cit. on pp. 2, 5, 12, 13).

[Lava] De Laval. *Cow Comfort: 9) Resting*. URL: http://www.milkproduction.com/Library/Scientific-articles/Housing/Cow-comfort-9/. (accessed: 2002) (cit. on p. 71).

[Lavb] De Laval. *Digestive physiology of the cow*. URL: http://www.milkproduction.com/Library/Scientific-articles/Animal-health/Digestive-Physiology-of-the-Cow/. (accessed: 2002) (cit. on pp. 7, 16).

[Lay] Dennis Layne. *Receiver Sensitivity and Equivalent Noise Bandwidth*. URL: https://www.highfrequencyelectronics.com/index.php?option=com_content%5C&view=article%5C&id=553:receiver-sensitivity-and-equivalent-noise-bandwidth%5C&catid=94:2014-06-june-articles%5C&Itemid=189. (accessed: 06.2014) (cit. on pp. 57, 58).

[Lima] Kahne Limited. *KB100008 Bolus low power transmitter User Manual KB1000 User Guide Kahne Limited*. URL: https://fccid.io/WO7KB100008/User-Manual/Users-Manual-1011828. (accessed: 2008-09-30) (cit. on pp. 14, 16).

[Limb] Well Cow Limited. *Well Cow System Overview*. URL: http://www.wellcow.org/overview.html. (accessed: 2010) (cit. on pp. 2, 4, 28).

[Mes] Schwarzbeck Mess. *VHF-UHF Biconical Broadband Antenna UBA 9116*. URL: http://schwarzbeck.de/Datenblatt/k9116.pdf (cit. on p. 53).

[Mob] Radio Mobile. *Linkbudgets*. URL: http://radiomobile.pe1mew.nl/?How_to:Linkbudgets. (accessed: 31.07.2018) (cit. on p. 57).

[Mot] Toby Mottram. *Biology of the rumen*. URL: https://www.ecow.co.uk/biology-of-the-rumen/. (accessed: 2018) (cit. on pp. 2, 6, 69).

[OECa] OECD-FAO. *Dairy and dairy products. In OECD-FAO agricultural outlook 2018-2027*. URL: http://www.fao.org/docrep/i9166e/i9166e_Chapter7_Dairy.pdf. (accessed: 2018-11-22) (cit. on p. 1).

[OECb] OECD-FAO. *Dairy Market Review*. URL: http://www.fao.org/3/I9210EN/i9210en.pdf. (accessed: 2018-04-15) (cit. on pp. 1, 2).

[SA] Schmid and Partner Enginnering AG. *MAINTENANCE OF TISSUE SIMULATING LIQUIDS*. URL: https://speag.swiss/assets/downloads/products/dasy/free_downloads/920-SLAAxyy-D.pdf. (accessed: 2011-04-21) (cit. on pp. 41, 52).

[See] Seeedstudio. *HC-12 Wireless RF UART Communication Module User Manual v2.4*. URL: http://statics3.seeedstudio.com/assets/file/bazaar/product/HC-12_english_datasheets.pdf. (accessed: 02.12.2016) (cit. on pp. 58, 86).

List of Figures

List of Tables

Declaration

I hereby declare that except where specific reference is made to the work of others, the contents of this doctoral thesis are original and have not been submitted in whole or in part for consideration for any other degree or qualification in this, or any other university. This dissertation is my own work and contains nothing which is the outcome of work done in collaboration with others, except as specified in the text and Acknowledgement. This doctoral thesis contains fewer than 65 000 words including appendices, bibliographies, footnotes, tables and equations, and has fewer than 150 figures.

Cerdanyola del Valles, Spain, February 5, 2019

Lu Wang